

RECEIVED: February 29, 2024 ACCEPTED: May 27, 2024 PUBLISHED: June 19, 2024

# Search for heavy neutral leptons in final states with electrons, muons, and hadronically decaying tau leptons in proton-proton collisions at $\sqrt{s}=13\,\text{TeV}$



# The CMS collaboration

E-mail: cms-publication-committee-chair@cern.ch

ABSTRACT: A search for heavy neutral leptons (HNLs) of Majorana or Dirac type using proton-proton collision data at  $\sqrt{s} = 13 \,\text{TeV}$  is presented. The data were collected by the CMS experiment at the CERN LHC and correspond to an integrated luminosity of  $138 \,\text{fb}^{-1}$ . Events with three charged leptons (electrons, muons, and hadronically decaying tau leptons) are selected, corresponding to HNL production in association with a charged lepton and decay of the HNL to two charged leptons and a standard model (SM) neutrino. The search is performed for HNL masses between 10 GeV and 1.5 TeV. No evidence for an HNL signal is observed in data. Upper limits at 95% confidence level are found for the squared coupling strength of the HNL to SM neutrinos, considering exclusive coupling of the HNL to a single SM neutrino generation, for both Majorana and Dirac HNLs. The limits exceed previously achieved experimental constraints for a wide range of HNL masses, and the limits on tau neutrino coupling scenarios with HNL masses above the W boson mass are presented for the first time.

Keywords: Beyond Standard Model, Hadron-Hadron Scattering

ARXIV EPRINT: 2403.00100

Contents					
1	Introduction				
<b>2</b>	The CMS detector and event reconstruction	3			
3	Event simulation	5			
4	Lepton selection	6			
5	Event selection and search strategy	7			
6	Background estimation	11			
7	Systematic uncertainties	18			
8	Results	20			
9	Interpretation	2			
10	10 Summary				
$\mathbf{T}$	The CMS collaboration 39				

# 1 Introduction

The observation of neutrino oscillations [1–3] implies that neutrinos have a nonzero mass [4]. Direct neutrino mass measurements [5, 6], as well as constraints from cosmological observations [7–9], indicate that the neutrino masses are much smaller than those of the other fermions in the standard model (SM) of particle physics. A possible mechanism for the generation of gauge-invariant neutrino mass terms and an explanation of their small scale is the see-saw mechanism [10–17], which introduces new heavy neutral leptons (HNLs) with right-handed chirality that are singlets under all SM gauge groups, but mix with the SM neutrinos. In addition, HNL models can provide a viable dark matter candidate [18, 19], and a mechanism to generate the matter-antimatter asymmetry of the universe [20–22].

We consider a simplified model with a single HNL (labelled N in diagrams and formulas) of Majorana or Dirac type that couples through the neutrino mixing matrix exclusively to a single generation of SM neutrinos [23, 24]. The signatures of such models in proton-proton (pp) collisions have been studied extensively [17, 25–35]. We focus on the production in association with a charged lepton  $\ell^{\pm}$ , which proceeds via the charged-current Drell-Yan (DY) process  $q\bar{q}' \to W^{\pm} \to N\ell^{\pm}$  [36, 37] or via the vector boson fusion (VBF) process  $q\gamma \to N\ell^{\pm}q'$  [38–41]. Several searches for this production mode have been performed by the ATLAS, CMS, and LHCb experiments at the CERN LHC [42–53]. The fully leptonic decay channel  $N \to \ell\ell\nu$  results in final states with three charged leptons, as illustrated in figure 1.

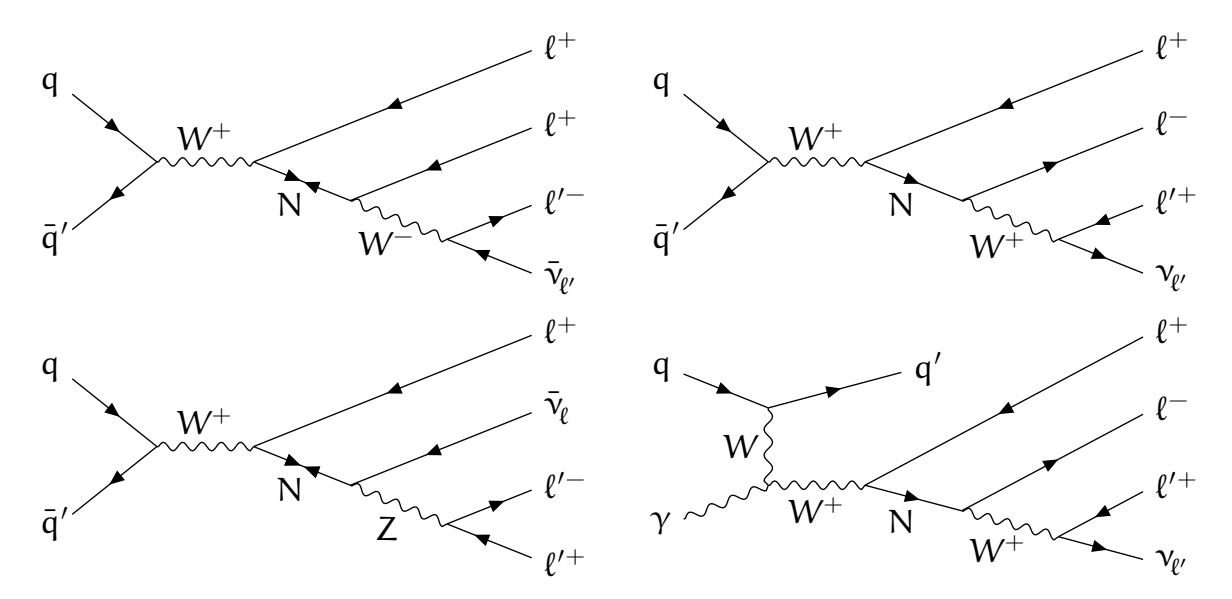


Figure 1. Examples of Feynman diagrams for production and decay of an HNL (indicated with the symbol N) resulting in final states with three charged leptons. The production processes DY (upper row and lower left) and VBF (lower right) are shown, with decays mediated by a W boson (upper row and lower right) or a Z boson (lower left). In the left column, HNLs of Majorana type with an LNV decay are shown, whereas the right column has HNLs of Dirac type with an LNC decay. The leptons that couple directly to the HNL (indicated with the symbol  $\ell$ ) are restricted to the SM generation that couples with the HNL, whereas the leptons from the W and Z boson decays (indicated with the symbol  $\ell'$ ) can be from any SM generation.

Due to the assumption of an exclusive coupling to a single SM generation, the charged lepton originating from the HNL production and the one from the first decay vertex in the case of W-boson-mediated decays are necessarily of the same flavour and from the generation to which the HNL couples. In the case of an HNL of Majorana type, both lepton number violating (LNV) and lepton number conserving (LNC) decays are possible, and as a result these two charged leptons can be of the same or opposite charge. For an HNL of Dirac type, only LNC decays are possible and these two charged leptons thus always have opposite charge.

In this article, we present a search for HNLs in events with three charged leptons (electrons e, muons  $\mu$ , and hadronically decaying tau leptons  $\tau_h$ , in the following referred to as "leptons"), using pp collision data collected in 2016–2018 at  $\sqrt{s}=13\,\mathrm{TeV}$  and corresponding to an integrated luminosity of  $138\,\mathrm{fb}^{-1}$ . We select events with all possible combinations of three light leptons (electrons and muons), resulting in the eee, ee $\mu$ , e $\mu\mu$ , and  $\mu\mu\mu$  flavour channels, as well as events with one  $\tau_h$  and any combination of two light leptons, resulting in the ee $\tau_h$ , e $\mu\tau_h$ , and  $\mu\mu\tau_h$  flavour channels. Events with an HNL decay mediated by a Z boson or with an LNC decay mediated by a W boson result in events with an opposite-sign same-flavour (OSSF) lepton pair, whereas events without such a pair are only possible for an LNV decay. The HNL scenarios with exclusive electron (muon) neutrino coupling are only probed in the eee and ee $\mu$  ( $\mu\mu\mu$  and e $\mu\mu$ ) channels. In the scenario of exclusive tau neutrino couplings, the two tau leptons can decay leptonically or hadronically, and thus the eee, ee $\mu$ , e $\mu\mu$ , and  $\mu\mu\mu$  channels provide sensitivity to HNL events where both tau leptons

decay leptonically, whereas the  $ee\tau_h$ ,  $e\mu\tau_h$ , and  $\mu\mu\tau_h$  channels provide sensitivity where one tau lepton each decays leptonically and hadronically. Two strategies based on event categorization or on machine-learning discriminants are employed to separate the HNL signal from the SM background, where diboson production is the most important contribution. Our results are interpreted for HNL masses  $m_N$  between 10 GeV and 1.5 TeV. To facilitate reinterpretations within more general HNL models [54, 55], we provide tabulated results in the HEPData record for this analysis [56].

The CMS Collaboration presented in ref. [46] a search in events with three light leptons using pp collision data collected in 2016 at  $\sqrt{s} = 13\,\text{TeV}$  and corresponding to an integrated luminosity of  $35.9\,\text{fb}^{-1}$ , constraining the mixing parameter  $|V_{\ell N}|^2$  between the HNL and the SM neutrino generation for  $m_N$  between 1 GeV and 1.2 TeV. This article supersedes those results, and improves them not only because of the larger data set, but also from refined light-lepton identification (ID) criteria, improved background estimation techniques, and signal-to-background discrimination based on machine learning. Additionally, we include for the first time in HNL searches at the LHC events with  $\tau_h$  and use state-of-the-art  $\tau_h$  ID techniques.

The mean lifetime of an HNL is proportional to  $m_{\rm N}^{-5}V_{\ell \rm N}^{-2}$  [57]. The HNL events that have a large decay length compared with the impact parameter resolution of the CMS tracker have a reduced selection efficiency in this analysis because we require that leptons originate from the primary interaction vertex (PV). Two dedicated HNL searches presented by the CMS Collaboration, based on the same pp collision data set used in this analysis, reconstruct the secondary HNL decay vertex in events with three light leptons [50] or apply a displaced jet tagger to events with two light leptons [52], and constrain long-lived HNL scenarios for  $1 < m_{\rm N} < 20\,{\rm GeV}$ . The results of this analysis are complementary since they probe short-lived HNL scenarios with  $m_{\rm N} > 10\,{\rm GeV}$  not excluded by the dedicated searches for long-lived HNLs.

# 2 The CMS detector and event reconstruction

The central feature of the CMS apparatus is a superconducting solenoid of 6 m internal diameter, providing a magnetic field of 3.8 T. Within the solenoid volume are a silicon pixel and strip tracker, a lead tungstate crystal electromagnetic calorimeter (ECAL), and a brass and scintillator hadron calorimeter (HCAL), each composed of a barrel and two endcap sections. Forward calorimeters extend the pseudorapidity ( $\eta$ ) coverage provided by the barrel and endcap detectors. Muons are measured in gas-ionization detectors embedded in the steel flux-return yoke outside the solenoid. A more detailed description of the CMS detector, together with a definition of the coordinate system used and the relevant kinematic variables, is reported in refs. [58, 59].

Events of interest are selected using a two-tiered trigger system. The first level, composed of custom hardware processors, uses information from the calorimeters and muon detectors to select events at a rate of around 100 kHz within a fixed latency of about  $4 \mu s$  [60]. The second level, known as the high-level trigger, consists of a farm of processors running a version of the full event reconstruction software optimized for fast processing, and reduces the event rate to around 1 kHz before data storage [61].

The global event reconstruction with the particle-flow (PF) algorithm [62] reconstructs and identifies each individual particle in an event, with an optimized combination of all subdetector information. In this process, the identification of the particle type (photon, electron, muon, charged or neutral hadron) plays an important role in the determination of the particle direction and energy. Photons are identified as ECAL energy clusters not linked to the extrapolation of any charged-particle trajectory to the ECAL. Electrons are identified as a charged-particle track and potentially many ECAL energy clusters corresponding to the extrapolation of this track to the ECAL and to possible bremsstrahlung photons emitted along the way through the tracker material. Muons are identified as tracks in the central tracker consistent with either a track or several hits in the muon system, and associated with calorimeter deposits compatible with the muon hypothesis. Charged hadrons are identified as charged-particle tracks neither identified as electrons, nor as muons. Finally, neutral hadrons are identified as HCAL energy clusters not linked to any charged-hadron trajectory, or as a combined ECAL and HCAL energy excess with respect to the expected charged-hadron energy deposit. The PV is taken to be the vertex corresponding to the hardest scattering in the event, evaluated using tracking information alone, as described in section 9.4.1 of ref. [63].

For each event, hadronic jets are clustered from these reconstructed particles using the infrared and collinear safe anti- $k_{\rm T}$  algorithm [64, 65] with a distance parameter of 0.4. Jet momentum is determined as the vectorial sum of all particle momenta in the jet, and is found from simulation to be, on average, within 5–10% of the true momentum over the entire transverse momentum ( $p_{\rm T}$ ) spectrum and detector acceptance. Additional pp interactions within the same or nearby bunch crossings (pileup) can contribute additional tracks and calorimetric energy depositions to the jet momentum. To mitigate this effect, charged particles identified to be originating from pileup vertices are discarded and an offset correction is applied to correct for remaining contributions. Jet energy corrections are derived from simulation to bring the measured response of jets to that of particle-level jets on average. In situ measurements of the momentum balance in dijet, photon+jet, Z+jet, and multijet events are used to correct for any residual differences in the jet energy scale between data and simulation [66]. Only jets with  $p_{\rm T} > 25\,{\rm GeV}$  and  $|\eta| < 2.4$  are considered in this analysis. Additional selection criteria are applied to each jet to remove jets potentially dominated by anomalous contributions from various subdetector components or reconstruction failures [67].

The missing transverse momentum vector  $\vec{p}_{\mathrm{T}}^{\mathrm{miss}}$  is computed as the negative  $\vec{p}_{\mathrm{T}}$  sum of all PF candidates in an event, and its magnitude is denoted as  $p_{\mathrm{T}}^{\mathrm{miss}}$  [68]. The  $\vec{p}_{\mathrm{T}}^{\mathrm{miss}}$  is modified to account for corrections to the energy scale of the reconstructed jets in the event. Anomalous high- $p_{\mathrm{T}}^{\mathrm{miss}}$  events can arise from a variety of reconstruction failures, detector malfunctions, or noncollisional backgrounds. Such events are rejected by event filters that identify more than 85% of the spurious high- $p_{\mathrm{T}}^{\mathrm{miss}}$  events with a mistagging rate of less than 0.1% [68].

The DEEPJET algorithm [69–71] is applied to identify jets arising from the hadronization of b hadrons. We use a loose working point to tag jets as "b jets" with a selection efficiency for b quark jets of more than 90%, and a misidentification rate for c quark jets (light quark and gluon jets) of 50 (20)%.

## 3 Event simulation

Event samples simulated with Monte Carlo event generators are used to evaluate the signal selection efficiency, to predict background contributions, to train machine learning discriminators, and to validate background estimation techniques based on control samples in data. The simulated event samples are processed with a full simulation of the CMS detector based on the GEANT4 toolkit [72], and are reconstructed with the same software as the data samples. Additional simulated pileup interactions are added to the simulated events to match the observed pileup distribution as well, with a mean pileup of 23 (32) in 2016 (2017–2018) [73]. Separate event samples are generated for each data-taking year, reflecting the differences in the LHC running conditions and the CMS detector performance.

For the signal process, event samples are generated with the MADGRAPH5 amc@nlo v2.6.5 program [74, 75], using a model that extends the SM particle content by up to three right-handed neutrinos [26, 33, 40, 41]. The DY production process is simulated for  $m_{\rm N}$  < 80 GeV at leading order (LO) in the strong coupling  $\alpha_{\rm S}$ , whereas the simulation is performed at next-to-LO (NLO) in all other cases. In the matrix element calculation, the NNPDF3.1 [76] parton distribution functions (PDFs) are used for the DY production process, and the NNPDF31.luxQED [77-79] PDFs for the VBF production process. Separate samples are generated for HNLs that couple to electron, muon, or tau neutrinos, and for different  $m_N$ values between 10 GeV and 1.5 TeV. The VBF samples are generated only for masses of at least 600 GeV, since the contribution from VBF production is only relevant at high masses. For  $m_{\rm N} > 30 \, {\rm GeV}$ , no HNL lifetime effects are included in the simulation and a fixed value of  $\left|V_{\ell N}\right|^2 = 10^{-4}$  is used. The HNL production cross section is proportional to  $\left|V_{\ell N}\right|^2$  [41], and thus the generated samples for a specific  $m_{\rm N}$  value can be used to emulate signal scenarios with the same  $m_{\rm N}$  and different  $|V_{\ell \rm N}|^2$  values by applying a corresponding normalization factor. At 30 GeV and lower, we calculate the HNL mean lifetime analytically [80] and include it in the simulation of the HNL decay. Samples are generated with one fixed  $|V_{\ell N}|^2$ value between  $10^{-6}$  and  $10^{-3}$  for each mass point, and we emulate other  $|V_{\ell N}|^2$  values by reweighting the HNL decay length distribution as described in ref. [50]. In all cases, the samples are generated assuming an HNL of Majorana nature, i.e. including both LNV and LNC decays. Samples for a Dirac HNL are obtained by selecting only the subset of simulated events with LNC decays, and the event weights are calculated using the same cross section but half the decay width of the Majorana HNL with the same mass and couplings.

Furthermore, the Madgraph5\_amc@nlo generator is used to simulate background samples at NLO for WZ and Z $\gamma$  diboson production, for Higgs boson (H) production in association with a vector boson or a top quark pair ( $t\bar{t}$ ), for triboson production, for  $t\bar{t}$  production in association with a W or Z boson, for s-channel and tZ single top quark production, and for four top quark production. It is also used at LO for DY vector boson production in association with jets (Z+jets and W+jets), H production in association with a single top quark,  $t\bar{t}$  production in association with two bosons, and three top quark production. Background samples for  $q\bar{q}$ -initiated WW and ZZ diboson production, gluon fusion and VBF H production,  $t\bar{t}$  production, and t-channel and tW single-t production are generated with the POWHEG 2 program [81–89] at NLO. The gluon-gluon-initiated ZZ diboson production is simulated with the MCFM v7.0.1 generator [90–92] at LO. In all cases,

the NNPDF3.1 PDFs are used.

The generators are interfaced with the PYTHIA v8.230 program [93] for the underlying event description with the CP5 tune [94], the parton shower simulation, and hadronization. For Madgraph5\_amc@nlo samples simulated at LO (NLO), jets from matrix element calculations are merged with those from the parton shower using the MLM [95] (FxFx [96]) matching scheme. In POWHEG samples for H production, the decay to four leptons is simulated with the JHUGEN v5.2.5 program [97].

# 4 Lepton selection

Electrons are measured in the range  $|\eta| < 2.5$ , and their momentum is estimated by combining the energy measurement in the ECAL with the momentum measurement in the tracker [98, 99]. Electrons with  $1.44 < |\eta| < 1.57$  in the transition region between the barrel and endcap are not considered in the analysis because of performance limitations of the electron reconstruction in this region. Muons are measured in the range  $|\eta| < 2.4$ , with detection planes made using three technologies: drift tubes, cathode strip chambers, and resistive plate chambers [100].

We select reconstructed electrons and muons with  $p_{\rm T}>10\,{\rm GeV}$  that are compatible with originating from the PV and isolated from other particles in the event. The relative isolation variable  $I_{\rm rel}$  is defined as the scalar  $p_{\rm T}$  sum of all PF particles reconstructed within a cone around the lepton direction divided by the lepton  $p_{\rm T}$ , with the cone size defined in terms of  $\Delta R = \sqrt{(\Delta \eta)^2 + (\Delta \phi)^2}$ , where  $\Delta \eta$  and  $\Delta \phi$  are the  $\eta$  and azimuthal angle difference between the particle and the lepton. We use a variable cone size of 0.2 for leptons with  $p_{\rm T}<50\,{\rm GeV}$ , of  $10\,{\rm GeV}/p_{\rm T}$  for  $50< p_{\rm T}<200\,{\rm GeV}$ , and of 0.05 for  $p_{\rm T}>200\,{\rm GeV}$ , which improves the efficiency for high- $p_{\rm T}$  leptons by removing the accidental overlap with other particles [101]. Additionally, corrections for pileup contributions to  $I_{\rm rel}$  are applied. All reconstructed electrons and muons are required to have  $I_{\rm rel}<0.4$ . For electrons, we additionally require that there be at most one tracker layer that contributes no hit on the track, to reduce contributions from photon conversions [98]. For muons, we additionally apply the "medium" set of ID criteria defined in ref. [100].

Electrons and muons produced directly from the prompt decay of HNLs, W and Z bosons, or tau leptons are referred to as "prompt" leptons. Background contributions with "nonprompt" leptons arise from events with genuine leptons produced in hadron decays and photon conversions, as well as from evens with jet constituents misidentified as leptons. To distinguish between prompt and nonprompt electrons and muons, the two additional sets of ID criteria defined in ref. [102] are applied, labelled "loose" and "tight". The tight ID is based on a multivariate analysis (MVA) discriminant using the methods developed for various CMS measurements and searches with multilepton signatures [103–108], described in more detail for the case of muons in ref. [109]. Tight electrons and muons are required to have the MVA discriminant exceed certain thresholds, resulting in a prompt electron (muon) selection efficiency of about 85 (92)%. The misidentification rate for nonprompt electrons (muons) is less than 0.6% (about 1%). The loose ID is defined by requiring that electrons and muons either pass the tight ID, or pass selection requirements on some properties that are also used as inputs to the MVA discriminant.

Jets are used to reconstruct  $\tau_h$  candidates with the hadrons-plus-strips algorithm [110], which combines one or three tracks with energy deposits in the calorimeters, to identify the  $\tau_h$  decay modes. Neutral pions are reconstructed as ECAL energy deposition "strips" with dynamic size in  $\eta$ - $\phi$  from reconstructed electrons and photons, where the strip size varies as a function of the  $p_T$  of the electron or photon candidate. The  $\tau_h$  decay mode is then obtained by combining the charged hadrons with the strips. We consider decay modes with one or three charged hadrons, with or without neutral pions, and require the  $\tau_h$  candidate to have  $p_T > 20\,\text{GeV}$  and  $|\eta| < 2.3$ .

To distinguish genuine  $\tau_h$  decays from jets originating from the hadronization of quarks or gluons, and from electrons and muons, the DEEPTAU algorithm is used [111]. Information from all individual reconstructed particles near the  $\tau_h$  axis is combined with properties of the  $\tau_h$  candidate and the event to provide a multiclassification output equivalent to a Bayesian probability of the  $\tau_h$  to originate from a genuine tau lepton, the hadronization of a quark or gluon, an electron, or a muon. We define a "loose" and a "tight" ID for  $\tau_h$  by choosing different working points of the DEEPTAU discriminant for genuine tau leptons. The rate of a jet to be misidentified as  $\tau_h$  by the DEEPTAU algorithm depends on the  $p_T$  and quark flavour of the jet. We estimate it in simulated events from W boson production in association with jets to be 0.43% for a genuine  $\tau_h$  identification efficiency of 70%. The misidentification rate for electrons (muons) is 2.6 (0.03)% for a genuine  $\tau_h$  identification efficiency of 80 (>99)%.

To avoid double counting of charged-particle candidates that pass both the electron and muon reconstruction, we remove reconstructed electrons that are within  $\Delta R < 0.05$  of any reconstructed muon. Furthermore, we require that  $\tau_{\rm h}$  candidates be separated from any reconstructed electron or muon passing the tight working point by  $\Delta R > 0.5$ . Any jet that is within  $\Delta R < 0.4$  of any reconstructed electron or muon that passes the loose ID or within  $\Delta R < 0.5$  of a  $\tau_{\rm h}$  candidate that passes the tight ID is removed as well.

### 5 Event selection and search strategy

We analyse events that were collected with various triggers that require the presence of one, two, or three light leptons, with  $p_{\rm T}$  thresholds that depend on the data-taking year and the flavour combination of the reconstructed leptons, as listed in table 1. The efficiency of the trigger selection is larger than 90% for three-lepton events everywhere, approaching 100% for events with large lepton  $p_{\rm T}$ .

We select events with exactly three leptons that pass the tight ID criteria. For a sideband enriched in events with nonprompt leptons, we retain events where at least one lepton fails the tight but passes the loose ID criteria. Events with additional loose leptons or with at least one b jet are removed, as well as events where all leptons have the same charge. The highest  $p_{\rm T}$  (leading) lepton, referred to as  $\ell_1$ , is required to have  $p_{\rm T}(\ell_1) > 15\,{\rm GeV}$ . To ensure a high trigger efficiency, higher  $p_{\rm T}$  thresholds are applied to the leading and second-highest  $p_{\rm T}$  (subleading) light lepton depending on the lepton flavours present in the event, as summarized in table 1. If OSSF lepton pairs are present in an event, they are required to have an invariant mass  $m(\ell^+\ell^-) > 5\,{\rm GeV}$  to remove contributions from low-mass resonances. Additionally, we require  $|m(\ell^+\ell^-) - m_{\rm Z}| > 15\,{\rm GeV}$  for any OSSF lepton pair, where  $m_{\rm Z} = 91.2\,{\rm GeV}$  is the Z boson mass [112], to remove background events with Z bosons.

$N_{ m e}$	$N_{\mu}$	Online selection	Offline selection
≥1	_	$p_{\rm T}({\rm e}_1) > 27 (32){\rm GeV}$	$p_{\rm T}({\rm e}_1) > 30 \ (35)  {\rm GeV}$
_	$\geq 1$	$p_{\mathrm{T}}(\mu_1) > 24\mathrm{GeV}$	$p_{\mathrm{T}}(\mu_1) > 25\mathrm{GeV}$
$\geq 2$	_	$p_{\rm T}({\rm e}_1) > 23{\rm GeV}, p_{\rm T}({\rm e}_2) > 12{\rm GeV}$	$p_{\rm T}({\rm e}_1) > 25{\rm GeV}, p_{\rm T}({\rm e}_2) > 15{\rm GeV}$
_	$\geq 2$	$p_{\rm T}(\mu_1) > 17{\rm GeV}, p_{\rm T}(\mu_2) > 8{\rm GeV}$	$p_{\mathrm{T}}(\mu_1) > 20\mathrm{GeV}$
$\geq 1$	$\geq 1$	$p_{\rm T}({\rm l}_1) > 23{\rm GeV}, p_{\rm T}({\rm l}_2) > 8\ (12){\rm GeV}$	$p_{\rm T}({\rm l}_1) > 25{\rm GeV}, p_{\rm T}({\rm l}_2) > 10\ (15){\rm GeV}$
$\geq 3$	_	$p_{\rm T}({\rm e}_1) > 16{\rm GeV}, p_{\rm T}({\rm e}_2) > 12{\rm GeV}, p_{\rm T}({\rm e}_3) > 8{\rm GeV}$	$p_{\rm T}({\rm e}_1) > 25{\rm GeV}, p_{\rm T}({\rm e}_2) > 15{\rm GeV}$
$\geq 2$	$\geq 1$	$p_{\rm T}({\rm e}_{1,2}) > 12{\rm GeV}, p_{\rm T}(\mu_1) > 8{\rm GeV}$	$p_{\rm T}({\rm e}_1) > 25{\rm GeV}, p_{\rm T}({\rm e}_2) > 15{\rm GeV}$
$\geq 1$	$\geq 2$	$p_{\mathrm{T}}(\mathrm{e}_{1}) > 9\mathrm{GeV}, p_{\mathrm{T}}(\mu_{1,2}) > 9\mathrm{GeV}$	_
_	$\geq 3$	$p_{\rm T}(\mu_1) > 12~(10)~{\rm GeV},~p_{\rm T}(\mu_2) > 10~(5)~{\rm GeV},~p_{\rm T}(\mu_3) > 5~{\rm GeV}$	_

Table 1. Requirements on the light-lepton  $p_{\rm T}$  values in the online and offline selections. The first two columns give the numbers of electrons and muons in the event ( $N_{\rm e}$  and  $N_{\rm \mu}$ ). The third column lists the  $p_{\rm T}$  thresholds on the reconstructed electrons and muons in the online trigger selection, where the indices 1, 2, and 3 refer to the highest  $p_{\rm T}$ , second-highest  $p_{\rm T}$ , and third-highest  $p_{\rm T}$  lepton, respectively. The fourth column lists the offline event selection requirements applied in addition to the baseline requirements of  $p_{\rm T}(\ell_1) > 15\,{\rm GeV}$  and  $p_{\rm T}(\ell_{2,3}) > 10\,{\rm GeV}$ , where  $\ell$  refers to reconstructed leptons of any flavour. For the e $\mu$  trigger, the requirements are given for the highest and second-highest  $p_{\rm T}$  light lepton, referred to as  $l_1$  and  $l_2$  to indicate that a  $\tau_{\rm h}$  present in the event is not considered for the ordering. The values in parentheses give the thresholds applied in 2017 and 2018, where they are different from 2016. All events are required to pass the conditions of at least one of the rows.

While this removes HNL signal events with decays mediated by an on-shell Z boson, the SM Z boson background is overwhelming in this phase space and thus the loss of sensitivity incurred by this requirement is negligible. Finally, events with b jets are removed to suppress background contributions with top quarks.

Events are categorized by the flavour of the selected leptons. For events with only electrons and muons, this results in the four categories eee, ee $\mu$ , e $\mu\mu$ , and  $\mu\mu\mu$ . For events with exactly one  $\tau_h$ , we distinguish the three categories ee $\tau_h$ , e $\mu\tau_h$ , and  $\mu\mu\tau_h$ . We do not select events with more than one  $\tau_h$ , since the typically smaller signal efficiency, higher background contamination, and lower resolution of the  $\tau_h$  reconstruction compared with those for electrons and muons result in a low signal acceptance and a significant background yield for these events.

For HNL models with  $m_{\rm N}$  below the W boson mass  $m_{\rm W}=80.4\,{\rm GeV}$  [112], the HNL decay proceeds via a virtual W or Z boson, resulting in typically low- $p_{\rm T}$  leptons. In the case of  $m_{\rm N}>m_{\rm W}$ , the decay will first proceed to an on-shell W boson and a lepton, with a subsequent leptonic decay of the W boson, resulting in typically higher  $p_{\rm T}$  for at least one of the leptons. Similarly for  $m_{\rm N}>m_{\rm Z}$ , the decay via an on-shell Z boson also results in events with leptons of typically higher  $p_{\rm T}$ . Other kinematic properties of the final-state leptons will be significantly different as well for the cases of  $m_{\rm N}< m_{\rm W}$  ("low mass") and  $>m_{\rm W}$  ("high mass"). Thus, we define two orthogonal event selections to target the two separate mass ranges, by categorizing events with  $p_{\rm T}(\ell_1)<55\,{\rm GeV}$  as low-mass and  $>55\,{\rm GeV}$  as high-mass events.

In the low-mass selection, events are further required to have  $p_{\rm T}^{\rm miss} < 75\,{\rm GeV}$  to remove background contributions with SM neutrinos, such as  ${\rm t\bar{t}}$  and diboson production, and to

have a trilepton invariant mass  $m(3\ell) < 80 \,\text{GeV}$  to remove Z $\gamma$  photon conversion events. In the high-mass selection, the subleading lepton is required to have  $p_{\rm T}(\ell_2) > 15 \,\text{GeV}$  to reduce background contributions with nonprompt leptons, and events with an OSSF lepton pair and  $|m(3\ell) - m_{\rm Z}| < 15 \,\text{GeV}$  are removed to reduce Z $\gamma$  photon conversion backgrounds. To remove background contributions with charge-misidentified electrons, events in the high-mass selection with two same-sign electrons and a muon are required to have consistent results between three independent charge measurements [113] for the two electrons and to have a dielectron mass more than 15 GeV away from  $m_{\rm Z}$ . Although charge-misidentified electrons can also play a role in other final states, their contribution to the background is small in other flavour channels. Charge mismeasurement for muons is negligible [114, 115].

Following the strategy applied in ref. [46], we define a number of orthogonal search regions (SRs) by classifying the events according to several kinematic variables that provide a good discrimination between signal and background contributions, as summarized in table 2. Events are first sorted based on whether they have an OSSF lepton pair or not, since background processes with a Z boson contribute primarily to the OSSF events. In the low-mass region, the SRs are then defined in bins of  $p_{\rm T}(\ell_1)$  and the smallest invariant mass of any opposite-sign (OS) lepton pair,  $\min m(\ell^+\ell^-)$ . The SRs with  $p_{\rm T}(\ell_1) < 30\,{\rm GeV}$  target HNL scenarios where  $m_{\rm N}$  is close to  $m_{\rm W}$ , such that both the lepton from the HNL production and the leptons from the HNL decay have low  $p_{\rm T}$ . The SRs with  $30 < p_{\rm T}(\ell_1) < 55\,{\rm GeV}$ , on the other hand, target HNL scenarios with a smaller  $m_{\rm N}$ , such that the lepton from the HNL production can have a large  $p_{\rm T}$ . The min  $m(\ell^+\ell^-)$  variable is bounded to be smaller than  $m_{\rm N}$  for HNL signal events, and thus provides sensitivity to distinguish different HNL signal scenarios.

In the high-mass region, the SRs are defined in bins of  $\min m(\ell^+\ell^-)$ ,  $m(3\ell)$ , and the transverse mass  $m_{\rm T}$  calculated with  $\vec{p}_{\rm T}^{\rm miss}$  and the lepton not used for  $\min m(\ell^+\ell^-)$ , defined as  $m_{\rm T} = \sqrt{2p_{\rm T}^{\rm miss}} p_{\rm T}(\ell)(1-\cos\Delta\phi)$ , where  $\Delta\phi$  is the  $\phi$  angle between the lepton and  $\vec{p}_{\rm T}^{\rm miss}$ . The variable  $\min m(\ell^+\ell^-)$  again provides discriminating power between different HNL masses, whereas  $m_{\rm T}$  is targeted at the reconstruction of a resonance decaying into the third lepton and an SM neutrino that causes the  $\vec{p}_{\rm T}^{\rm miss}$  in the events. Although the HNL signal events have no such resonance and thus are distributed towards high  $m_{\rm T}$  values, SM background processes like WZ production with W  $\to \ell \nu$  decays will have a distribution of  $m_{\rm T}$  mostly below  $m_{\rm W}$ . Finally,  $m(3\ell)$  measures a lower bound on the energy of the s-channel resonance that produced the leptons in the event, with larger values as  $m_{\rm N}$  increases due to the large partonic centre-of-mass energy required to produce high-mass HNLs, and a distribution at lower values for the SM backgrounds that generally have a lower production threshold.

To further improve the separation of signal and background events, we employ machine learning classifiers based on boosted decision trees (BDTs) as implemented in the TMVA package [116]. The classifiers are trained to distinguish HNL signal events from background events taken from simulated samples for the Z+jets,  $t\bar{t}$ , and WZ background processes, using both selected and sideband events to also train against nonprompt-lepton background events. We train separate BDTs for different HNL coupling scenarios and  $m_N$  ranges, using different event selections and categories, and label these trainings as "BDT( $m_N$ ,  $\ell$ ,  $i\tau_h$ )". The first argument specifies one of the five  $m_N$  ranges (in GeV), where we use the low-mass (high-mass) selection for the ranges 10–40 and 50–75 GeV (85–150, 200–250, and 300–400 GeV). The

OSSF pair	$p_{\rm T}(\ell_1) $ (GeV)	$m(3\ell)$ (GeV)	$\min m(\ell^+\ell^-)$ (GeV)	$m_{ m T}$ (GeV)	SR name
	Low-mass selection				
No	< 30	< 80	<10	any	La1
			10 – 20		La2
			20 – 30		La3
			>30		La4
	30 – 55	< 80	<10	any	La5
			10-20	V	La6
			20-30		La7
			>30		La8
Yes	< 30	<80	<10	any	Lb1
105	<b>\30</b>	<b>\00</b>	10-20	any	Lb1
			20–30		Lb2
			>30		Lb3
	20 55	<b>~</b> 90			
	30 – 55	<80	<10	any	Lb5
			10–20		Lb6
			20–30		Lb7
			>30		Lb8
High- $m$			$mass\ selection$		
No	> 55	< 100	any	< 100	Ha1
				> 100	Ha2
		>100	< 100	<100	Ha3
				100 – 150	Ha4
				150 - 250	Ha5
				> 250	Ha6
			100-200	<100	Ha7
				>100	Ha8
			>200	any	Ha9
Yes	> 55	< 75	any	<100	Hb1
				100 - 200	Hb2
				>200	Hb3
		>105	< 100	<100	Hb4
		<i>&gt;</i> 100	(100	100-200	Hb5
				200-300	Hb6
				300-400	Hb7
				>400	Hb8
			100-200	<100	Hb9
			100 200	100-200	Hb10
				200–300	Hb11
				>300	Hb12
			>200	<100	Hb13
			/200	100-200	Hb14
				200–300	Hb15
				>300	Hb16
				/500	11010

**Table 2.** Definitions of the search regions (SRs) for events in the low-mass (upper part) and high-mass (lower part) selections.

second argument specifies the lepton flavour of the neutrino generation to which the HNL couples exclusively. The third argument specifies the event categories used in the training: for electron and muon neutrino couplings, the event categories without  $\tau_h$  are used, i.e. eee, ee $\mu$ , e $\mu\mu$ , and  $\mu\mu\mu$ , labelled as " $0\tau_h$ ". For tau neutrino couplings, separate trainings are performed for final states with no  $\tau_h$  at generator level, using the  $0\tau_h$  event categories, and for final states with at least one  $\tau_h$  at generator level, using the ee $\tau_h$ , e $\mu\tau_h$ , and  $\mu\mu\tau_h$  event categories, labelled as " $1\tau_h$ ".

The input variables to the BDTs are the kinematic properties of the reconstructed leptons; invariant and transverse masses of different dilepton and trilepton systems; the number of jets; kinematic properties of the reconstructed jets;  $\Delta R$  between different lepton and lepton-jet pairs;  $p_{\rm T}^{\rm miss}$ ; and the sum of the  $p_{\rm T}$  of all reconstructed jets (leptons), referred to as  $H_{\rm T}$  ( $L_{\rm T}$ ). Additional input variables to the BDTs trained with the low-mass selection are various  $\Delta \phi$  between  $\vec{p}_{\rm T}^{\rm miss}$  and leptons or jets. Furthermore, the BDTs trained with the low-mass selection in the  $0\tau_{\rm h}$  categories have the flavours and charges of the reconstructed electrons and muons as additional input variables. A selection of the most discriminating variables used in the different trainings is shown in figures 2–4. It can be seen that the different distributions provide sensitivity to distinguish between HNL signal and background distributions, but also show differences in the expected distributions for different  $m_{\rm N}$  values, which is the reason to train separate BDTs for different mass ranges. Generally good agreement is observed between data and background prediction.

The BDTs calculate event scores based on these input variables, and the score can be interpreted as a measure of how likely an event is to originate from the HNL signals used in the respective BDT training. The agreement between data and background prediction is validated for all BDT input variables and output scores in the control regions (CRs) defined in section 6, and good agreement is found.

For the final results, we combine the approaches based on SRs and BDTs. In the low-mass selection, the background events used in the BDT training predominantly have an OSSF lepton pair, whereas the SRs with no OSSF pair have only small background yields and no significant separation between signal and background contributions is provided by the BDTs for these events. Thus, we analyse together the BDT score distributions for the combined SRs with an OSSF pair (i.e. Lb1–8, as defined in table 2) and the yields in the SRs without an OSSF pair (i.e. La1–8). In the high-mass selection, good sensitivity to the HNL signal is provided by the BDT scores for  $m_{\rm N}$  up to 400 GeV for electron and muon neutrino couplings, whereas the low expected signal yields for larger  $m_{\rm N}$  or exclusive couplings to tau neutrinos result in a loss of sensitivity for the BDT approach. Consequentially, we use the BDT score distributions for the combined SRs Ha1–9 and Hb1–16 when targeting  $m_{\rm N}$  up to 400 GeV for electron or muon neutrino couplings, and the yields in these SRs otherwise.

### 6 Background estimation

Background contributions from SM processes are estimated with a combination of methods based on CRs in data and simulated event samples. We distinguish between background contributions where all three selected leptons are prompt and those that have at least one nonprompt lepton. For prompt-lepton backgrounds, we additionally treat processes separately

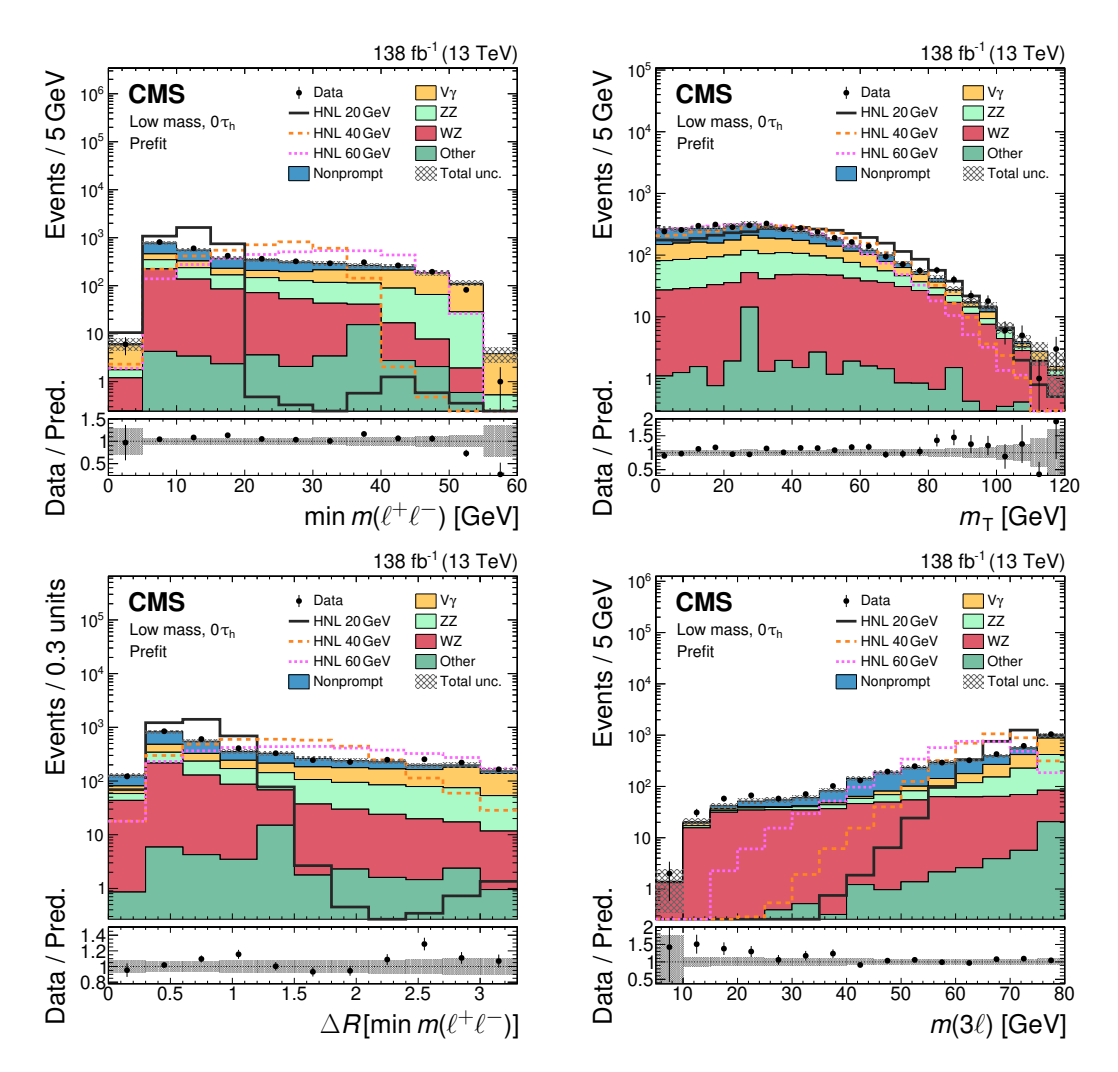


Figure 2. Comparison of observed (points) and predicted (coloured histograms) distributions in the low-mass selection for the  $0\tau_{\rm h}$  categories combined. Important input variables to the BDT training are shown:  $\min m(\ell^+\ell^-)$  (upper left),  $m_{\rm T}$  (upper right),  $\Delta R$  between the two leptons used for  $\min m(\ell^+\ell^-)$  ( $\Delta R[\min m(\ell^+\ell^-)]$ , lower left),  $m(3\ell)$  (lower right). The predicted background yields are shown before the fit to the data ("prefit"). The HNL predictions for three different  $m_{\rm N}$  values with exclusive coupling to tau neutrinos are shown with coloured lines, and are normalized to the total background yield. The vertical bars on the points represent the statistical uncertainties in the data, and the hatched bands the total uncertainties in the predictions. The last bins include the overflow contributions. In the lower panels, the ratios of the event yield in data to the overall sum of the predictions are shown.

that have a charge-misidentified electron (referred to as "charge misID") or at least one lepton originating from the conversion of a prompt photon produced at the interaction point. Prompt-lepton backgrounds are estimated from the simulated event samples discussed in section 3, and are dominated by WZ and ZZ diboson production, where the latter includes resonant contributions from  $H \to ZZ$  production. All other prompt-lepton background contributions, of which the largest is from associated top quark and triboson production, are grouped together with charge-misID contributions as "Other" in the figures.

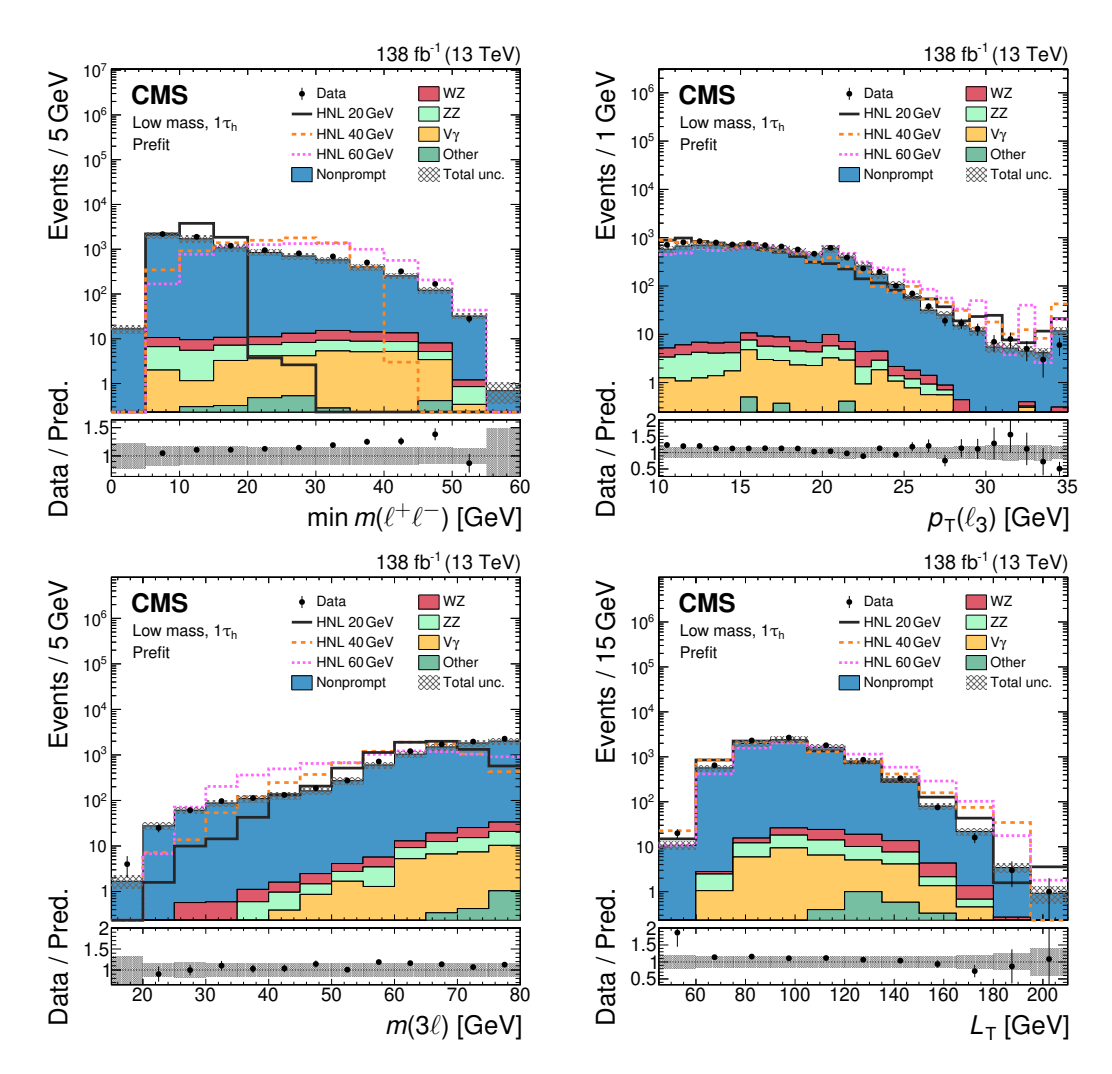


Figure 3. Comparison of observed (points) and predicted (coloured histograms) distributions in the low-mass selection for the  $1\tau_h$  categories combined. Important input variables to the BDT training are shown:  $\min m(\ell^+\ell^-)$  (upper left),  $p_T(\ell_3)$  (upper right),  $m(3\ell)$  (lower left),  $L_T$  (lower right). The predicted background yields are shown before the fit to the data ("prefit"). The HNL predictions for three different  $m_N$  values with exclusive coupling to tau neutrinos are shown with coloured lines, and are normalized to the total background yield. The vertical bars on the points represent the statistical uncertainties in the data, and the hatched bands the total uncertainties in the predictions. The last bins include the overflow contributions. In the lower panels, the ratios of the event yield in data to the overall sum of the predictions are shown.

To validate the modelling of the dominant diboson background contributions in the simulated event samples, we define three CRs that are orthogonal to the SRs by the requirement of an OSSF lepton pair consistent with  $m_{\rm Z}$ . These CRs target WZ and ZZ production, as well as Z $\gamma$  production with photon conversion. The total yield predicted by the SM backgrounds is compared with the observed data yield, and a correction factor is derived where necessary. Additionally, the distributions for several observables relevant in the SR definitions and the BDTs are compared to ensure that these background contributions are well modelled, and to derive uncertainties in the background normalizations.

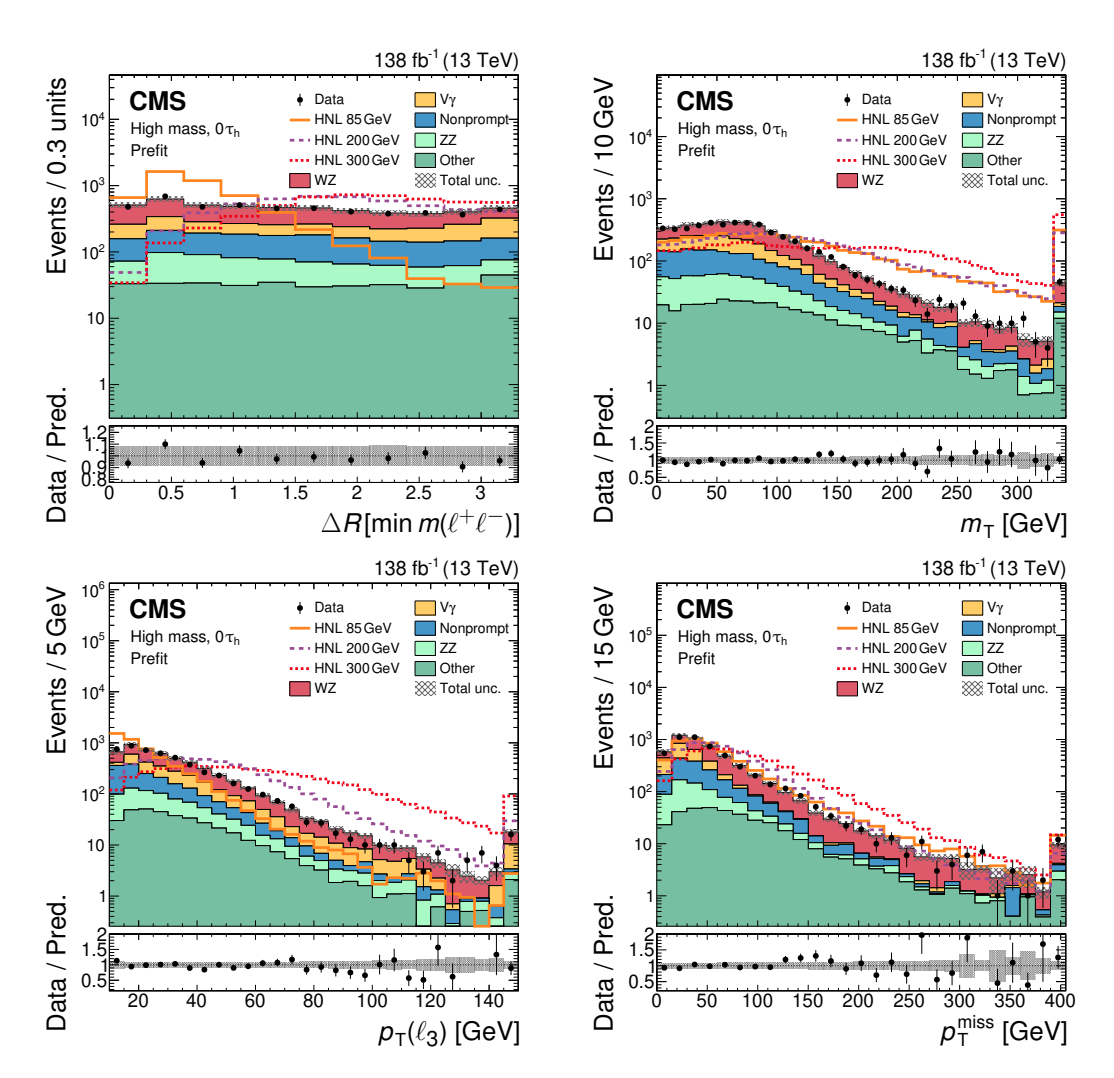


Figure 4. Comparison of observed (points) and predicted (coloured histograms) distributions in the high-mass selection for the  $0\tau_h$  categories combined. Important input variables to the BDT training are shown:  $\Delta R[\min m(\ell^+\ell^-)]$  (upper left),  $m_T$  (upper right),  $p_T(\ell_3)$  (lower left),  $p_T^{miss}$  (lower right). The predicted background yields are shown before the fit to the data ("prefit"). The HNL predictions for three different  $m_N$  values with exclusive coupling to tau neutrinos are shown with coloured lines, and are normalized to the total background yield. The vertical bars on the points represent the statistical uncertainties in the data, and the hatched bands the total uncertainties in the predictions. The last bins include the overflow contributions. In the lower panels, the ratios of the event yield in data to the overall sum of the predictions are shown.

The WZ CR is defined by selecting events with exactly three tight light leptons with  $p_{\rm T}(\ell_1) > 25\,{\rm GeV}$  and  $p_{\rm T}(\ell_2) > 15\,{\rm GeV}$ , where two leptons form an OSSF pair with  $|m(\ell^+\ell^-) - m_{\rm Z}| < 15\,{\rm GeV}$ . Events with b jets are excluded to reduce contributions from associated top quark production,  $p_{\rm T}^{\rm miss} > 50\,{\rm GeV}$  is required to account for the SM neutrino from the W boson decay, and the requirement of  $|m(3\ell) - m_{\rm Z}| > 15\,{\rm GeV}$  removes contributions with photon conversions. More than 80% of the events in the CR originate from WZ production. Signal contributions to this CR are negligible, with predicted yields of signal processes not excluded by ref. [46] less than 0.5% of the total background yield for all mass points in this

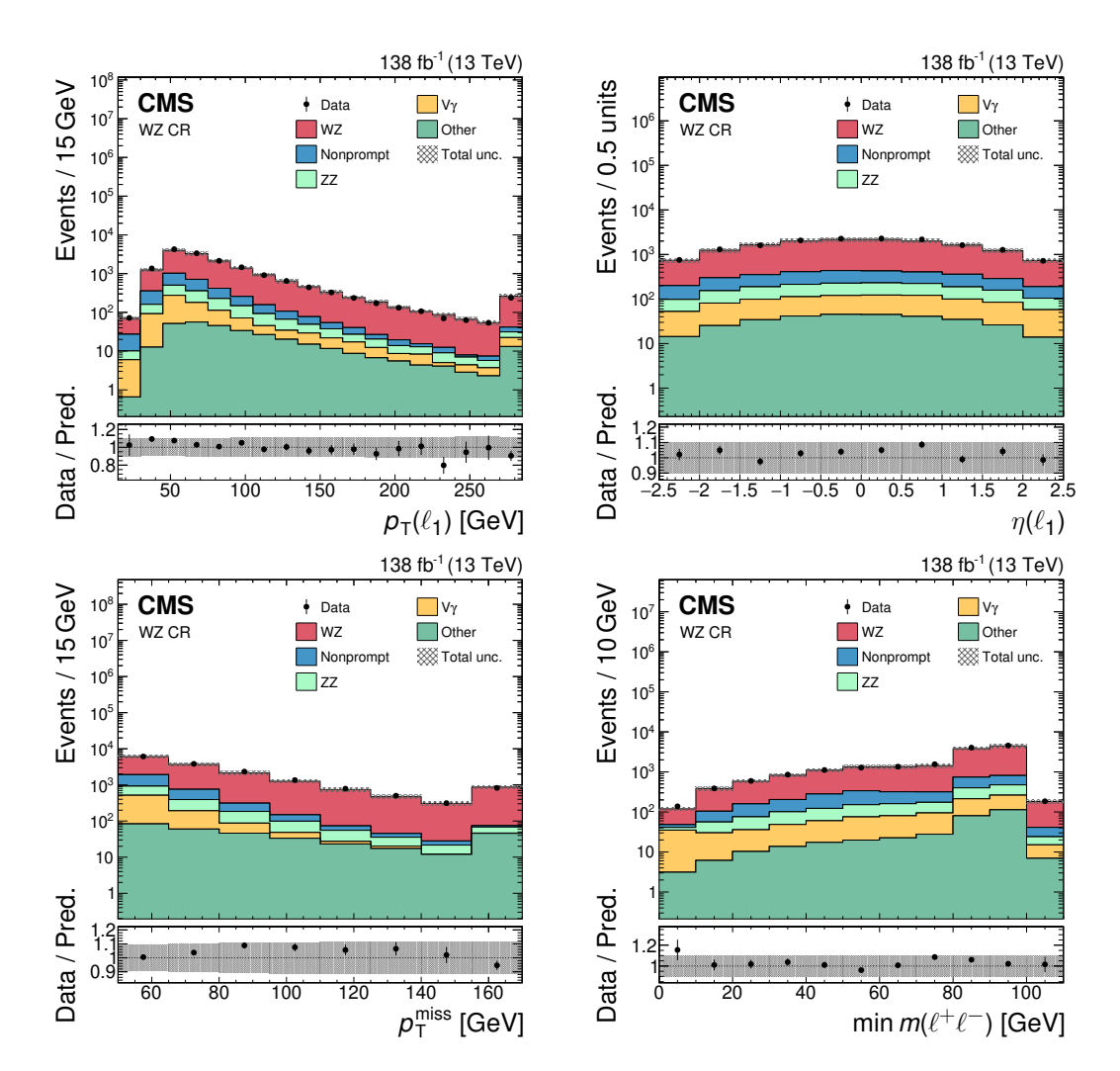


Figure 5. Comparison of observed (points) and predicted (coloured histograms) distributions in the WZ CR. The leading lepton  $p_{\rm T}$  (upper left) and  $\eta$  (upper right), as well as  $p_{\rm T}^{\rm miss}$  (lower left) and min  $m(\ell^+\ell^-)$  (lower right) are shown. The vertical bars on the points represent the statistical uncertainties in the data, and the hatched bands the total uncertainties in the predictions. The last bins include the overflow contributions. In the lower panels, the ratios of the event yield in data to the overall sum of the predictions are shown.

analysis. The total yields observed in the data agree with the prediction. The comparison of the distributions for several observables in figure 5 demonstrates good agreement as well, with deviations smaller than 10% in most bins.

The ZZ CR is defined by selecting events with exactly four tight light leptons with  $p_{\rm T}(\ell_1) > 15\,{\rm GeV}$ , where the four leptons form two OSSF pairs with  $|m(\ell^+\ell^-) - m_{\rm Z}| < 15\,{\rm GeV}$  each. In the case of four leptons of the same flavour, the pairs are chosen such that the sum of the mass differences with respect to  $m_{\rm Z}$  is minimized. The OSSF pair with the invariant mass further away from  $m_{\rm Z}$  is labelled "Z<sub>2</sub>". Events with b jets are removed to reduce contributions from associated top quark production, and  $m(\ell^+\ell^-) > 12\,{\rm GeV}$  is required for every OS lepton pair to remove contributions from low-mass resonances. Contributions from background processes other than ZZ production or from signal contamination are negligible

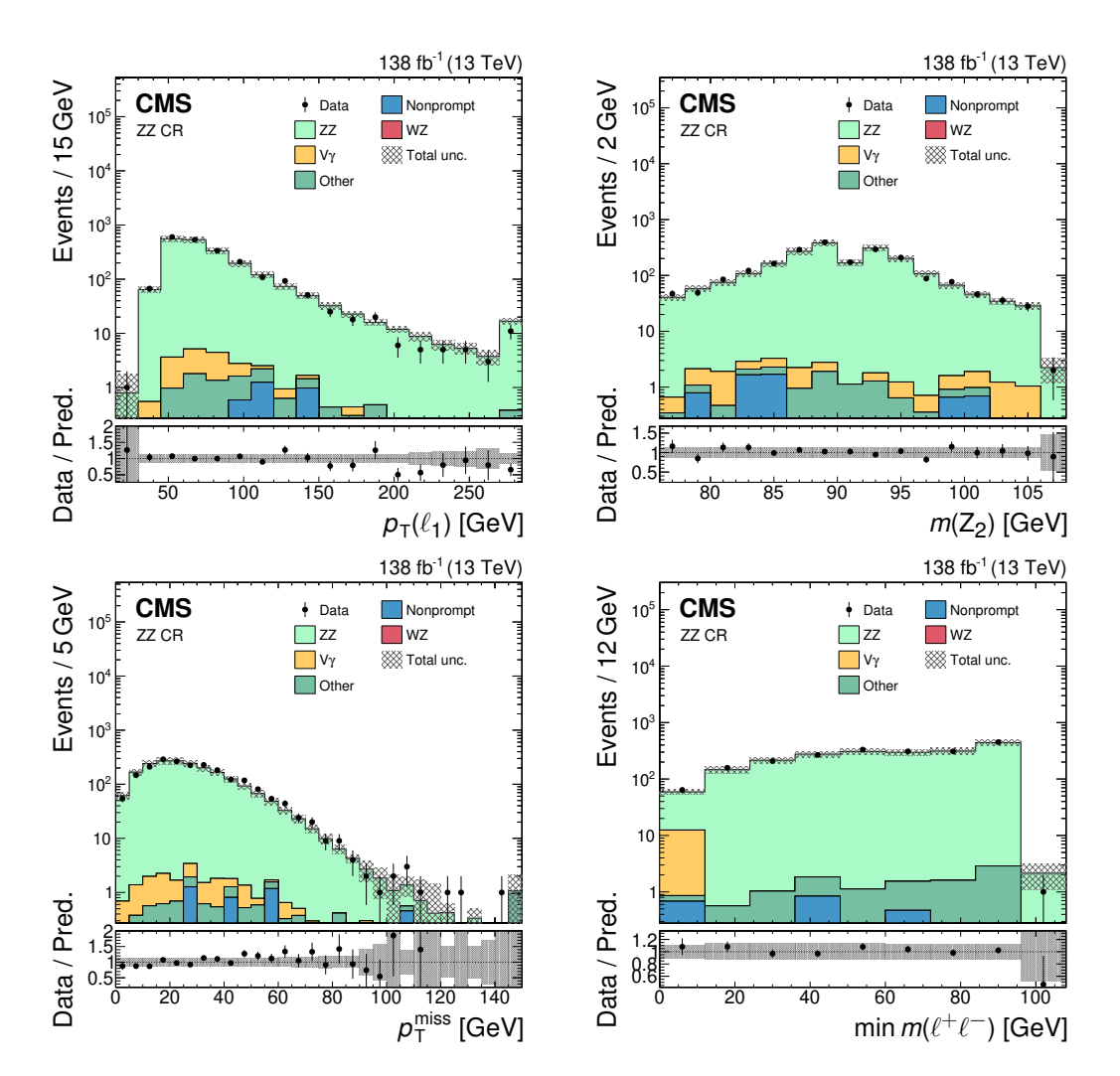


Figure 6. Comparison of observed (points) and predicted (coloured histograms) distributions in the ZZ CR. The leading lepton  $p_{\rm T}$  (upper left),  $m(\ell^+\ell^-)$  of  $Z_2$  ( $m(Z_2)$ , upper right),  $p_{\rm T}^{\rm miss}$  (lower left), and  $\min m(\ell^+\ell^-)$  (lower right) are shown. The ZZ prediction is scaled with a normalization factor of 1.12, as discussed in the text. The vertical bars on the points represent the statistical uncertainties in the data, and the hatched bands the total uncertainties in the predictions. The last bins include the overflow contributions. In the lower panels, the ratios of the event yield in data to the overall sum of the predictions are shown.

in this CR. We find the observed yields to be larger than the prediction, and assign a scale factor of 1.12 to the simulated ZZ samples to correct for the difference in the total yield. After applying the scale factor, good agreement between the prediction and the observation is found across several observables, some of which are shown in figure 6. Except for a few bins with lower statistical precision, the agreement is generally better than 10%.

Background contributions from processes with photon conversions are also estimated from simulated samples. The main photon conversion background arises from  $Z\gamma$  production, where the photon undergoes an asymmetric conversion into two leptons of which one has very low  $p_T$  and is not reconstructed. For the  $Z\gamma$  CR, events with exactly three tight light leptons with  $p_T(\ell_1) > 15\,\text{GeV}$  are selected. To select  $Z\gamma$  events where the photon is radiated from

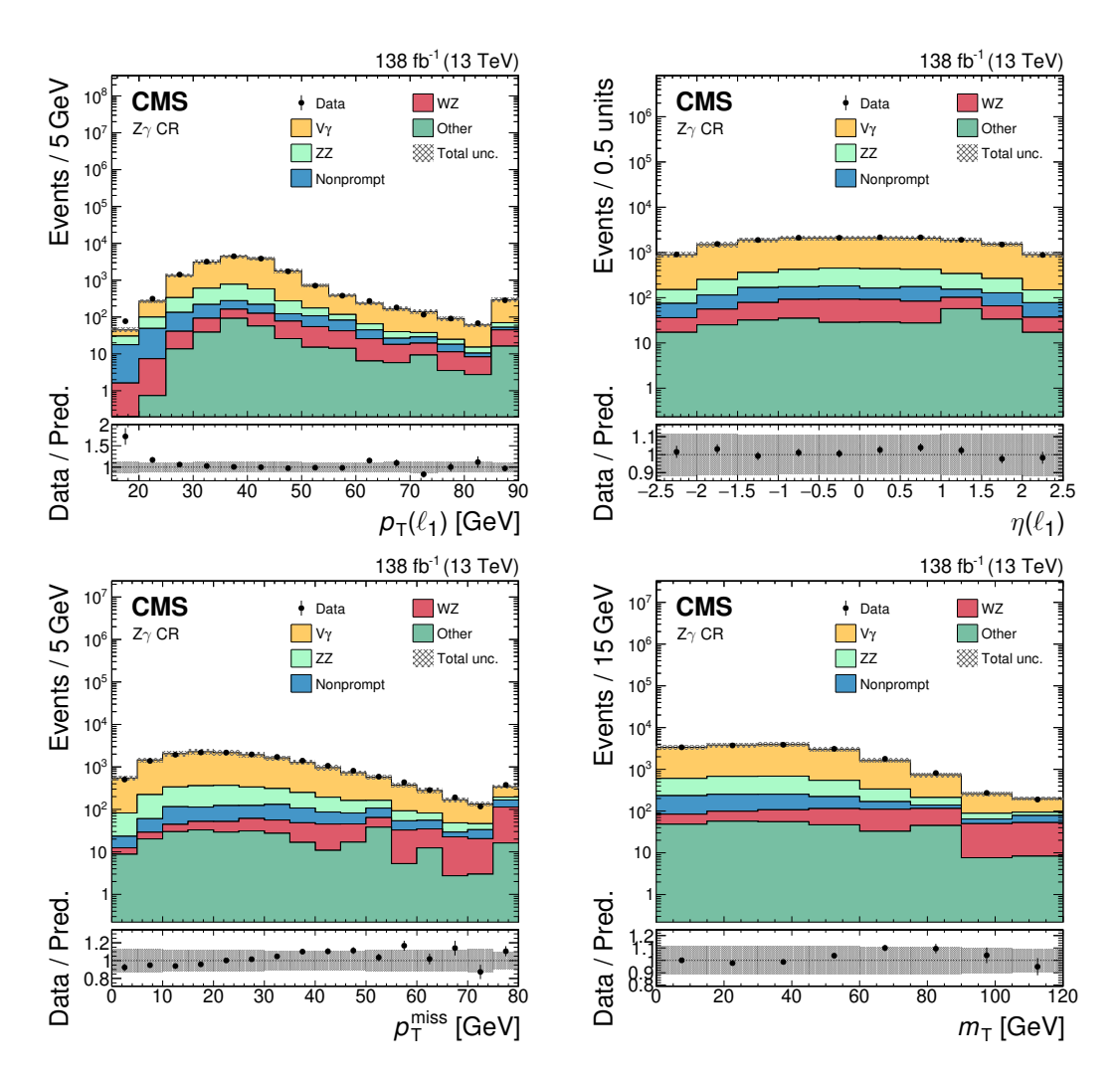


Figure 7. Comparison of observed (points) and predicted (coloured histograms) distributions in the  $Z\gamma$  CR. The leading lepton  $p_T$  (upper left) and  $\eta$  (upper right),  $p_T^{miss}$  (lower left), and  $m_T$  (lower right) are shown. The  $Z\gamma$  prediction is scaled with a normalization factor of 1.11, as discussed in the text. The vertical bars on the points represent the statistical uncertainties in the data, and the hatched bands the total uncertainties in the predictions. The last bins include the overflow contributions. In the lower panels, the ratios of the event yield in data to the overall sum of the predictions are shown.

one of the leptons from the Z boson decay but at the same time remove contributions from Z+jets and WZ production, we require  $|m(3\ell) - m_Z| < 10 \,\text{GeV}$ , as well as that two leptons form an OSSF pair with  $|m(\ell^+\ell^-) - m_Z| > 15 \,\text{GeV}$ . Events with b jets are removed. In this CR, about 70% of the events originate from photon conversions. Expected signal yields for processes not excluded by ref. [46] are below 0.5% of the total yield. To correct for differences in the total yield between data and prediction, we apply a scale factor of 1.11 to simulated  $Z\gamma$  samples. Figure 7 shows the data and predicted distributions for several observables, with the scale factor applied, and exhibits agreement that is typically better than 10%.

Simulated event samples are used to predict background contributions with charge-misID electrons. The misID rate in simulation depends strongly on the material included in the detector model, and is validated by dedicated measurements in data by comparing event yields

with same- and opposite-sign electron pairs [102]. It is found that the misidentification rate is overestimated (underestimated) in 2016 (2017–2018) samples by about 10 (50)%, and we apply correction factors to the normalization of the charge-misID background correspondingly.

Nonprompt-lepton background contributions arise mostly from  $t\bar{t}$  and Z+jets production with an additional nonprompt lepton. They are especially relevant in the  $1\tau_h$  categories. A "tight-to-loose" ratio method [105, 117, 118] is applied to estimate the nonprompt-lepton background contributions from control samples in data. The tight-to-loose ratio is defined as the probability f for a loose lepton to also satisfy the tight ID selection. It is evaluated separately for the different lepton flavours, and is measured as a function of  $p_T$  and  $|\eta|$ . For electrons and muons, f is measured in a sample enriched in SM events composed uniquely of jets produced through the strong interaction selected with nonisolated single-lepton triggers. For  $\tau_h$ , f is measured in samples enriched in Z+jets and  $t\bar{t}$  events. The measured values of f are applied as weights to events that pass the SR selection but have one or more leptons that pass the loose and fail the tight selection. Both simulated events and data samples enriched in nonprompt leptons are used to validate the tight-to-loose ratio method for all lepton flavours. Good agreement of better than 30% is found in these tests in the most relevant kinematic distributions, with larger deviations up to 50% only for nonprompt electrons with  $p_T > 55\,\text{GeV}$ .

### 7 Systematic uncertainties

Multiple sources of systematic uncertainty affect the signal prediction, the background event yields, and the distributions of the observables used for the signal extraction. The sources and their correlations between the data-taking years are described below, and their impact on the fits described in section 9 is summarized in table 3.

The integrated luminosities for the three data-taking years have individual uncertainties between 1.2 and 2.5% [119–121], and the overall uncertainty for the 2016–2018 period is 1.6%. This uncertainty affects the normalization of the background contributions from simulated event samples, as well as the extraction of cross section limits from the final estimate of the limit on the number of signal events.

The distribution of the number of additional pp interactions per event in simulation is matched to data by reweighting the profile of the true number of interactions to the one inferred from the instantaneous luminosity profile in data. The systematic uncertainty is estimated from a variation of the total inelastic cross section used for this reweighting by  $\pm 4.6\%$ , which is treated as correlated among the data-taking years.

The trigger selection efficiency is measured in data with independent trigger paths based on hadronic activity and  $p_{\rm T}^{\rm miss}$  signatures, and agrees with the efficiency estimated in simulation within 3%. Thus, no correction is applied to the simulated event samples and a systematic uncertainty of 3% is assigned that is correlated between the data-taking years. Additionally, the statistical uncertainty in the measured trigger efficiencies in data is considered, separately for each data-taking year.

During the 2016 and 2017 data-taking periods, a gradual shift in the timing of the inputs of the ECAL level-1 trigger in the region  $|\eta| > 2.0$  caused a specific trigger inefficiency [60]. For events containing an electron (a jet) with  $p_T > 50$  (100) GeV in the region  $2.5 < |\eta| < 3.0$ 

Uncertainty source		$m_{\rm N} = 40{\rm GeV}$			$m_{\mathrm{N}} = 200\mathrm{GeV}$		
		μ	τ	e	μ	τ	
Luminosity, pileup reweighting	5.0%	2.6%	11.3%	5.8%	7.6%	4.4%	
Trigger efficiency	2.4%	10.6%	26.4%	2.9%	6.9%	5.1%	
Light-lepton selection efficiency $\&$ energy calibration	8.7%	15.5%	7.9%	10.4%	18.3%	1.2%	
$\tau_{\rm h}$ selection efficiency			2.7%		_	14.2%	
Jet energy calibration, $p_{\mathrm{T}}^{\mathrm{miss}}$ , b tagging efficiency	10.6%	8.4%	34.4%	8.6%	12.4%	24.0%	
WZ background normalization	1.1%	9.6%	7.4%	2.8%	5.4%	4.0%	
ZZ background normalization	3.9%	9.9%	8.0%	4.1%	6.1%	6.5%	
$\mathrm{Z}\gamma$ background normalization	7.4%	8.3%	5.1%	1.9%	1.5%	12.1%	
Other background normalization	1.4%	5.6%	1.6%	13.8%	6.3%	10.5%	
Nonprompt light-lepton background	10.8%	16.0%	20.9%	15.6%	26.4%	9.1%	
Nonprompt $\tau_{\rm h}$ background	_	_	14.3%	_		66.7%	
HNL cross section prediction	4.7%	3.5%	3.8%	3.7%	3.0%	2.1%	
Total systematic	23.3%	25.5%	55.1%	27.7%	35.8%	75.5%	
Statistical	96.8%	96.5%	83.4%	96.1%	93.3%	65.5%	

**Table 3.** Relative impacts of the uncertainty sources in fits for six different fit models specified with  $m_{\rm N}$  value and coupling scenario, where the relative impact is defined as the ratio between the uncertainty from the respective source and the total uncertainty in the HNL signal strength. The symbol "—" indicates that the corresponding uncertainty source is not applicable.

the efficiency loss is  $\approx 10$ –20%, depending on  $p_{\rm T}$ ,  $\eta$ , and time. Correction factors are derived from data and applied to the acceptance evaluated by simulation, and the impact on our results is small.

The efficiency of the tight ID selection of light leptons is measured in data and simulation using a "tag-and-probe" method applied to  $Z \to \ell^+\ell^-$  events [122]. Per-lepton corrections are derived separately for electrons, muons, and  $\tau_h$ . Statistical and systematic uncertainties in the correction factors are included, with the former (latter) treated as uncorrelated (correlated) between the data-taking years. Corrections for the differences in the electron energy scale and resolution between data and simulation are derived from  $Z \to ee$  events using only ECAL information [98], and systematic uncertainties are considered that are correlated between the data-taking years.

Uncertainties in the jet energy scale and resolution are evaluated from the  $p_{\rm T}$  variations of the reconstructed jets in simulated events [66]. The variation due to the jet energy scale, as well as an additional variation to account for the uncertainty in the contribution from unclustered PF particles [68], is propagated to  $p_{\rm T}^{\rm miss}$ . The jet energy scale (jet energy resolution and unclustered energy) variation is treated as correlated (uncorrelated) between the data-taking years. Differences in the b tagging efficiency between data and simulation are corrected by applying scale factors to simulated events. Uncertainties in the scale factors are evaluated by separate variations for light- and heavy-flavour jets, where both correlated and uncorrelated variations between the three data-taking years are considered [69].

Several uncertainties are considered for the normalization of the background processes. For the dominant WZ, ZZ, and Zγ contributions, we assign an uncertainty of 10% each, corresponding to the level of agreement in the CRs described in section 6. The SM predictions for triboson production have a precision of about 10% [123–127], which is assigned as a normalization uncertainty to the triboson background. For associated top quark production, a normalization uncertainty of 10% is assigned, matching the experimental precision of the latest CMS measurements of the most important contributions [108, 118]. The uncertainty in the charge-misID contribution originates from the correction factors and is taken to be 15% [102]. For all remaining contributions in the "Other" category, we assign a normalization uncertainty of 20% corresponding to the experimental precision in the signal strength of H production in association with a vector boson [128].

The uncertainties in the nonprompt background contributions stem from the tight-to-loose ratio method. For nonprompt light leptons, a normalization uncertainty of 30% is applied when the leading nonprompt lepton is a muon, and a  $p_{\rm T}$ -dependent uncertainty when it is an electron. In the latter case, the uncertainty is 15% for  $p_{\rm T} < 35\,{\rm GeV}$  of the electron, 30% for 35  $< p_{\rm T} < 55\,{\rm GeV}$ , and 50% for  $p_{\rm T} > 55\,{\rm GeV}$ . In the case of nonprompt  $\tau_{\rm h}$  leptons, a normalization uncertainty of 30% is assigned to account for observed differences in the validation, separately for events with and without an OSSF lepton pair because of the different composition of sources of nonprompt  $\tau_{\rm h}$  leptons in these two event selections.

The HNL signal samples for  $m_{\rm N} < m_{\rm W}$  are simulated at LO accuracy, and their normalization is scaled with the ratio between the SM cross sections of W boson production evaluated at next-to-NLO with the FEWZ v3.1 program [129–132] and at LO with MAD-GRAPH5\_amc@nlo, using settings identical to those of the signal samples. The uncertainty in the signal cross section is then evaluated from the variations of the renormalization and factorization scale and of the PDFs in the next-to-NLO calculation and amounts to 4% in total [50]. For the HNL signal samples with  $m_{\rm N} > m_{\rm W}$ , the simulation is done at NLO accuracy, and no additional scale factor is applied. From the evaluation of scale variations and the PDF choice, we find a signal cross section uncertainty of 3 (15)% for the DY (VBF) production mode.

# 8 Results

The statistical analysis is performed with the CMS tool COMBINE [133], which is based on the RooFit [134] and RooStats [135] frameworks. For each HNL signal scenario, a binned likelihood function  $L(r,\theta)$  is constructed from the product of Poisson probabilities to obtain the observed yields in the relevant distributions, given the HNL signal prediction scaled with a signal strength r and the SM background estimates. Additional terms are included to account for the systematic uncertainty sources, where  $\theta$  denotes the full set of corresponding nuisance parameters [136]. Statistical uncertainties in the predicted yields are implemented through a single nuisance parameter in each bin for all processes [137, 138]. We consider the cases of exclusive HNL couplings to electron, muon, and tau neutrinos separately, and use different distributions to construct L depending on the coupling scenario and  $m_N$ , as listed in table 4. To obtain background-only fits, the maximum likelihood estimator of  $\theta$  with a fixed r=0 is evaluated for specific fit setups. In figure 8, the number of observed events in data is compared with the background predictions in the SRs, separately combined

for the  $0\tau_h$  and  $1\tau_h$  categories, after simultaneous background-only fits to the SRs of all flavour channels. Furthermore, the distributions of the BDT output scores are compared between data and prediction in figures 9–11, after the background-only fits corresponding to the fit setups in table 4 where the corresponding BDT is used. In all figures, the signal prediction for several HNL mass points is shown as well, with  $|V_{\ell N}|^2$  values chosen such that the predicted signal yield matches roughly the total background yield.

The number of observed events in data is in good agreement with the SM background expectations within the statistical and systematic uncertainties. No significant excess is found for any final state or in any SR.

# 9 Interpretation

To derive exclusion limits at 95% confidence level (CL) on HNL signal scenarios, we apply the modified frequentist  $CL_s$  approach [136, 139–141]. Distributions of the LHC test statistic [136], based on the profile likelihood method, are evaluated in the asymptotic approximation [141] and used to calculate the  $CL_s$  value [139, 140]. We exclude a signal scenario if the signal strength of r=1 is excluded at 95% CL or greater.

The limits are obtained under the assumption of a Majorana or a Dirac HNL, and are evaluated at a grid of points in the  $(m_{\rm N}, |V_{\ell \rm N}|^2)$  parameter space. For electron and muon neutrino couplings, masses of up to 1.5 TeV are considered, whereas tau neutrino couplings are evaluated only up to 1 TeV since the exclusion limit passes above  $|V_{\tau \rm N}|^2=1$  already at this mass point. The results are shown in figure 12. The obtained limits are connected with straight lines between neighbouring mass points for which the same fit distributions are used. For  $m_{\rm N}$  values at which the fit distributions change, the limits are evaluated for both strategies and shown separately. Since the BDTs are trained with nonoverlapping mass ranges, the sensitivity is generally different for two strategies evaluated at the same  $m_{\rm N}$  value, and we thus obtain disjoint limit curves for several of these mass points. The expected and observed exclusion limits generally agree within one standard deviation, with a few exceptions discussed in the following.

For exclusive couplings to electron neutrinos and  $m_{\rm N} < m_{\rm W}$ , we exclude  $|V_{\rm eN}|^2$  values for Majorana (Dirac) HNL of  $4.8\times 10^{-6}$  ( $2.23\times 10^{-5}$ ) at a mass of 20 GeV, of  $1.5\times 10^{-5}$  ( $3.3\times 10^{-5}$ ) at 60 GeV, and of  $3.3\times 10^{-4}$  ( $9.6\times 10^{-4}$ ) at 75 GeV, which is the highest simulated mass point below  $m_{\rm W}$ . For masses below 30 GeV, the HNLs become long-lived and have a reduced selection efficiency, with, e.g., 16 times fewer events selected at  $m_{\rm N}=10$  GeV and  $|V_{\rm eN}|^2=10^{-5}$  compared with a prompt HNL of the same mass, resulting in less stringent limits. In the high-mass selection, we exclude  $|V_{\rm eN}|^2$  values for Majorana (Dirac) HNL of  $1.2\times 10^{-3}$  ( $1.5\times 10^{-3}$ ) at 85 GeV, which is the lightest simulated mass point above  $m_{\rm W}$ , of  $8.8\times 10^{-4}$  ( $1.3\times 10^{-3}$ ) at 100 GeV, and of  $7.8\times 10^{-2}$  ( $8.2\times 10^{-2}$ ) at 600 GeV. The most notable discrepancies between observed and expected limits are for HNL masses between 250 and 400 GeV (125 and 250 GeV) in the case of a Majorana (Dirac) HNL, caused by a small excess (deficit) in the last bin of the corresponding BDT score distribution. Similarly a discrepancy is observed at HNL masses below 40 GeV in case of a Dirac HNL. This is due to a small excess in the relevant BDT distribution, which leads the sensitivity in the Dirac requirement of an OSSF electron pair in the final selection. Compared with the results of the previous prompt

HNL model	Selection	Categories	OSSF	Fitted distributions
(10-40GeV,e)	low mass	$0\tau_{\rm h}$	no	La1-8
		$0\tau_{\rm h}$	yes	$BDT(1040,e,0\tau_h)$
$(4075\mathrm{GeV},\mathrm{e})$	low mass	$0\tau_{\rm h}$	no	La1-8
		$0\tau_{\rm h}$	yes	$\mathrm{BDT}(5075,\mathrm{e},0\tau_\mathrm{h})$
(85-125GeV,e)	high mass	$0\tau_{\rm h}$	any	$BDT(85150,e,0\tau_h)$
$(125-250{\rm GeV},{\rm e})$	high mass	$0\tau_{\rm h}$	any	$BDT(200250,e,0\tau_h)$
$(250-400{\rm GeV},{\rm e})$	high mass	$0\tau_{\rm h}$	any	$BDT(300400,e,0\tau_h)$
$(\geq 400\mathrm{GeV},\mathrm{e})$	high mass	$0\tau_{\rm h}$	any	Ha1-9, Hb1-16
$(1040\text{GeV},\mu)$	low mass	$0\tau_{\rm h}$	no	La1-8
		$0\tau_{\rm h}$	yes	$BDT(1040,\mu,0\tau_h)$
$(4075\mathrm{GeV},\mu)$	low mass	$0\tau_{\rm h}$	no	La1-8
		$0\tau_{\rm h}$	yes	$\mathrm{BDT}(5075,\mu,0\tau_h)$
$(85125\mathrm{GeV},\mu)$	high mass	$0\tau_{\rm h}$	any	$BDT(85150,\mu,0\tau_h)$
$(125200\mathrm{GeV},\mu)$	high mass	$0\tau_{\rm h}$	any	$\mathrm{BDT}(200250,\mu,0\tau_h)$
$(200400\mathrm{GeV},\mu)$	high mass	$0\tau_{\rm h}$	any	$\mathrm{BDT}(300400,\mu,0\tau_h)$
$({\geq}400{\rm GeV},\mu)$	high mass	$0  au_{ m h}$	any	Ha1-9, Hb1-16
$(1040\text{GeV},\tau)$	low mass	$0\tau_{\rm h}$	no	La1-8
		$0\tau_{\rm h}$	yes	$BDT(1040,\tau,0\tau_h)$
		$1\tau_{\rm h}$	no	La1-8
		$1 au_{ m h}$	yes	$BDT(1040,\tau,1\tau_h)$
$(4075\mathrm{GeV},\tau)$	low mass	$0\tau_{\rm h}$	no	La1-8
		$0\tau_{\rm h}$	yes	$BDT(5075,\tau,0\tau_h)$
		$1 au_{ m h}$	no	La1-8
		$1 au_{ m h}$	yes	$BDT(50-75, \tau, 1\tau_h)$
$({\ge}85{\rm GeV},\tau)$	high mass	all	any	Ha1-9, Hb1-16

**Table 4.** Summary of the selections, categories, and distributions used in the maximum likelihood fits for the HNL signal points.

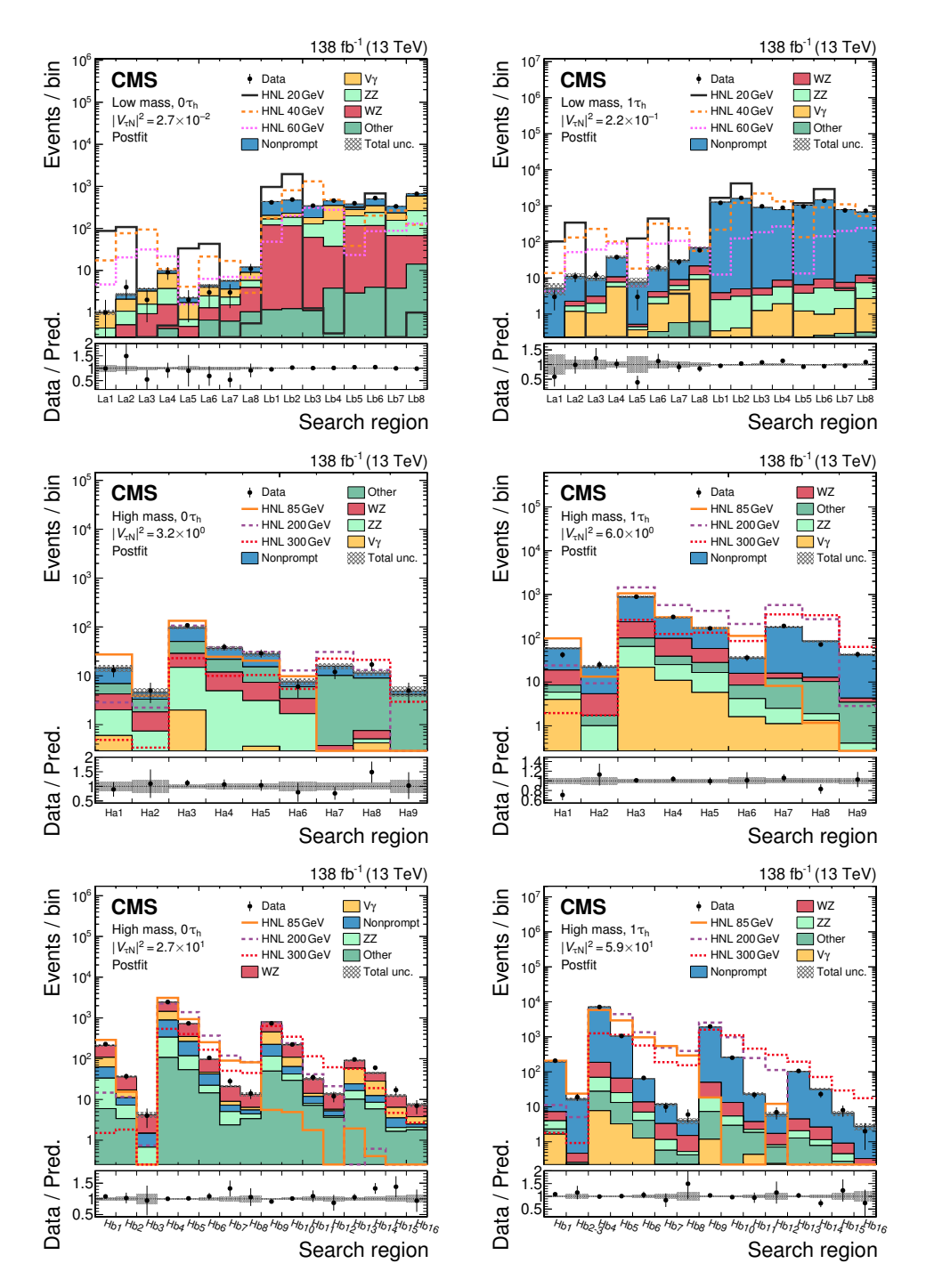


Figure 8. Comparison of the number of observed (points) and predicted (coloured histograms) events in the SR bins, shown for the  $0\tau_h$  (left column) and  $1\tau_h$  (right column) categories combined. The La1–8 and Lb1–8 (upper row), Ha1–Ha9 (middle row), and Hb1–16 (lower row) are displayed. The predicted background yields are shown with the values of the normalizations and nuisance parameters obtained in background-only fits applied ("postfit"). The HNL predictions for three different  $m_N$  values with exclusive coupling to tau neutrinos are shown with coloured lines. The vertical bars on the points represent the statistical uncertainties in the data, and the hatched bands the total uncertainties in the background predictions as obtained from the fits. In the lower panels, the ratios of the event yield in data to the overall sum of the background predictions are shown.

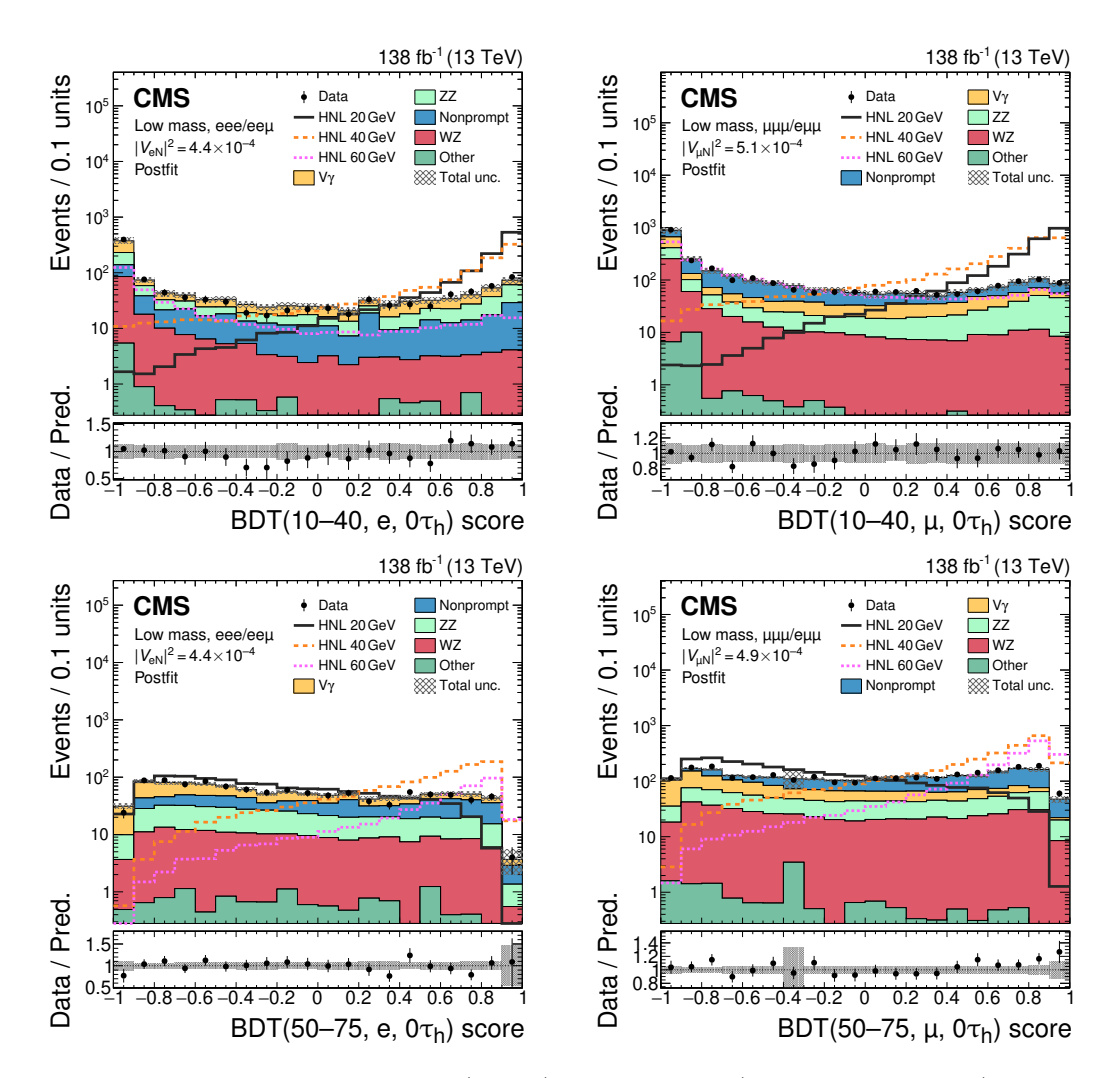


Figure 9. Comparison of the observed (points) and predicted (coloured histograms) BDT output distributions of the low-mass selection, shown for the eee and eeμ channels combined (left column) and the eμμ and μμμ channels combined (right column). The output scores BDT(10–40, e,  $0\tau_h$ ) (upper left), BDT(10–40, μ,  $0\tau_h$ ) (upper right), BDT(50–75, e,  $0\tau_h$ ) (lower left), and BDT(50–75, μ,  $0\tau_h$ ) (lower right) are displayed. The predicted background yields are shown with the values of the normalizations and nuisance parameters obtained in background-only fits applied ("postfit"). The HNL predictions for three different  $m_N$  values with exclusive coupling to electron (left column) or muon (right column) neutrinos are shown with coloured lines. The vertical bars on the points represent the statistical uncertainties in the data, and the hatched bands the total uncertainties in the background predictions as obtained from the fits. In the lower panels, the ratios of the event yield in data to the overall sum of the background predictions are shown.

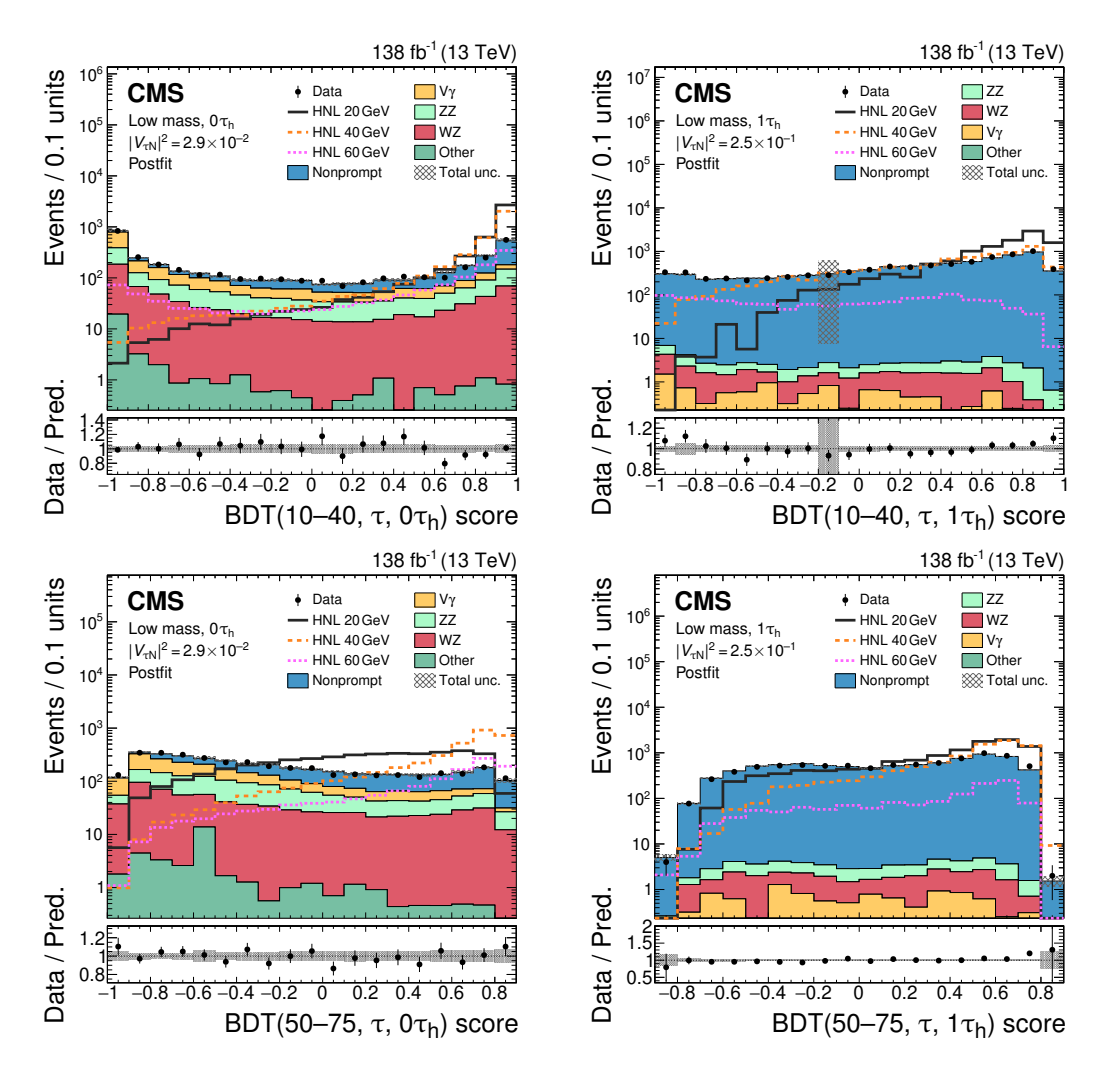


Figure 10. Comparison of the observed (points) and predicted (coloured histograms) BDT output distributions of the low-mass selection, shown for the  $0\tau_h$  channels combined (left column) and the  $1\tau_h$  channels combined (right column). The output scores BDT(10–40,  $\tau$ ,  $0\tau_h$ ) (upper left), BDT(10–40,  $\tau$ ,  $1\tau_h$ ) (upper right), BDT(50–75,  $\tau$ ,  $0\tau_h$ ) (lower left), and BDT(50–75,  $\tau$ ,  $0\tau_h$ ) (lower right) are displayed. The predicted background yields are shown with the values of the normalizations and nuisance parameters obtained in background-only fits applied ("postfit"). The HNL predictions for three different  $m_N$  values with exclusive coupling to tau neutrinos are shown with coloured lines. The vertical bars on the points represent the statistical uncertainties in the data, and the hatched bands the total uncertainties in the background predictions as obtained from the fits. In the lower panels, the ratios of the event yield in data to the overall sum of the background predictions are shown.

HNL search presented in ref. [46] for Majorana HNL, the limits improve by up to one order of magnitude. For masses below 20 GeV, we exclude short-lived HNL scenarios not excluded by the displaced HNL searches presented in refs. [50, 52]. The exclusion limits obtained by the DELPHI Collaboration [142] for  $m_{\rm N} < m_{\rm W}$  are less stringent (similar) compared with our results for the case of Majorana (Dirac) HNL.

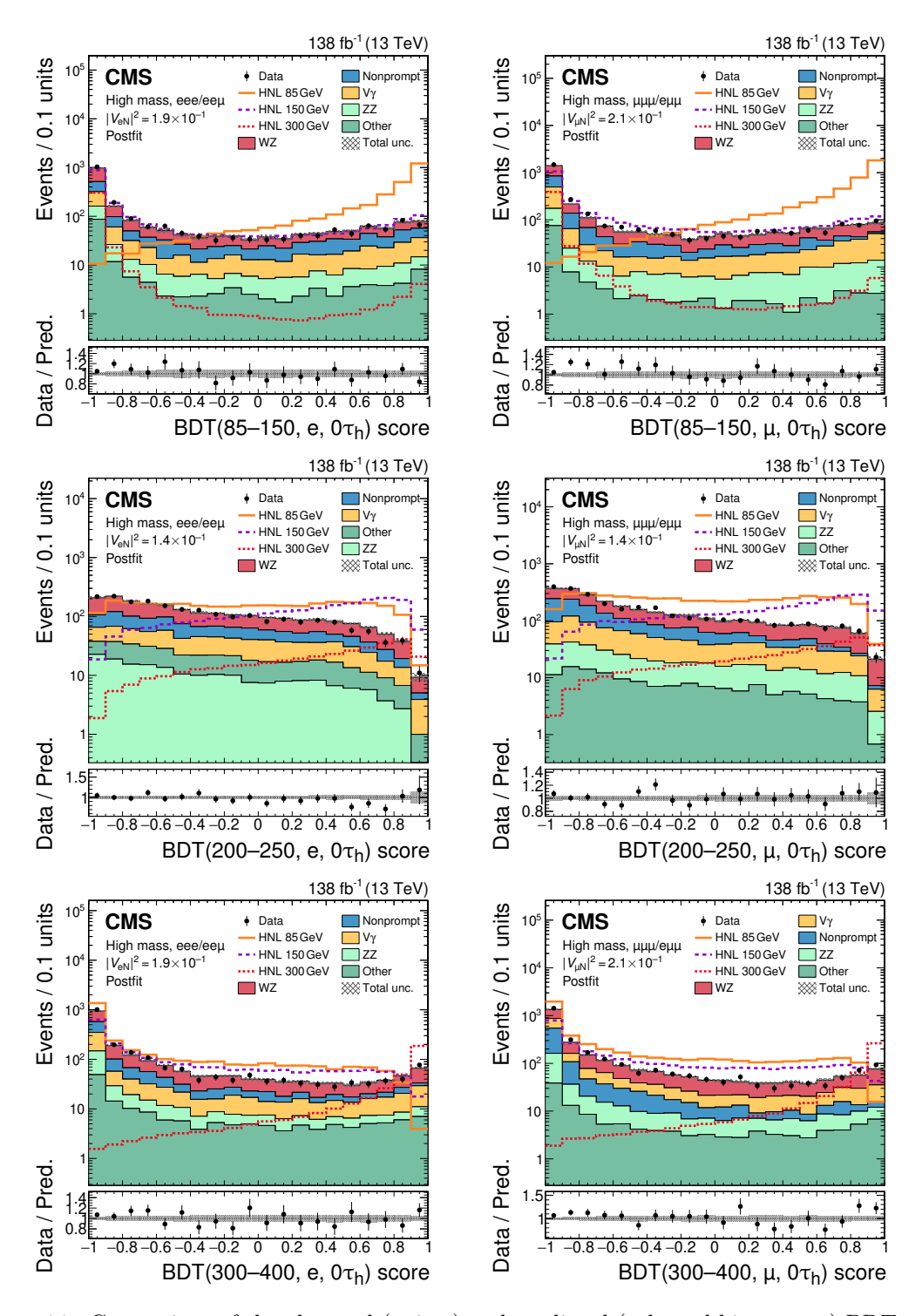


Figure 11. Comparison of the observed (points) and predicted (coloured histograms) BDT output distributions of the high-mass selection, shown for the eee and eeμ channels combined (left column) and the eμμ and μμμ channels combined (right column). The output scores BDT(85–150, e,  $0\tau_h$ ) (upper left), BDT(85–150, μ,  $0\tau_h$ ) (upper right), BDT(200–250, e,  $0\tau_h$ ) (middle left), BDT(200–250, μ,  $0\tau_h$ ) (middle right), BDT(300–400, e,  $0\tau_h$ ) (lower left), and BDT(300–400, μ,  $0\tau_h$ ) (lower right) are displayed. Notations as in figure 9.

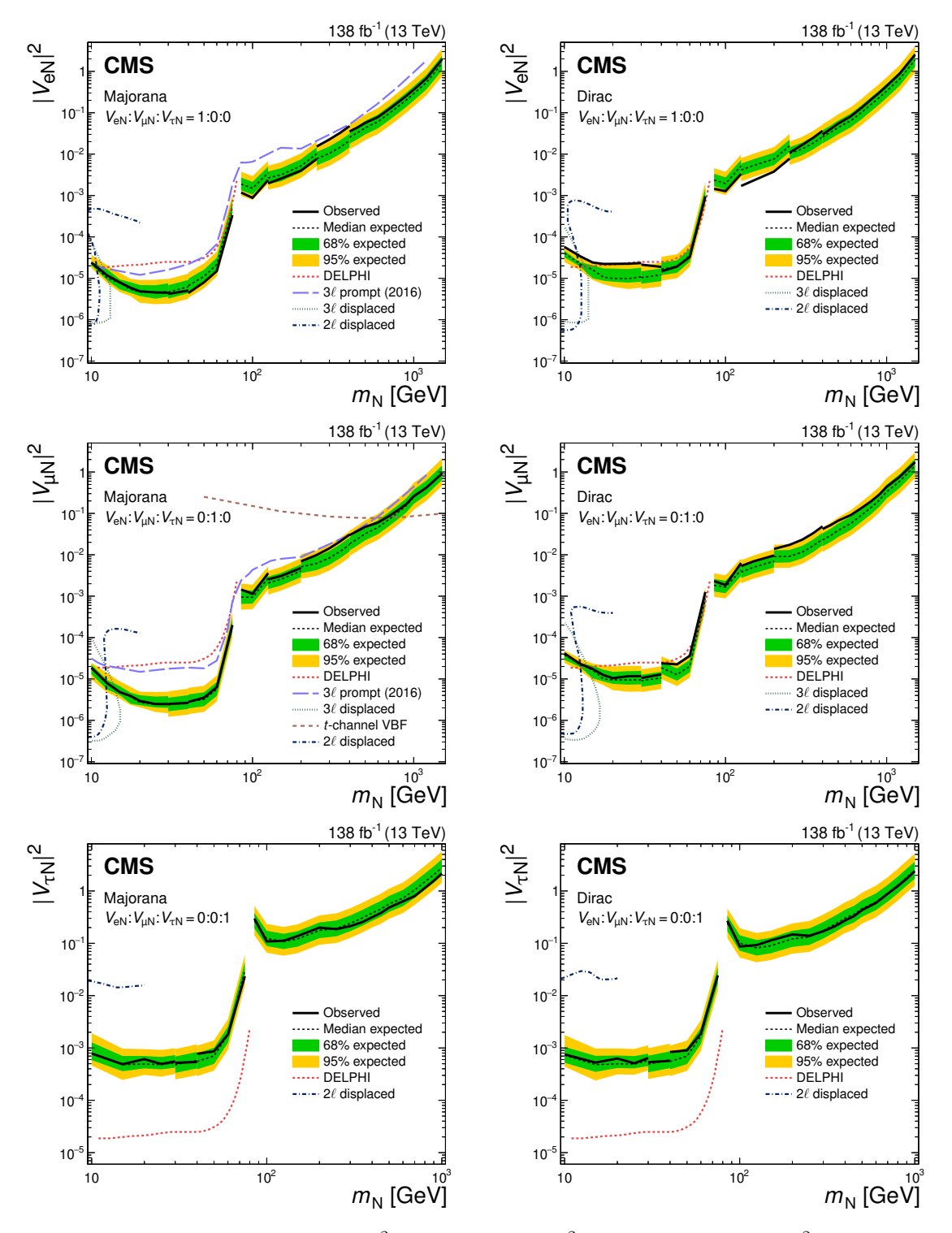


Figure 12. The 95% CL limits on  $|V_{\rm eN}|^2$  (upper row),  $|V_{\mu \rm N}|^2$  (middle row), and  $|V_{\tau \rm N}|^2$  (lower row) as functions of  $m_{\rm N}$  for a Majorana (left) and Dirac (right) HNL. The area above the solid (dashed) black curve indicates the observed (expected) exclusion region. Previous results from the DELPHI Collaboration [142] are shown for reference. The previous CMS result "3 $\ell$  prompt (2016)" [46] is shown to highlight the improvements achieved in our analysis, and the results "3 $\ell$  displaced" [50], "2 $\ell$  displaced" [52], and " $\ell$ -channel VBF" [143] are shown to highlight the complementarity to other search strategies.

Using the low-mass selection and considering exclusive couplings to muon neutrinos, we find limits on  $|V_{\mu \rm N}|^2$  for Majorana (Dirac) HNL of  $2.9 \times 10^{-6}$  ( $1.0 \times 10^{-5}$ ) at  $m_{\rm N}=20$  GeV, of  $6.3 \times 10^{-6}$  ( $3.6 \times 10^{-5}$ ) at 60 GeV, and of  $2.0 \times 10^{-4}$  ( $1.3 \times 10^{-3}$ ) at 75 GeV. Below 30 GeV, the limits are less stringent because of the impact of the long HNL lifetime, with 34 times fewer events selected at  $m_{\rm N}=10$  GeV and  $|V_{\mu \rm N}|^2=10^{-5}$  compared with a prompt HNL. Above  $m_{\rm W}$ , we exclude  $|V_{\mu \rm N}|^2$  values for Majorana (Dirac) HNL of  $1.4 \times 10^{-3}$  ( $2.3 \times 10^{-3}$ ) at a mass of 85 GeV, of  $1.1 \times 10^{-3}$  ( $1.9 \times 10^{-3}$ ) at 100 GeV, and of  $6.0 \times 10^{-2}$  ( $9.1 \times 10^{-2}$ ) at 600 GeV. We improve the exclusion limits from the previous prompt HNL search [46] by up to one order of magnitude, and complement the limits from previous displaced HNL searches [50, 52] for short-lived HNLs below 20 GeV. For  $m_{\rm N} < m_{\rm W}$ , our exclusion limits are more stringent (similar) in the case of Majorana (Dirac) HNLs compared with the results of the DELPHI Collaboration [142]. Compared with a CMS result that searches for high-mass Majorana HNLs with muon neutrino couplings in t-channel VBF production [143], our results provide stricter exclusion limits up to  $m_{\rm N} \approx 700$  GeV.

The case of HNLs at the GeV scale with exclusive tau neutrino couplings was probed before only by the DELPHI Collaboration for  $m_{\rm N} < m_{\rm W}$  [142], by the BaBar Collaboration for  $m_{\rm N} < 1.3\,{\rm GeV}$  [144], and recently by the CMS Collaboration in displaced HNL searches for  $m_{\rm N} < 20\,{\rm GeV}$  [52]. Using the low-mass selection, we exclude Majorana (Dirac) HNLs with  $|V_{\tau \rm N}|^2$  values of  $6.1\times10^{-4}$  ( $6.3\times10^{-4}$ ) at a mass of 20 GeV, of  $1.8\times10^{-3}$  ( $1.9\times10^{-3}$ ) at 60 GeV, and of  $2.3\times10^{-2}$  ( $2.4\times10^{-2}$ ) at 75 GeV. The DELPHI limits for  $m_{\rm N} < m_{\rm W}$  are up to two orders of magnitude more stringent than our results. Above  $m_{\rm W}$ , the tau neutrino couplings are probed for the first time, and we find limits for Majorana (Dirac) HNLs of  $3.0\times10^{-1}$  ( $2.7\times10^{-1}$ ) at  $85\,{\rm GeV}$ ,  $1.1\times10^{-1}$  ( $8.6\times10^{-2}$ ) at  $100\,{\rm GeV}$ , and  $5.9\times10^{-1}$  ( $5.0\times10^{-2}$ ) at  $600\,{\rm GeV}$ .

# 10 Summary

A search for heavy neutral leptons (HNLs) produced in proton-proton collisions at  $\sqrt{s} = 13 \,\text{TeV}$  has been presented. The data were collected with the CMS experiment at the LHC and correspond to an integrated luminosity of  $138 \, \text{fb}^{-1}$ . Events with three charged leptons (electrons, muons, and hadronically decaying tau leptons) are selected, and dedicated identification criteria based on machine learning techniques are applied to reduce the contribution from nonprompt leptons not originating from the hard scattering process. Remaining standard model (SM) background contributions with nonprompt leptons are estimated from control samples in data, whereas other SM contributions that mostly stem from diboson production are estimated from Monte Carlo event simulations. A combination of categorization by kinematic properties and machine learning discriminants achieves optimal separation of the predicted signal and SM background contributions.

No significant deviations from the SM predictions are observed. Exclusion limits at 95% confidence level are evaluated, assuming exclusive HNL couplings to a single generation of SM neutrinos in the mass range  $10~{\rm GeV}-1.5~{\rm TeV}$ , for both Majorana and Dirac HNLs. These results exceed previous experimental constraints over large parts of the mass range. Constraints on tau neutrino couplings for HNL masses above the W boson mass are presented for the first time.

# Acknowledgments

We congratulate our colleagues in the CERN accelerator departments for the excellent performance of the LHC and thank the technical and administrative staffs at CERN and at other CMS institutes for their contributions to the success of the CMS effort. In addition, we gratefully acknowledge the computing centres and personnel of the Worldwide LHC Computing Grid and other centres for delivering so effectively the computing infrastructure essential to our analyses. Finally, we acknowledge the enduring support for the construction and operation of the LHC, the CMS detector, and the supporting computing infrastructure provided by the following funding agencies: SC (Armenia), BMBWF and FWF (Austria); FNRS and FWO (Belgium); CNPq, CAPES, FAPERJ, FAPERGS, and FAPESP (Brazil); MES and BNSF (Bulgaria); CERN; CAS, MoST, and NSFC (China); MINCIENCIAS (Colombia); MSES and CSF (Croatia); RIF (Cyprus); SENESCYT (Ecuador); ERC PRG, RVTT3 and MoER TK202 (Estonia); Academy of Finland, MEC, and HIP (Finland); CEA and CNRS/IN2P3 (France); SRNSF (Georgia); BMBF, DFG, and HGF (Germany); GSRI (Greece); NKFIH (Hungary); DAE and DST (India); IPM (Iran); SFI (Ireland); INFN (Italy); MSIP and NRF (Republic of Korea); MES (Latvia); LMTLT (Lithuania); MOE and UM (Malaysia); BUAP, CINVESTAV, CONACYT, LNS, SEP, and UASLP-FAI (Mexico); MOS (Montenegro); MBIE (New Zealand); PAEC (Pakistan); MES and NSC (Poland); FCT (Portugal); MESTD (Serbia); MCIN/AEI and PCTI (Spain); MOSTR (Sri Lanka); Swiss Funding Agencies (Switzerland); MST (Taipei); MHESI and NSTDA (Thailand); TUBITAK and TENMAK (Turkey); NASU (Ukraine); STFC (United Kingdom); DOE and NSF (U.S.A.).

Individuals have received support from the Marie-Curie programme and the European Research Council and Horizon 2020 Grant, contract Nos. 675440, 724704, 752730, 758316, 765710, 824093, 101115353, and COST Action CA16108 (European Union); the Leventis Foundation; the Alfred P. Sloan Foundation; the Alexander von Humboldt Foundation; the Science Committee, project no. 22rl-037 (Armenia); the Belgian Federal Science Policy Office; the Fonds pour la Formation à la Recherche dans l'Industrie et dans l'Agriculture (FRIA-Belgium); the Agentschap voor Innovatie door Wetenschap en Technologie (IWT-Belgium); the F.R.S.-FNRS and FWO (Belgium) under the "Excellence of Science — EOS" — be.h project n. 30820817; the Beijing Municipal Science & Technology Commission, No. Z191100007219010 and Fundamental Research Funds for the Central Universities (China); the Ministry of Education, Youth and Sports (MEYS) of the Czech Republic; the Shota Rustaveli National Science Foundation, grant FR-22-985 (Georgia); the Deutsche Forschungsgemeinschaft (DFG), under Germany's Excellence Strategy — EXC 2121 "Quantum Universe" — 390833306, and under project number 400140256 — GRK2497; the Hellenic Foundation for Research and Innovation (HFRI), Project Number 2288 (Greece); the Hungarian Academy of Sciences, the New National Excellence Program — ÚNKP, the NKFIH research grants K 124845. K 124850, K 128713, K 128786, K 129058, K 131991, K 133046, K 138136, K 143460, K 143477, 2020-2.2.1-ED-2021-00181, and TKP2021-NKTA-64 (Hungary); the Council of Science and Industrial Research, India; ICSC — National Research Centre for High Performance Computing, Big Data and Quantum Computing, funded by the NexGeneration EU program (Italy); the Latvian Council of Science; the Ministry of Education and Science, project no. 2022/WK/14, and the National Science Center, contracts Opus 2021/41/B/ST2/01369

and 2021/43/B/ST2/01552 (Poland); the Fundação para a Ciência e a Tecnologia, grant CEECIND/01334/2018 (Portugal); the National Priorities Research Program by Qatar National Research Fund; MCIN/AEI/10.13039/501100011033, ERDF "a way of making Europe", and the Programa Estatal de Fomento de la Investigación Científica y Técnica de Excelencia María de Maeztu, grant MDM-2017-0765 and Programa Severo Ochoa del Principado de Asturias (Spain); the Chulalongkorn Academic into Its 2nd Century Project Advancement Project, and the National Science, Research and Innovation Fund via the Program Management Unit for Human Resources & Institutional Development, Research and Innovation, grant B37G660013 (Thailand); the Kavli Foundation; the Nvidia Corporation; the SuperMicro Corporation; the Welch Foundation, contract C-1845; and the Weston Havens Foundation (U.S.A.).

**Open Access.** This article is distributed under the terms of the Creative Commons Attribution License (CC-BY4.0), which permits any use, distribution and reproduction in any medium, provided the original author(s) and source are credited.

### References

- [1] SUPER-KAMIOKANDE collaboration, Evidence for oscillation of atmospheric neutrinos, Phys. Rev. Lett. 81 (1998) 1562 [hep-ex/9807003] [INSPIRE].
- [2] SNO collaboration, Direct evidence for neutrino flavor transformation from neutral current interactions in the Sudbury Neutrino Observatory, Phys. Rev. Lett. 89 (2002) 011301 [nucl-ex/0204008] [INSPIRE].
- [3] KAMLAND collaboration, First results from KamLAND: evidence for reactor anti-neutrino disappearance, Phys. Rev. Lett. **90** (2003) 021802 [hep-ex/0212021] [INSPIRE].
- [4] S. Bilenky, Neutrino oscillations: from a historical perspective to the present status, Nucl. Phys. B 908 (2016) 2 [arXiv:1602.00170] [INSPIRE].
- [5] J.A. Formaggio, A.L.C. de Gouvêa and R.G.H. Robertson, *Direct measurements of neutrino mass*, *Phys. Rept.* **914** (2021) 1 [arXiv:2102.00594] [INSPIRE].
- [6] KATRIN collaboration, Direct neutrino-mass measurement with sub-electronvolt sensitivity, Nature Phys. 18 (2022) 160 [arXiv:2105.08533] [INSPIRE].
- [7] Planck collaboration, Planck 2018 results. VI. Cosmological parameters, Astron. Astrophys. 641 (2020) A6 [Erratum ibid. 652 (2021) C4] [arXiv:1807.06209] [INSPIRE].
- [8] EBOSS collaboration, Completed SDSS-IV extended Baryon Oscillation Spectroscopic Survey: cosmological implications from two decades of spectroscopic surveys at the Apache Point Observatory, Phys. Rev. D 103 (2021) 083533 [arXiv:2007.08991] [INSPIRE].
- [9] Z. Sakr, A short review on the latest neutrinos mass and number constraints from cosmological observables, Universe 8 (2022) 284 [INSPIRE].
- [10] P. Minkowski,  $\mu \to e \gamma$  at a rate of one out of  $10^9$  muon decays?, Phys. Lett. B **67** (1977) 421 [INSPIRE].
- [11] T. Yanagida, Horizontal gauge symmetry and masses of neutrinos, in Proc. workshop on the unified theories and the baryon number in the universe, Tsukuba, Japan, 13–14 February 1979 [Conf. Proc. C 7902131 (1979) 95] [INSPIRE].

- [12] M. Gell-Mann, P. Ramond and R. Slansky, Complex spinors and unified theories, Conf. Proc. C 790927 (1979) 315 [arXiv:1306.4669] [INSPIRE].
- [13] S.L. Glashow, The future of elementary particle physics, NATO Sci. Ser. B 61 (1980) 687 [INSPIRE].
- [14] R.N. Mohapatra and G. Senjanović, Neutrino mass and spontaneous parity nonconservation, Phys. Rev. Lett. 44 (1980) 912 [INSPIRE].
- [15] J. Schechter and J.W.F. Valle, Neutrino masses in  $SU(2) \times U(1)$  theories, Phys. Rev. D 22 (1980) 2227 [INSPIRE].
- [16] R.E. Shrock, General theory of weak leptonic and semileptonic decays. 1. Leptonic pseudoscalar meson decays, with associated tests for, and bounds on, neutrino masses and lepton mixing, Phys. Rev. D 24 (1981) 1232 [INSPIRE].
- [17] Y. Cai, T. Han, T. Li and R. Ruiz, Lepton number violation: seesaw models and their collider tests, Front. in Phys. 6 (2018) 40 [arXiv:1711.02180] [INSPIRE].
- [18] S. Dodelson and L.M. Widrow, Sterile-neutrinos as dark matter, Phys. Rev. Lett. 72 (1994) 17 [hep-ph/9303287] [INSPIRE].
- [19] A. Boyarsky et al., Sterile neutrino dark matter, Prog. Part. Nucl. Phys. 104 (2019) 1 [arXiv:1807.07938] [INSPIRE].
- [20] M. Fukugita and T. Yanagida, Baryogenesis without grand unification, Phys. Lett. B 174 (1986) 45 [INSPIRE].
- [21] E.J. Chun et al., Probing leptogenesis, Int. J. Mod. Phys. A 33 (2018) 1842005 [arXiv:1711.02865] [INSPIRE].
- [22] M. Drewes, Y. Georis and J. Klarić, Mapping the viable parameter space for testable leptogenesis, Phys. Rev. Lett. 128 (2022) 051801 [arXiv:2106.16226] [INSPIRE].
- [23] J. Beacham et al., Physics beyond colliders at CERN: beyond the standard model working group report, J. Phys. G 47 (2020) 010501 [arXiv:1901.09966] [INSPIRE].
- [24] M. Drewes, J. Klarić and J. López-Pavón, New benchmark models for heavy neutral lepton searches, Eur. Phys. J. C 82 (2022) 1176 [arXiv:2207.02742] [INSPIRE].
- [25] F. del Aguila and J.A. Aguilar-Saavedra, Distinguishing seesaw models at LHC with multi-lepton signals, Nucl. Phys. B 813 (2009) 22 [arXiv:0808.2468] [INSPIRE].
- [26] A. Atre, T. Han, S. Pascoli and B. Zhang, The search for heavy Majorana neutrinos, JHEP 05 (2009) 030 [arXiv:0901.3589] [INSPIRE].
- [27] V. Tello et al., Left-right symmetry: from LHC to neutrinoless double beta decay, Phys. Rev. Lett. 106 (2011) 151801 [arXiv:1011.3522] [INSPIRE].
- [28] A. Das and N. Okada, Inverse seesaw neutrino signatures at the LHC and ILC, Phys. Rev. D 88 (2013) 113001 [arXiv:1207.3734] [INSPIRE].
- [29] F.F. Deppisch, P.S. Bhupal Dev and A. Pilaftsis, Neutrinos and collider physics, New J. Phys. 17 (2015) 075019 [arXiv:1502.06541] [INSPIRE].
- [30] A. Das and N. Okada, Bounds on heavy Majorana neutrinos in type-I seesaw and implications for collider searches, Phys. Lett. B 774 (2017) 32 [arXiv:1702.04668] [INSPIRE].
- [31] A. Das, P. Konar and A. Thalapillil, Jet substructure shedding light on heavy Majorana neutrinos at the LHC, JHEP 02 (2018) 083 [arXiv:1709.09712] [INSPIRE].

- [32] A. Bhardwaj, A. Das, P. Konar and A. Thalapillil, Looking for minimal inverse seesaw scenarios at the LHC with jet substructure techniques, J. Phys. G 47 (2020) 075002 [arXiv:1801.00797] [INSPIRE].
- [33] S. Pascoli, R. Ruiz and C. Weiland, Heavy neutrinos with dynamic jet vetoes: multilepton searches at  $\sqrt{s} = 14$ , 27, and 100 TeV, JHEP **06** (2019) 049 [arXiv:1812.08750] [INSPIRE].
- [34] A.M. Abdullahi et al., The present and future status of heavy neutral leptons, J. Phys. G 50 (2023) 020501 [arXiv:2203.08039] [INSPIRE].
- [35] C. Antel et al., Feebly-interacting particles: FIPs 2022 workshop report, Eur. Phys. J. C 83 (2023) 1122 [arXiv:2305.01715] [INSPIRE].
- [36] W.-Y. Keung and G. Senjanovic, Majorana neutrinos and the production of the right-handed charged gauge boson, Phys. Rev. Lett. **50** (1983) 1427 [INSPIRE].
- [37] S.T. Petcov, Possible signature for production of Majorana particles in e<sup>+</sup>e<sup>-</sup> and pp̄ collisions, Phys. Lett. B **139** (1984) 421 [INSPIRE].
- [38] A. Datta, M. Guchait and A. Pilaftsis, Probing lepton number violation via Majorana neutrinos at hadron supercolliders, Phys. Rev. D 50 (1994) 3195 [hep-ph/9311257] [INSPIRE].
- [39] P.S.B. Dev, A. Pilaftsis and U.-K. Yang, New production mechanism for heavy neutrinos at the LHC, Phys. Rev. Lett. 112 (2014) 081801 [arXiv:1308.2209] [INSPIRE].
- [40] D. Alva, T. Han and R. Ruiz, Heavy Majorana neutrinos from Wγ fusion at hadron colliders, JHEP 02 (2015) 072 [arXiv:1411.7305] [INSPIRE].
- [41] C. Degrande, O. Mattelaer, R. Ruiz and J. Turner, Fully-automated precision predictions for heavy neutrino production mechanisms at hadron colliders, Phys. Rev. D 94 (2016) 053002 [arXiv:1602.06957] [INSPIRE].
- [42] CMS collaboration, Search for heavy Majorana neutrinos in  $\mu^{\pm}\mu^{\pm}$ + jets and  $e^{\pm}e^{\pm}$ + jets events in pp collisions at  $\sqrt{s} = 7$  TeV, Phys. Lett. B 717 (2012) 109 [arXiv:1207.6079] [INSPIRE].
- [43] CMS collaboration, Search for heavy Majorana neutrinos in  $\mu^{\pm}\mu^{\pm}$ + jets events in proton-proton collisions at  $\sqrt{s}=8$  TeV, Phys. Lett. B **748** (2015) 144 [arXiv:1501.05566] [INSPIRE].
- [44] ATLAS collaboration, Search for heavy Majorana neutrinos with the ATLAS detector in pp collisions at  $\sqrt{s} = 8$  TeV, JHEP **07** (2015) 162 [arXiv:1506.06020] [INSPIRE].
- [45] CMS collaboration, Search for heavy Majorana neutrinos in  $e^{\pm}e^{\pm}$  + jets and  $e^{\pm}\mu^{\pm}$  + jets events in proton-proton collisions at  $\sqrt{s} = 8$  TeV, JHEP **04** (2016) 169 [arXiv:1603.02248] [INSPIRE].
- [46] CMS collaboration, Search for heavy neutral leptons in events with three charged leptons in proton-proton collisions at  $\sqrt{s} = 13$  TeV, Phys. Rev. Lett. 120 (2018) 221801 [arXiv:1802.02965] [INSPIRE].
- [47] CMS collaboration, Search for heavy Majorana neutrinos in same-sign dilepton channels in proton-proton collisions at  $\sqrt{s} = 13$  TeV, JHEP **01** (2019) 122 [arXiv:1806.10905] [INSPIRE].
- [48] ATLAS collaboration, Search for heavy neutral leptons in decays of W bosons produced in 13 TeV pp collisions using prompt and displaced signatures with the ATLAS detector, JHEP 10 (2019) 265 [arXiv:1905.09787] [INSPIRE].
- [49] LHCb collaboration, Search for heavy neutral leptons in  $W^+ \to \mu^+ \mu^\pm$  jet decays, Eur. Phys. J. C 81 (2021) 248 [arXiv:2011.05263] [INSPIRE].
- [50] CMS collaboration, Search for long-lived heavy neutral leptons with displaced vertices in proton-proton collisions at  $\sqrt{s} = 13$  TeV, JHEP **07** (2022) 081 [arXiv:2201.05578] [INSPIRE].

- [51] ATLAS collaboration, Search for heavy neutral leptons in decays of W bosons using a dilepton displaced vertex in √s = 13 TeV pp collisions with the ATLAS detector, Phys. Rev. Lett. 131 (2023) 061803 [arXiv:2204.11988] [INSPIRE].
- [52] CMS collaboration, Search for long-lived heavy neutral leptons with lepton flavour conserving or violating decays to a jet and a charged lepton, JHEP 03 (2024) 105 [arXiv:2312.07484] [INSPIRE].
- [53] CMS collaboration, Review of searches for vector-like quarks, vector-like leptons, and heavy neutral leptons in proton-proton collisions at  $\sqrt{s} = 13$  TeV at the CMS experiment, submitted to Phys. Rept. [arXiv:2405.17605] [INSPIRE].
- [54] A. Abada, N. Bernal, M. Losada and X. Marcano, *Inclusive displaced vertex searches for heavy neutral leptons at the LHC*, *JHEP* **01** (2019) 093 [arXiv:1807.10024] [INSPIRE].
- [55] J.-L. Tastet, O. Ruchayskiy and I. Timiryasov, Reinterpreting the ATLAS bounds on heavy neutral leptons in a realistic neutrino oscillation model, JHEP 12 (2021) 182 [arXiv:2107.12980] [INSPIRE].
- [56] CMS collaboration, HEPData record for this analysis, CMS-EXO-22-011, CERN, Geneva, Switzerland (2024).
- [57] T. Asaka, S. Blanchet and M. Shaposhnikov, The νMSM, dark matter and neutrino masses, Phys. Lett. B 631 (2005) 151 [hep-ph/0503065] [INSPIRE].
- [58] CMS collaboration, The CMS experiment at the CERN LHC, 2008 JINST 3 S08004 [INSPIRE].
- [59] CMS collaboration, Development of the CMS detector for the CERN LHC run 3, 2024 JINST 19 P05064 [arXiv:2309.05466] [INSPIRE].
- [60] CMS collaboration, Performance of the CMS level-1 trigger in proton-proton collisions at  $\sqrt{s} = 13 \text{ TeV}$ , 2020 JINST 15 P10017 [arXiv:2006.10165] [INSPIRE].
- [61] CMS collaboration, The CMS trigger system, 2017 JINST 12 P01020 [arXiv:1609.02366] [INSPIRE].
- [62] CMS collaboration, Particle-flow reconstruction and global event description with the CMS detector, 2017 JINST 12 P10003 [arXiv:1706.04965] [INSPIRE].
- [63] D. Contardo et al., Technical proposal for the phase-II upgrade of the CMS detector, CERN-LHCC-2015-010 CERN, Geneva, Switzerland (2015) [DOI:10.17181/CERN.VU8I.D59J].
- [64] M. Cacciari, G.P. Salam and G. Soyez, The anti- $k_t$  jet clustering algorithm, JHEP **04** (2008) 063 [arXiv:0802.1189] [INSPIRE].
- [65] M. Cacciari, G.P. Salam and G. Soyez, FastJet user manual, Eur. Phys. J. C 72 (2012) 1896 [arXiv:1111.6097] [INSPIRE].
- [66] CMS collaboration, Jet energy scale and resolution in the CMS experiment in pp collisions at 8 TeV, 2017 JINST 12 P02014 [arXiv:1607.03663] [INSPIRE].
- [67] CMS collaboration, Jet algorithms performance in 13 TeV data, CMS-PAS-JME-16-003, CERN, Geneva, Switzerland (2017).
- [68] CMS collaboration, Performance of missing transverse momentum reconstruction in proton-proton collisions at  $\sqrt{s} = 13$  TeV using the CMS detector, 2019 JINST 14 P07004 [arXiv:1903.06078] [INSPIRE].
- [69] CMS collaboration, Identification of heavy-flavour jets with the CMS detector in pp collisions at 13 TeV, 2018 JINST 13 P05011 [arXiv:1712.07158] [INSPIRE].

- [70] E. Bols et al., Jet flavour classification using DeepJet, 2020 JINST 15 P12012 [arXiv:2008.10519] [INSPIRE].
- [71] CMS collaboration, Performance summary of AK4 jet b tagging with data from proton-proton collisions at 13 TeV with the CMS detector, CMS-DP-2023-005 (2023).
- [72] GEANT4 collaboration, GEANT4 a simulation toolkit, Nucl. Instrum. Meth. A 506 (2003) 250 [INSPIRE].
- [73] CMS collaboration, Pileup mitigation at CMS in 13 TeV data, 2020 JINST 15 P09018 [arXiv:2003.00503] [INSPIRE].
- [74] J. Alwall et al., The automated computation of tree-level and next-to-leading order differential cross sections, and their matching to parton shower simulations, JHEP **07** (2014) 079 [arXiv:1405.0301] [INSPIRE].
- [75] P. Artoisenet, R. Frederix, O. Mattelaer and R. Rietkerk, Automatic spin-entangled decays of heavy resonances in Monte Carlo simulations, JHEP 03 (2013) 015 [arXiv:1212.3460] [INSPIRE].
- [76] NNPDF collaboration, Parton distributions from high-precision collider data, Eur. Phys. J. C 77 (2017) 663 [arXiv:1706.00428] [INSPIRE].
- [77] A. Manohar, P. Nason, G.P. Salam and G. Zanderighi, How bright is the proton? A precise determination of the photon parton distribution function, Phys. Rev. Lett. 117 (2016) 242002 [arXiv:1607.04266] [INSPIRE].
- [78] A.V. Manohar, P. Nason, G.P. Salam and G. Zanderighi, The photon content of the proton, JHEP 12 (2017) 046 [arXiv:1708.01256] [INSPIRE].
- [79] NNPDF collaboration, Illuminating the photon content of the proton within a global PDF analysis, SciPost Phys. 5 (2018) 008 [arXiv:1712.07053] [INSPIRE].
- [80] K. Bondarenko, A. Boyarsky, D. Gorbunov and O. Ruchayskiy, *Phenomenology of GeV-scale heavy neutral leptons*, *JHEP* 11 (2018) 032 [arXiv:1805.08567] [INSPIRE].
- [81] P. Nason, A new method for combining NLO QCD with shower Monte Carlo algorithms, JHEP 11 (2004) 040 [hep-ph/0409146] [INSPIRE].
- [82] S. Frixione, P. Nason and G. Ridolfi, A positive-weight next-to-leading-order Monte Carlo for heavy flavour hadroproduction, JHEP 09 (2007) 126 [arXiv:0707.3088] [INSPIRE].
- [83] S. Frixione, P. Nason and C. Oleari, Matching NLO QCD computations with parton shower simulations: the POWHEG method, JHEP 11 (2007) 070 [arXiv:0709.2092] [INSPIRE].
- [84] S. Alioli, P. Nason, C. Oleari and E. Re, NLO single-top production matched with shower in POWHEG: s- and t-channel contributions, JHEP 09 (2009) 111 [Erratum ibid. 02 (2010) 011] [arXiv:0907.4076] [INSPIRE].
- [85] P. Nason and C. Oleari, NLO Higgs boson production via vector-boson fusion matched with shower in POWHEG, JHEP 02 (2010) 037 [arXiv:0911.5299] [INSPIRE].
- [86] S. Alioli, P. Nason, C. Oleari and E. Re, A general framework for implementing NLO calculations in shower Monte Carlo programs: the POWHEG BOX, JHEP 06 (2010) 043 [arXiv:1002.2581] [INSPIRE].
- [87] E. Re, Single-top Wt-channel production matched with parton showers using the POWHEG method, Eur. Phys. J. C 71 (2011) 1547 [arXiv:1009.2450] [INSPIRE].

- [88] E. Bagnaschi, G. Degrassi, P. Slavich and A. Vicini, Higgs production via gluon fusion in the POWHEG approach in the SM and in the MSSM, JHEP 02 (2012) 088 [arXiv:1111.2854] [INSPIRE].
- [89] P. Nason and G. Zanderighi, W<sup>+</sup>W<sup>-</sup>, WZ and ZZ production in the POWHEG-BOX-V2, Eur. Phys. J. C **74** (2014) 2702 [arXiv:1311.1365] [INSPIRE].
- [90] J.M. Campbell and R.K. Ellis, An update on vector boson pair production at hadron colliders, Phys. Rev. D 60 (1999) 113006 [hep-ph/9905386] [INSPIRE].
- [91] J.M. Campbell, R.K. Ellis and C. Williams, Vector boson pair production at the LHC, JHEP 07 (2011) 018 [arXiv:1105.0020] [INSPIRE].
- [92] J.M. Campbell, R.K. Ellis and W.T. Giele, A multi-threaded version of MCFM, Eur. Phys. J. C 75 (2015) 246 [arXiv:1503.06182] [INSPIRE].
- [93] T. Sjöstrand et al., An introduction to PYTHIA 8.2, Comput. Phys. Commun. 191 (2015) 159 [arXiv:1410.3012] [INSPIRE].
- [94] CMS collaboration, Extraction and validation of a new set of CMS PYTHIA8 tunes from underlying-event measurements, Eur. Phys. J. C 80 (2020) 4 [arXiv:1903.12179] [INSPIRE].
- [95] J. Alwall et al., Comparative study of various algorithms for the merging of parton showers and matrix elements in hadronic collisions, Eur. Phys. J. C 53 (2008) 473 [arXiv:0706.2569] [INSPIRE].
- [96] R. Frederix and S. Frixione, Merging meets matching in MC@NLO, JHEP 12 (2012) 061 [arXiv:1209.6215] [INSPIRE].
- [97] S. Bolognesi et al., On the spin and parity of a single-produced resonance at the LHC, Phys. Rev. D 86 (2012) 095031 [arXiv:1208.4018] [INSPIRE].
- [98] CMS collaboration, Electron and photon reconstruction and identification with the CMS experiment at the CERN LHC, 2021 JINST 16 P05014 [arXiv:2012.06888] [INSPIRE].
- [99] CMS collaboration, ECAL 2016 refined calibration and Run2 summary plots, CMS-DP-2020-021, CERN, Geneva, Switzerland (2020).
- [100] CMS collaboration, Performance of the CMS muon detector and muon reconstruction with proton-proton collisions at  $\sqrt{s} = 13$  TeV, 2018 JINST 13 P06015 [arXiv:1804.04528] [INSPIRE].
- [101] K. Rehermann and B. Tweedie, Efficient identification of boosted semileptonic top quarks at the LHC, JHEP 03 (2011) 059 [arXiv:1007.2221] [INSPIRE].
- [102] CMS collaboration, Observation of four top quark production in proton-proton collisions at  $\sqrt{s} = 13$  TeV, Phys. Lett. B 847 (2023) 138290 [arXiv:2305.13439] [INSPIRE].
- [103] CMS collaboration, Evidence for associated production of a Higgs boson with a top quark pair in final states with electrons, muons, and hadronically decaying  $\tau$  leptons at  $\sqrt{s} = 13$  TeV, JHEP 08 (2018) 066 [arXiv:1803.05485] [INSPIRE].
- [104] CMS collaboration, Observation of single top quark production in association with a Z boson in proton-proton collisions at  $\sqrt{s} = 13$  TeV, Phys. Rev. Lett. 122 (2019) 132003 [arXiv:1812.05900] [INSPIRE].
- [105] CMS collaboration, Measurement of the Higgs boson production rate in association with top quarks in final states with electrons, muons, and hadronically decaying tau leptons at  $\sqrt{s} = 13$  TeV, Eur. Phys. J. C 81 (2021) 378 [arXiv:2011.03652] [INSPIRE].

- [106] CMS collaboration, Search for electroweak production of charginos and neutralinos in proton-proton collisions at  $\sqrt{s} = 13$  TeV, JHEP **04** (2022) 147 [arXiv:2106.14246] [INSPIRE].
- [107] CMS collaboration, Measurements of the electroweak diboson production cross sections in proton-proton collisions at  $\sqrt{s} = 5.02$  TeV using leptonic decays, Phys. Rev. Lett. 127 (2021) 191801 [arXiv:2107.01137] [INSPIRE].
- [108] CMS collaboration, Inclusive and differential cross section measurements of single top quark production in association with a Z boson in proton-proton collisions at  $\sqrt{s} = 13$  TeV, JHEP 02 (2022) 107 [arXiv:2111.02860] [INSPIRE].
- [109] CMS collaboration, Muon identification using multivariate techniques in the CMS experiment in proton-proton collisions at  $\sqrt{s} = 13$  TeV, 2024 JINST 19 P02031 [arXiv:2310.03844] [INSPIRE].
- [110] CMS collaboration, Performance of reconstruction and identification of  $\tau$  leptons decaying to hadrons and  $\nu_{\tau}$  in pp collisions at  $\sqrt{s}=13$  TeV, 2018 JINST 13 P10005 [arXiv:1809.02816] [INSPIRE].
- [111] CMS collaboration, *Identification of hadronic tau lepton decays using a deep neural network*, 2022 JINST 17 P07023 [arXiv:2201.08458] [INSPIRE].
- [112] Particle Data Group collaboration, Review of particle physics, PTEP **2022** (2022) 083C01 [INSPIRE].
- [113] CMS collaboration, Performance of electron reconstruction and selection with the CMS detector in proton-proton collisions at  $\sqrt{s} = 8$  TeV, 2015 JINST 10 P06005 [arXiv:1502.02701] [INSPIRE].
- [114] CMS collaboration, Performance of CMS muon reconstruction in cosmic-ray events, 2010 JINST 5 T03022 [arXiv:0911.4994] [INSPIRE].
- [115] CMS collaboration, Performance of the reconstruction and identification of high-momentum muons in proton-proton collisions at  $\sqrt{s} = 13$  TeV, 2020 JINST 15 P02027 [arXiv:1912.03516] [INSPIRE].
- [116] H. Voss, A. Höcker, J. Stelzer and F. Tegenfeldt, TMVA, the toolkit for multivariate data analysis with ROOT, PoS ACAT (2007) 040 [physics/0703039] [INSPIRE].
- [117] CMS collaboration, Search for new physics in same-sign dilepton events in proton-proton collisions at  $\sqrt{s} = 13$  TeV, Eur. Phys. J. C 76 (2016) 439 [arXiv:1605.03171] [INSPIRE].
- [118] CMS collaboration, Measurement of the cross section of top quark-antiquark pair production in association with a W boson in proton-proton collisions at  $\sqrt{s} = 13$  TeV, JHEP **07** (2023) 219 [arXiv:2208.06485] [INSPIRE].
- [119] CMS collaboration, Precision luminosity measurement in proton-proton collisions at  $\sqrt{s} = 13$  TeV in 2015 and 2016 at CMS, Eur. Phys. J. C 81 (2021) 800 [arXiv:2104.01927] [INSPIRE].
- [120] CMS collaboration, CMS luminosity measurement for the 2017 data-taking period at  $\sqrt{s} = 13 \text{ TeV}$ , CMS-PAS-LUM-17-004, CERN, Geneva, Switzerland (2018).
- [121] CMS collaboration, CMS luminosity measurement for the 2018 data-taking period at  $\sqrt{s} = 13 \text{ TeV}$ , CMS-PAS-LUM-18-002, CERN, Geneva, Switzerland (2019).
- [122] CMS collaboration, Measurements of inclusive W and Z cross sections in pp collisions at  $\sqrt{s} = 7$  TeV, JHEP **01** (2011) 080 [arXiv:1012.2466] [INSPIRE].

- [123] A. Lazopoulos, K. Melnikov and F. Petriello, QCD corrections to tri-boson production, Phys. Rev. D 76 (2007) 014001 [hep-ph/0703273] [INSPIRE].
- [124] T. Binoth, G. Ossola, C.G. Papadopoulos and R. Pittau, NLO QCD corrections to tri-boson production, JHEP 06 (2008) 082 [arXiv:0804.0350] [INSPIRE].
- [125] V. Hankele and D. Zeppenfeld, QCD corrections to hadronic WWZ production with leptonic decays, Phys. Lett. B 661 (2008) 103 [arXiv:0712.3544] [INSPIRE].
- [126] F. Campanario et al., QCD corrections to charged triple vector boson production with leptonic decay, Phys. Rev. D 78 (2008) 094012 [arXiv:0809.0790] [INSPIRE].
- [127] S. Dittmaier, A. Huss and G. Knippen, Next-to-leading-order QCD and electroweak corrections to WWW production at proton-proton colliders, JHEP 09 (2017) 034 [arXiv:1705.03722] [INSPIRE].
- [128] CMS collaboration, A portrait of the Higgs boson by the CMS experiment ten years after the discovery, Nature 607 (2022) 60 [arXiv:2207.00043] [INSPIRE].
- [129] K. Melnikov and F. Petriello, Electroweak gauge boson production at hadron colliders through  $O(\alpha_s^2)$ , Phys. Rev. D **74** (2006) 114017 [hep-ph/0609070] [INSPIRE].
- [130] R. Gavin, Y. Li, F. Petriello and S. Quackenbush, FEWZ 2.0: a code for hadronic Z production at next-to-next-to-leading order, Comput. Phys. Commun. 182 (2011) 2388 [arXiv:1011.3540] [INSPIRE].
- [131] R. Gavin, Y. Li, F. Petriello and S. Quackenbush, W physics at the LHC with FEWZ 2.1, Comput. Phys. Commun. 184 (2013) 208 [arXiv:1201.5896] [INSPIRE].
- [132] Y. Li and F. Petriello, Combining QCD and electroweak corrections to dilepton production in FEWZ, Phys. Rev. D 86 (2012) 094034 [arXiv:1208.5967] [INSPIRE].
- [133] CMS collaboration, The CMS statistical analysis and combination tool: COMBINE, arXiv:2404.06614 [INSPIRE].
- [134] W. Verkerke and D.P. Kirkby, *The RooFit toolkit for data modeling*, eConf C **0303241** (2003) MOLT007 [physics/0306116] [INSPIRE].
- [135] L. Moneta et al., The RooStats project, PoS ACAT2010 (2010) 057 [arXiv:1009.1003] [INSPIRE].
- [136] THEATLAS et al. collaborations, Procedure for the LHC Higgs boson search combination in Summer 2011, CMS-NOTE-2011-005, CERN, Geneva, Switzerland (2011).
- [137] R.J. Barlow and C. Beeston, Fitting using finite Monte Carlo samples, Comput. Phys. Commun. 77 (1993) 219 [INSPIRE].
- [138] J.S. Conway, Incorporating nuisance parameters in likelihoods for multisource spectra, in the proceedings of the PHYSTAT 2011, (2011) [DOI:10.5170/CERN-2011-006.115] [arXiv:1103.0354] [INSPIRE].
- [139] T. Junk, Confidence level computation for combining searches with small statistics, Nucl. Instrum. Meth. A 434 (1999) 435 [hep-ex/9902006] [INSPIRE].
- [140] A.L. Read, Presentation of search results: the  $CL_s$  technique, J. Phys. G **28** (2002) 2693 [INSPIRE].
- [141] G. Cowan, K. Cranmer, E. Gross and O. Vitells, Asymptotic formulae for likelihood-based tests of new physics, Eur. Phys. J. C 71 (2011) 1554 [Erratum ibid. 73 (2013) 2501] [arXiv:1007.1727] [INSPIRE].

- [142] DELPHI collaboration, Search for neutral heavy leptons produced in Z decays, Z. Phys. C 74 (1997) 57 [Erratum ibid. 75 (1997) 580] [INSPIRE].
- [143] CMS collaboration, Probing heavy Majorana neutrinos and the Weinberg operator through vector boson fusion processes in proton-proton collisions at  $\sqrt{s} = 13$  TeV, Phys. Rev. Lett. 131 (2023) 011803 [arXiv:2206.08956] [INSPIRE].
- [144] BABAR collaboration, Search for heavy neutral leptons using tau lepton decays at BaBaR, Phys. Rev. D 107 (2023) 052009 [arXiv:2207.09575] [INSPIRE].

#### The CMS collaboration

### Yerevan Physics Institute, Yerevan, Armenia

A. Hayrapetyan, A. Tumasyan 10 1

### Institut für Hochenergiephysik, Vienna, Austria

```
W. Adam, J.W. Andrejkovic, T. Bergauer, S. Chatterjee, K. Damanakis, M. Dragicevic, P.S. Hussain, M. Jeitler, N. Krammer, A. Li, D. Liko, J. Mikulec, J. Schieck, R. Schöfbeck, D. Schwarz, M. Sonawane, S. Templ, W. Waltenberger, C.-E. Wulz,
```

### Universiteit Antwerpen, Antwerpen, Belgium

M.R. Darwish <sup>1</sup> , T. Janssen <sup>1</sup> , P. Van Mechelen <sup>1</sup>

### Vrije Universiteit Brussel, Brussel, Belgium

```
E.S. Bols<sup>®</sup>, N. Breugelmans, J. D'Hondt<sup>®</sup>, S. Dansana<sup>®</sup>, A. De Moor<sup>®</sup>, M. Delcourt<sup>®</sup>, F. Heyen, S. Lowette<sup>®</sup>, I. Makarenko<sup>®</sup>, D. Müller<sup>®</sup>, S. Tavernier<sup>®</sup>, M. Tytgat<sup>®</sup>, G.P. Van Onsem<sup>®</sup>, S. Van Putte<sup>®</sup>, D. Vannerom<sup>®</sup>
```

### Université Libre de Bruxelles, Bruxelles, Belgium

```
B. Clerbaux, A.K. Das, G. De Lentdecker, H. Evard, L. Favart, P. Gianneios, D. Hohov, J. Jaramillo, A. Khalilzadeh, F.A. Khan, K. Lee, M. Mahdavikhorrami, A. Malara, S. Paredes, L. Thomas, M. Vanden Bemden, C. Vander Velde, P. Vanlaer,
```

### Ghent University, Ghent, Belgium

```
M. De Coen, D. Dobur, Y. Hong, J. Knolle, L. Lambrecht, G. Mestdach, K. Mota Amarilo, C. Rendón, A. Samalan, K. Skovpen, N. Van Den Bossche, J. van der Linden, L. Wezenbeek
```

#### Université Catholique de Louvain, Louvain-la-Neuve, Belgium

```
A. Benecke, A. Bethani, G. Bruno, C. Caputo, C. Delaere, I.S. Donertas, A. Giammanco, Sa. Jain, V. Lemaitre, J. Lidrych, P. Mastrapasqua, T.T. Tran, S. Wertz
```

### Centro Brasileiro de Pesquisas Fisicas, Rio de Janeiro, Brazil

```
G.A. Alves, E. Coelho, C. Hensel, T. Menezes De Oliveira, A. Moraes, P. Rebello Teles, M. Soeiro, A. Vilela Pereira,
```

### Universidade do Estado do Rio de Janeiro, Rio de Janeiro, Brazil

```
W.L. Aldá Júnior, M. Alves Gallo Pereira, M. Barroso Ferreira Filho, H. Brandao Malbouisson, W. Carvalho, J. Chinellato, E.M. Da Costa, G.G. Da Silveira, T. D. De Jesus Damiao, S. Fonseca De Souza, R. Gomes De Souza, M. Macedo, J. Martins, C. Mora Herrera, L. Mundim, H. Nogima, J.P. Pinheiro, A. Santoro, A. Sznajder, M. Thiel,
```

```
Universidade Estadual Paulista, Universidade Federal do ABC, São Paulo, Brazil C.A. Bernardes o<sup>7</sup>, L. Calligaris o, T.R. Fernandez Perez Tomei o, E.M. Gregores o, I. Maietto Silverio o, P.G. Mercadante o, S.F. Novaes o, B. Orzari o, Sandra S. Padula o Institute for Nuclear Research and Nuclear Energy, Bulgarian Academy of Sciences, Sofia, Bulgaria

A. Aleksandrov o, G. Antchev o, R. Hadjiiska o, P. Iaydjiev o, M. Misheva o, M. Shopova o, G. Sultanov o
University of Sofia, Sofia, Bulgaria

A. Dimitrov o, L. Litov o, B. Pavlov o, P. Petkov o, A. Petrov o, E. Shumka o
```

# Instituto De Alta Investigación, Universidad de Tarapacá, Casilla 7 D, Arica, Chile

S. Keshri, S. Thakur

### Beihang University, Beijing, China

T. Cheng, T. Javaid, L. Yuan

### Department of Physics, Tsinghua University, Beijing, China

Z. Hu, Z. Liang, J. Liu, K. Yi, 10, 10, 10

### Institute of High Energy Physics, Beijing, China

```
G.M. Chen 11, H.S. Chen 11, M. Chen 11, F. Iemmi 1, C.H. Jiang, A. Kapoor 12, H. Liao , Z.-A. Liu 13, R. Sharma 14, J.N. Song 3, J. Tao 5, C. Wang 11, J. Wang 15, Z. Wang 11, H. Zhang 15
```

# State Key Laboratory of Nuclear Physics and Technology, Peking University, Beijing, China

```
A. Agapitos, Y. Ban, A. Levin, C. Li, Q. Li, Y. Mao, S. Qian, S.J. Qian, X. Sun, D. Wang, H. Yang, L. Zhang, Y. Zhao, C. Zhou
```

### Sun Yat-Sen University, Guangzhou, China

Z. You

### University of Science and Technology of China, Hefei, China

K. Jaffel<sup>®</sup>, N. Lu<sup>®</sup>

### Nanjing Normal University, Nanjing, China

G. Bauer<sup>15</sup>

# Institute of Modern Physics and Key Laboratory of Nuclear Physics and Ion-beam Application (MOE) — Fudan University, Shanghai, China X. Gao © 16

### Zhejiang University, Hangzhou, Zhejiang, China

Z. Lin<sup>®</sup>, C. Lu<sup>®</sup>, M. Xiao<sup>®</sup>

### Universidad de Los Andes, Bogota, Colombia

C. Avila, D.A. Barbosa Trujillo, A. Cabrera, C. Florez, J. Fraga, J.A. Reyes Vega

### Universidad de Antioquia, Medellin, Colombia

J. Mejia Guisao, F. Ramirez, M. Rodriguez, J.D. Ruiz Alvarez

### University of Split, Faculty of Electrical Engineering, Mechanical Engineering and Naval Architecture, Split, Croatia

D. Giljanovic, N. Godinovic, D. Lelas, A. Sculac

### University of Split, Faculty of Science, Split, Croatia

M. Kovac<sup>®</sup>, A. Petkovic, T. Sculac<sup>®</sup>

### Institute Rudjer Boskovic, Zagreb, Croatia

P. Bargassa<sup>®</sup>, V. Brigljevic<sup>®</sup>, B.K. Chitroda<sup>®</sup>, D. Ferencek<sup>®</sup>, K. Jakovcic, S. Mishra<sup>®</sup>, A. Starodumov<sup>®</sup><sup>17</sup>, T. Susa<sup>®</sup>

### University of Cyprus, Nicosia, Cyprus

A. Attikis, K. Christoforou, A. Hadjiagapiou, C. Leonidou, J. Mousa, C. Nicolaou, L. Paizanos, F. Ptochos, P.A. Razis, H. Rykaczewski, H. Saka, A. Stepennov

### Charles University, Prague, Czech Republic

M. Finger D, M. Finger Jr. D, A. Kveton D

### Escuela Politecnica Nacional, Quito, Ecuador

E. Ayala 10

#### Universidad San Francisco de Quito, Quito, Ecuador

E. Carrera Jarrin

### Academy of Scientific Research and Technology of the Arab Republic of Egypt, Egyptian Network of High Energy Physics, Cairo, Egypt

Y. Assran<sup>18,19</sup>, S. Elgammal<sup>19</sup>

### Center for High Energy Physics (CHEP-FU), Fayoum University, El-Fayoum, Egypt

M. Abdullah Al-Mashad, M.A. Mahmoud

### National Institute of Chemical Physics and Biophysics, Tallinn, Estonia

K. Ehataht, M. Kadastik, T. Lange, S. Nandan, C. Nielsen, J. Pata, M. Raidal, L. Tani, C. Veelken

### Department of Physics, University of Helsinki, Helsinki, Finland

H. Kirschenmann, K. Osterberg, M. Voutilainen

### Helsinki Institute of Physics, Helsinki, Finland

- S. Bharthuar, E. Brücken, F. Garcia, K.T.S. Kallonen, R. Kinnunen, T. Lampén,
- K. Lassila-Perini, S. Lehti, T. Lindén, L. Martikainen, M. Myllymäki, M.m. Rantanen,
- H. Siikonen, E. Tuominen, J. Tuominiemi

### Lappeenranta-Lahti University of Technology, Lappeenranta, Finland

P. Luukka, H. Petrow

### IRFU, CEA, Université Paris-Saclay, Gif-sur-Yvette, France

- M. Besancon, F. Couderc, M. Dejardin, D. Denegri, J.L. Faure, F. Ferri, S. Ganjour,
- P. Gras<sup>®</sup>, G. Hamel de Monchenault<sup>®</sup>, V. Lohezic<sup>®</sup>, J. Malcles<sup>®</sup>, F. Orlandi<sup>®</sup>, L. Portales<sup>®</sup>,
- J. Rander, A. Rosowsky, M.Ö. Sahin, A. Savoy-Navarro, P. Simkina, M. Titov, M. Tornago

# Laboratoire Leprince-Ringuet, CNRS/IN2P3, Ecole Polytechnique, Institut Polytechnique de Paris, Palaiseau, France

- F. Beaudette, A. Buchot Perraguin, P. Busson, A. Cappati, C. Charlot, M. Chiusi,
- F. Damas, O. Davignon, A. De Wit, I.T. Ehle, B.A. Fontana Santos Alves, S. Ghosh,
- A. Gilbert, R. Granier de Cassagnac, A. Hakimi, B. Harikrishnan, L. Kalipoliti, G. Liu, G.
- J. Motta, M. Nguyen, C. Ochando, R. Salerno, J.B. Sauvan, Y. Sirois, A. Tarabini,
- E. Vernazza, A. Zabi, A. Zghiche

### Université de Strasbourg, CNRS, IPHC UMR 7178, Strasbourg, France

- J.-L. Agram <sup>©</sup> <sup>21</sup>, J. Andrea <sup>©</sup>, D. Apparu <sup>©</sup>, D. Bloch <sup>©</sup>, J.-M. Brom <sup>©</sup>, E.C. Chabert <sup>©</sup>,
- C. Collard, S. Falke, U. Goerlach, C. Grimault, R. Haeberle, A.-C. Le Bihan, M. Meena,
- G. Saha<sup>®</sup>, M.A. Sessini<sup>®</sup>, P. Van Hove<sup>®</sup>

### Institut de Physique des 2 Infinis de Lyon (IP2I), Villeurbanne, France

- D. Amram, S. Beauceron, B. Blancon, G. Boudoul, N. Chanon, D. Contardo,
- P. Depasse, C. Dozen, H. El Mamouni, J. Fay, S. Gascon, M. Gouzevitch, C. Greenberg,
- G. Grenier, B. Ille, E. Jourd'huy, I.B. Laktineh, M. Lethuillier, L. Mirabito, S. Perries,
- A. Purohit, M. Vander Donckt, P. Verdier, J. Xiao

### Georgian Technical University, Tbilisi, Georgia

A. Khvedelidze <sup>17</sup>, I. Lomidze , Z. Tsamalaidze <sup>17</sup>

### RWTH Aachen University, I. Physikalisches Institut, Aachen, Germany

V. Botta<sup>®</sup>, L. Feld<sup>®</sup>, K. Klein<sup>®</sup>, M. Lipinski<sup>®</sup>, D. Meuser<sup>®</sup>, A. Pauls<sup>®</sup>, N. Röwert<sup>®</sup>, M. Teroerde<sup>®</sup>

#### RWTH Aachen University, III. Physikalisches Institut A, Aachen, Germany

- S. Diekmann, A. Dodonova, N. Eich, D. Eliseev, F. Engelke, J. Erdmann,
- M. Erdmann , P. Fackeldey , B. Fischer , T. Hebbeker , K. Hoepfner , F. Ivone , A. Jung ,
- M.y. Lee, F. Mausolf, M. Merschmeyer, A. Meyer, S. Mukherjee, D. Noll, F. Nowotny,
- A. Pozdnyakov<sup>®</sup>, Y. Rath, W. Redjeb<sup>®</sup>, F. Rehm, H. Reithler<sup>®</sup>, U. Sarkar<sup>®</sup>, V. Sarkisovi<sup>®</sup>,

- A. Schmidt<sup>®</sup>, A. Sharma<sup>®</sup>, J.L. Spah<sup>®</sup>, A. Stein<sup>®</sup>, F. Torres Da Silva De Araujo<sup>®</sup>, S. Wiedenbeck<sup>®</sup>, S. Zaleski
- RWTH Aachen University, III. Physikalisches Institut B, Aachen, Germany
- C. Dziwok  $^{\odot}$ , G. Flügge  $^{\odot}$ , W. Haj Ahmad  $^{\odot}^{24}$ , T. Kress  $^{\odot}$ , A. Nowack  $^{\odot}$ , O. Pooth  $^{\odot}$ , A. Stahl  $^{\odot}$ ,
- T. Ziemons, A. Zotz

### Deutsches Elektronen-Synchrotron, Hamburg, Germany

- H. Aarup Petersen, M. Aldaya Martin, J. Alimena, S. Amoroso, Y. An, J. Bach,
- S. Baxter, M. Bayatmakou, H. Becerril Gonzalez, O. Behnke, A. Belvedere,
- S. Bhattacharya, F. Blekman, K. Borras, A. Campbell, A. Cardini, C. Cheng,
- F. Colombina, S. Consuegra Rodríguez, G. Correia Silva, M. De Silva, G. Eckerlin,
- D. Eckstein, L.I. Estevez Banos, O. Filatov, E. Gallo, A. Geiser, A. Giraldi, A. Giraldi,
- V. Guglielmi, M. Guthoff, A. Hinzmann, L. Jeppe, B. Kaech, M. Kasemann,
- C. Kleinwort, R. Kogler, M. Komm, D. Krücker, W. Lange, D. Leyva Pernia,
- K. Lipka <sup>©</sup> <sup>27</sup>, W. Lohmann <sup>©</sup> <sup>28</sup>, F. Lorkowski <sup>©</sup>, R. Mankel <sup>©</sup>, I.-A. Melzer-Pellmann <sup>©</sup>,
- M. Mendizabal Morentin, A.B. Meyer, G. Milella, K. Moral Figueroa, A. Mussgiller,
- L.P. Nair, A. Nürnberg, Y. Otarid, J. Park, D. Pérez Adán, E. Ranken, A. Raspereza, A.
- D. Rastorguev, B. Ribeiro Lopes, J. Rübenach, L. Rygaard, A. Saggio, M. Scham 29,26,
- S. Schnake <sup>26</sup>, P. Schütze , C. Schwanenberger <sup>25</sup>, D. Selivanova , K. Sharko ,
- M. Shchedrolosiev<sup>®</sup>, R.E. Sosa Ricardo<sup>®</sup>, D. Stafford, F. Vazzoler<sup>®</sup>, A. Ventura Barroso<sup>®</sup>,
- R. Walsh, D. Wang, Q. Wang, Y. Wen, K. Wichmann, L. Wiens, C. Wissing,
- Y. Yang, A. Zimermmane Castro Santos

#### University of Hamburg, Hamburg, Germany

- A. Albrecht, S. Albrecht, M. Antonello, S. Bein, L. Benato, S. Bollweg, M. Bonanomi, A. Albrecht, S. Bollweg, M. Bonanomi, A. Albrecht, S. Bollweg, M. Bonanomi, S. Bein, L. Benato, S. Bollweg, M. Bonanomi, S. Bein, S. Bollweg, M. Bonanomi, S. Bein, S. Bollweg, M. Bonanomi, S. Bein, S. Bein,
- P. Connor, K. El Morabit, Y. Fischer, E. Garutti, A. Grohsjean, J. Haller,
- H.R. Jabusch, G. Kasieczka, P. Keicher, R. Klanner, W. Korcari, T. Kramer, C.c. Kuo,
- V. Kutzner, F. Labe, J. Lange, A. Lobanov, C. Matthies, L. Moureaux, M. Mrowietz,
- A. Nigamova, Y. Nissan, A. Paasch, K.J. Pena Rodriguez, T. Quadfasel, B. Raciti,
- M. Rieger, D. Savoiu, J. Schindler, P. Schleper, M. Schröder, J. Schwandt, ,
- M. Sommerhalder, H. Stadie, G. Steinbrück, A. Tews, M. Wolf

### Karlsruher Institut fuer Technologie, Karlsruhe, Germany

- S. Brommer, M. Burkart, E. Butz, T. Chwalek, A. Dierlamm, A. Droll, N. Faltermann,
- M. Giffels, A. Gottmann, F. Hartmann, R. Hofsaess, M. Horzela, U. Husemann,
- J. Kieseler, M. Klute, R. Koppenhöfer, J.M. Lawhorn, M. Link, A. Lintuluoto,
- B. Maier, S. Maier, S. Mitra, M. Mormile, Th. Müller, M. Neukum, M. Oh,
- E. Pfeffer, M. Presilla, G. Quast, K. Rabbertz, B. Regnery, N. Shadskiy, I. Shvetsov,
- H.J. Simonis, M. Toms, N. Trevisani, R.F. Von Cube, M. Wassmer, S. Wieland,
- F. Wittig, R. Wolf, X. Zuo

### Institute of Nuclear and Particle Physics (INPP), NCSR Demokritos, Aghia Paraskevi, Greece

G. Anagnostou, G. Daskalakis, A. Kyriakis, A. Papadopoulos<sup>30</sup>, A. Stakia

### National and Kapodistrian University of Athens, Athens, Greece

P. Kontaxakis<sup>®</sup>, G. Melachroinos, Z. Painesis<sup>®</sup>, A. Panagiotou, I. Papavergou<sup>®</sup>, I. Paraskevas<sup>®</sup>,

N. Saoulidou, K. Theofilatos, E. Tziaferi, K. Vellidis, I. Zisopoulos

### National Technical University of Athens, Athens, Greece

G. Bakas<sup>10</sup>, T. Chatzistavrou, G. Karapostoli<sup>10</sup>, K. Kousouris<sup>10</sup>, I. Papakrivopoulos<sup>10</sup>,

E. Siamarkou, G. Tsipolitis, A. Zacharopoulou

### University of Ioánnina, Ioánnina, Greece

K. Adamidis, I. Bestintzanos, I. Evangelou, C. Foudas, C. Kamtsikis, P. Katsoulis, P. Kokkas, C. Kamtsikis, P. Katsoulis, P. K

P.G. Kosmoglou Kioseoglou, N. Manthos, I. Papadopoulos, J. Strologas

### HUN-REN Wigner Research Centre for Physics, Budapest, Hungary

M. Bartók <sup>31</sup>, C. Hajdu, D. Horvath <sup>32,33</sup>, K. Márton, A.J. Rádl <sup>34</sup>, F. Sikler, F. Sikler, F. Sikler, R. S

V. Veszpremi

## MTA-ELTE Lendület CMS Particle and Nuclear Physics Group, Eötvös Loránd University, Budapest, Hungary

M. Csanád, K. Farkas, A. Fehérkuti, M.M.A. Gadallah, Á. Kadlecsik, P. Major,

K. Mandal, G. Pásztor, G.I. Veres

### Faculty of Informatics, University of Debrecen, Debrecen, Hungary

P. Raics, B. Ujvari, G. Zilizi

### Institute of Nuclear Research ATOMKI, Debrecen, Hungary

G. Bencze, S. Czellar, J. Molnar, Z. Szillasi

### Karoly Robert Campus, MATE Institute of Technology, Gyongyos, Hungary

T. Csorgo <sup>1</sup><sup>35</sup>, F. Nemes <sup>1</sup><sup>35</sup>, T. Novak <sup>1</sup>

### Panjab University, Chandigarh, India

J. Babbar, S. Bansal, S.B. Beri, V. Bhatnagar, G. Chaudhary, S. Chauhan,

N. Dhingra <sup>37</sup>, A. Kaur , A. Kaur , H. Kaur , M. Kaur , S. Kumar , K. Sandeep ,

T. Sheokand, J.B. Singh, A. Singla

#### University of Delhi, Delhi, India

A. Ahmed 🗓 , A. Bhardwaj 🗓 , A. Chhetri 🗓 , B.C. Choudhary 🗓 , A. Kumar 🗓 , A. Kumar 🕞 ,

M. Naimuddin, K. Ranjan, S. Saumya

#### Saha Institute of Nuclear Physics, HBNI, Kolkata, India

S. Baradia, S. Barman, S. Bhattacharya, S. Das Gupta, S. Dutta, S. Dutta, S. Sarkar

### Indian Institute of Technology Madras, Madras, India

 $M.M.\ Ameen @,\ P.K.\ Behera @,\ S.C.\ Behera @,\ S.\ Chatterjee @,\ G.\ Dash @,\ P.\ Jana @,\ P.\ Kalbhor @,$ 

S. Kamble, J.R. Komaragiri, D. Kumar, P.R. Pujahari, N.R. Saha, A. Sharma,

A.K. Sikdar<sup>®</sup>, R.K. Singh, P. Verma, S. Verma<sup>®</sup>, A. Vijay

### Tata Institute of Fundamental Research-A, Mumbai, India

S. Dugad, M. Kumar, G.B. Mohanty, M. Shelake, P. Suryadevara

### Tata Institute of Fundamental Research-B, Mumbai, India

A. Bala, S. Banerjee, R.M. Chatterjee, R.K. Dewanjee, M. Guchait, Sh. Jain, A. Jaiswal, S. Kumar, G. Majumder, K. Mazumdar, S. Parolia, A. Thachayath

### National Institute of Science Education and Research, An OCC of Homi Bhabha National Institute, Bhubaneswar, Odisha, India

S. Bahinipati  $\mathbb{D}^{41}$ , C. Kar  $\mathbb{D}$ , D. Maity  $\mathbb{D}^{42}$ , P. Mal  $\mathbb{D}$ , T. Mishra  $\mathbb{D}$ , V.K. Muraleedharan Nair Bindhu  $\mathbb{D}^{42}$ , K. Naskar  $\mathbb{D}^{42}$ , A. Nayak  $\mathbb{D}^{42}$ , S. Nayak, P. Sadangi, S.K. Swain  $\mathbb{D}$ , S. Varghese  $\mathbb{D}^{42}$ , D. Vats  $\mathbb{D}^{42}$ 

### Indian Institute of Science Education and Research (IISER), Pune, India

S. Acharya <sup>6</sup> <sup>43</sup>, A. Alpana <sup>6</sup>, S. Dube <sup>6</sup>, B. Gomber <sup>6</sup> <sup>43</sup>, P. Hazarika <sup>6</sup>, B. Kansal <sup>6</sup>, A. Laha <sup>6</sup>, B. Sahu <sup>6</sup> <sup>43</sup>, S. Sharma <sup>6</sup>, K.Y. Vaish

### Isfahan University of Technology, Isfahan, Iran

H. Bakhshiansohi • 44, A. Jafari • 45, M. Zeinali • 46

### Institute for Research in Fundamental Sciences (IPM), Tehran, Iran

S. Bashiri, S. Chenarani  $^{647}$ , S.M. Etesami  $^{6}$ , Y. Hosseini  $^{6}$ , M. Khakzad  $^{6}$ , E. Khazaie  $^{648}$ , M. Mohammadi Najafabadi  $^{6}$ , S. Tizchang  $^{6}$ 

### University College Dublin, Dublin, Ireland

M. Grunewald •

### INFN Sezione di Bari<sup>a</sup>, Università di Bari<sup>b</sup>, Politecnico di Bari<sup>c</sup>, Bari, Italy

M. Abbrescia  $\mathbb{D}^{a,b}$ , R. Aly  $\mathbb{D}^{a,c,49}$ , A. Colaleo  $\mathbb{D}^{a,b}$ , D. Creanza  $\mathbb{D}^{a,c}$ , B. D'Anzi  $\mathbb{D}^{a,b}$ ,

N. De Filippis $\mathbb{O}^{a,c}$ , M. De Palma $\mathbb{O}^{a,b}$ , A. Di Florio $\mathbb{O}^{a,c}$ , W. Elmetenawee $\mathbb{O}^{a,b,49}$ , L. Fiore $\mathbb{O}^a$ ,

G. Iaselli $^{\bullet a,c}$ , M. Louka $^{a,b}$ , G. Maggi $^{\bullet a,c}$ , M. Maggi $^{\bullet a}$ , I. Margjeka $^{\bullet a,b}$ , V. Mastrapasqua $^{\bullet a,b}$ ,

S.  $\text{My}^{\textcircled{\tiny{a,b}}}$ , S.  $\text{Nuzzo}^{\textcircled{\tiny{a,b}}}$ , A. Pellecchia $\textcircled{\tiny{a,b}}$ , A. Pompili $\textcircled{\tiny{a,b}}$ , G. Pugliese $\textcircled{\tiny{a,c}}$ , R. Radogna $\textcircled{\tiny{a,b}}$ 

G. Ramirez-Sanchez  $\mathbb{O}^{a,c}$ , D. Ramos  $\mathbb{O}^a$ , A. Ranieri  $\mathbb{O}^a$ , L. Silvestris  $\mathbb{O}^a$ , F.M. Simone  $\mathbb{O}^{a,b}$ ,

Ü. Sözbilir $^{lacktriangle}{}^a$ , A. Stamerra $^{lacktriangle}{}^a$ , D. Troiano $^{lacktriangle}{}^a$ , R. Venditti $^{lacktriangle}{}^a$ , P. Verwilligen $^{lacktriangle}{}^a$ , A. Zaza $^{lacktriangle}{}^{a,b}$ 

### INFN Sezione di Bologna $^a,$ Università di Bologna $^b,$ Bologna, Italy

G. Abbiendi <sup>©</sup><sup>a</sup>, C. Battilana <sup>©</sup><sup>a,b</sup>, D. Bonacorsi <sup>©</sup><sup>a,b</sup>, L. Borgonovi <sup>©</sup><sup>a</sup>, P. Capiluppi <sup>©</sup><sup>a,b</sup>, A. Castro <sup>©</sup><sup>a,b</sup>, F.R. Cavallo <sup>©</sup><sup>a</sup>, M. Cuffiani <sup>©</sup><sup>a,b</sup>, G.M. Dallavalle <sup>©</sup><sup>a</sup>, T. Diotalevi <sup>©</sup><sup>a,b</sup>, F. Fabbri <sup>©</sup><sup>a</sup>.

A. Fanfani  $\bigcirc^{a,b}$ , D. Fasanella  $\bigcirc^{a,b}$ , P. Giacomelli  $\bigcirc^{a}$ , L. Giommi  $\bigcirc^{a,b}$ , C. Grandi  $\bigcirc^{a}$ , L. Guiducci  $\bigcirc^{a,b}$ ,

S. Lo Meo $\textcircled{o}^{a,50}$ , M. Loruss $\textcircled{o}^{a,b}$ , L. Lunerti $\textcircled{o}^{a,b}$ , S. Marcellini $\textcircled{o}^{a}$ , G. Masetti $\textcircled{o}^{a}$ , F.L. Navarria $\textcircled{o}^{a,b}$ ,

A. Perrotta  $\mathbb{D}^a$ , F. Primavera  $\mathbb{D}^{a,b}$ , A.M. Rossi  $\mathbb{D}^{a,b}$ , S. Rossi Tisbeni  $\mathbb{D}^{a,b}$ , T. Rovelli  $\mathbb{D}^{a,b}$ , G.P. Siroli  $\mathbb{D}^{a,b}$ 

### INFN Sezione di Catania<sup>a</sup>, Università di Catania<sup>b</sup>, Catania, Italy

S. Costa $^{\bullet a,b,51}$ , A. Di Mattia $^{\bullet a}$ , R. Potenza $^{a,b}$ , A. Tricomi $^{\bullet a,b,51}$ , C. Tuve $^{\bullet a,b}$ 

### INFN Sezione di Firenze<sup>a</sup>, Università di Firenze<sup>b</sup>, Firenze, Italy

- P. Assiouras  $\mathbb{D}^a$ , G. Barbagli  $\mathbb{D}^a$ , G. Bardelli  $\mathbb{D}^{a,b}$ , B. Camaiani  $\mathbb{D}^{a,b}$ , A. Cassese  $\mathbb{D}^a$ , R. Ceccarelli  $\mathbb{D}^a$ ,
- V. Ciulli $\mathbb{D}^{a,b}$ , C. Civinini $\mathbb{D}^a$ , R. D'Alessandro $\mathbb{D}^{a,b}$ , E. Focardi $\mathbb{D}^{a,b}$ , T. Kello $^a$ , G. Latino $\mathbb{D}^{a,b}$ ,
- P. Lenzi $\mathbb{O}^{a,b}$ , M. Lizzo $\mathbb{O}^a$ , M. Meschini $\mathbb{O}^a$ , S. Paoletti $\mathbb{O}^a$ , A. Papanastassiou $^{a,b}$ , G. Sguazzoni $\mathbb{O}^a$ , L. Viliani $\mathbb{O}^a$

### INFN Laboratori Nazionali di Frascati, Frascati, Italy

L. Benussi, S. Bianco, S. Meola, D. Piccolo

### INFN Sezione di Genova<sup>a</sup>, Università di Genova<sup>b</sup>, Genova, Italy

P. Chatagnon a, F. Ferro a, E. Robutti a, S. Tosi a, b

### INFN Sezione di Milano-Bicocca<sup>a</sup>, Università di Milano-Bicocca<sup>b</sup>, Milano, Italy

- A. Benaglia a, G. Boldrini a, F. Brivio a, F. Cetorelli a, F. De Guio a, M.E. Dinardo a,
- P. Dini $^{\bullet a}$ , S. Gennai $^{\bullet a}$ , R. Gerosa $^{\bullet a,b}$ , A. Ghezzi $^{\bullet a,b}$ , P. Govoni $^{\bullet a,b}$ , L. Guzzi $^{\bullet a}$ ,
- M.T. Lucchini $^{\bullet a,b}$ , M. Malberti $^{\bullet a}$ , S. Malvezzi $^{\bullet a}$ , A. Massironi $^{\bullet a}$ , D. Menasce $^{\bullet a}$ , L. Moroni $^{\bullet a}$ ,
- M. Paganoni $\mathbb{D}^{a,b}$ , S. Palluotto $\mathbb{D}^{a,b}$ , D. Pedrini $\mathbb{D}^{a}$ , B.S. Pinolini $^{a}$ , G. Pizzati $^{a,b}$ , S. Ragazzi $\mathbb{D}^{a,b}$ ,
- T. Tabarelli de Fatis $\mathbb{D}^{a,b}$

# INFN Sezione di Napoli<sup>a</sup>, Università di Napoli 'Federico II'<sup>b</sup>, Napoli, Italy; Università della Basilicata<sup>c</sup>, Potenza, Italy; Scuola Superiore Meridionale (SSM)<sup>d</sup>, Napoli, Italy

S. Buontempo  $\mathbb{D}^a$ , A. Cagnotta  $\mathbb{D}^{a,b}$ , F. Carnevali $\mathbb{D}^{a,b}$ , N. Cavallo  $\mathbb{D}^{a,c}$ , F. Fabozzi  $\mathbb{D}^{a,c}$ , A.O.M. Iorio  $\mathbb{D}^{a,b}$ , L. Lista  $\mathbb{D}^{a,b,53}$ , P. Paolucci  $\mathbb{D}^{a,30}$ , B. Rossi  $\mathbb{D}^a$ , C. Sciacca  $\mathbb{D}^{a,b}$ 

# INFN Sezione di Padova<sup>a</sup>, Università di Padova<sup>b</sup>, Padova, Italy; Università di Trento<sup>c</sup>, Trento, Italy

- R. Ardino  $\mathbb{D}^a$ , P. Azzi  $\mathbb{D}^a$ , N. Bacchetta  $\mathbb{D}^{a,54}$ , D. Bisello  $\mathbb{D}^{a,b}$ , P. Bortignon  $\mathbb{D}^a$ , G. Bortolato  $\mathbb{D}^a$ ,
- A. Bragagnolo a, A.C.M. Bulla a, R. Carlin a, P. Checchia a, T. Dorigo a, F. Gasparini a, F. Gasparini
- U. Gasparini $\mathbb{D}^{a,b}$ , M. Gulmini $\mathbb{D}^{a,55}$ , E. Lusiani $\mathbb{D}^a$ , M. Margoni $\mathbb{D}^{a,b}$ , F. Marini $\mathbb{D}^a$ , G. Maron $\mathbb{D}^{a,55}$ ,
- M. Migliorini  $\mathbb{D}^{a,b}$ , J. Pazzini  $\mathbb{D}^{a,b}$ , P. Ronchese  $\mathbb{D}^{a,b}$ , R. Rossin  $\mathbb{D}^{a,b}$ , F. Simonetto  $\mathbb{D}^{a,b}$ , G. Strong  $\mathbb{D}^{a}$ ,
- M.  $Tosi \bigcirc^{a,b}$ , A.  $Triossi \bigcirc^{a,b}$ , S.  $Ventura \bigcirc^{a}$ , M.  $Zanetti \bigcirc^{a,b}$ , P.  $Zotto \bigcirc^{a,b}$ , A.  $Zucchetta \bigcirc^{a,b}$

### INFN Sezione di Pavia<sup>a</sup>, Università di Pavia<sup>b</sup>, Pavia, Italy

S. Abu Zeid  $\mathbb{D}^{a,56}$ , C. Aimè  $\mathbb{D}^{a,b}$ , A. Braghieri  $\mathbb{D}^a$ , S. Calzaferri  $\mathbb{D}^a$ , D. Fiorina  $\mathbb{D}^a$ , P. Montagna  $\mathbb{D}^{a,b}$ , V. Re  $\mathbb{D}^a$ , C. Riccardi  $\mathbb{D}^{a,b}$ , P. Salvini  $\mathbb{D}^a$ , I. Vai  $\mathbb{D}^{a,b}$ , P. Vitulo  $\mathbb{D}^{a,b}$ 

### INFN Sezione di Perugia $^a,$ Università di Perugia $^b,$ Perugia, Italy

# INFN Sezione di Pisa<sup>a</sup>, Università di Pisa<sup>b</sup>, Scuola Normale Superiore di Pisa<sup>c</sup>, Pisa, Italy; Università di Siena<sup>d</sup>, Siena, Italy

C.A. Alexe  $\mathbb{O}^{a,c}$ , P. Asenov  $\mathbb{O}^{a,b}$ , P. Azzurri  $\mathbb{O}^a$ , G. Bagliesi  $\mathbb{O}^a$ , R. Bhattacharya  $\mathbb{O}^a$ , L. Bianchini  $\mathbb{O}^{a,b}$ , T. Boccali  $\mathbb{O}^a$ , E. Bossini  $\mathbb{O}^a$ , D. Bruschini  $\mathbb{O}^{a,c}$ , R. Castaldi  $\mathbb{O}^a$ , M.A. Ciocci  $\mathbb{O}^{a,b}$ , M. Cipriani  $\mathbb{O}^{a,b}$ ,

```
V. D'Amante o<sup>a,d</sup>, R. Dell'Orso o<sup>a</sup>, S. Donato o<sup>a</sup>, A. Giassi o<sup>a</sup>, F. Ligabue o<sup>a,c</sup>,
D. Matos Figueiredo \bigcirc^a, A. Messineo \bigcirc^{a,b}, M. Musich \bigcirc^{a,b}, F. Palla \bigcirc^a, A. Rizzi \bigcirc^{a,b},
G. Rolandi \mathbb{D}^{a,c}, S. Roy Chowdhury \mathbb{D}^a, T. Sarkar \mathbb{D}^a, A. Scribano \mathbb{D}^a, P. Spagnolo \mathbb{D}^a,
R. Tenchini \mathbb{D}^a, G. Tonelli \mathbb{D}^{a,b}, N. Turini \mathbb{D}^{a,d}, F. Vaselli \mathbb{D}^{a,c}, A. Venturi \mathbb{D}^a, P.G. Verdini \mathbb{D}^a
INFN Sezione di Roma<sup>a</sup>, Sapienza Università di Roma<sup>b</sup>, Roma, Italy
C. Baldenegro Barrera a<sup>a,b</sup>, P. Barria a<sup>a</sup>, C. Basile a<sup>a,b</sup>, M. Campana a<sup>a,b</sup>, F. Cavallari a<sup>a</sup>,
L. Cunqueiro Mendez o<sup>a,b</sup>, D. Del Re o<sup>a,b</sup>, E. Di Marco o<sup>a</sup>, M. Diemoz o<sup>a</sup>, F. Errico o<sup>a,b</sup>,
E. Longo \mathbb{D}^{a,b}, P. Meridiani \mathbb{D}^{a}, J. Mijuskovic \mathbb{D}^{a,b}, G. Organtini \mathbb{D}^{a,b}, F. Pandolfi \mathbb{D}^{a},
R. Paramatti • a, C. Quaranta • S. Rahatlou • C. Rovelli • F. Santanastasio • A, C. Rovelli • F. Santanastasio
L. Soffi\bigcirc^a
INFN Sezione di Torino<sup>a</sup>, Università di Torino<sup>b</sup>, Torino, Italy; Università del
Piemonte Orientale<sup>c</sup>, Novara, Italy
N. Amapane \mathbb{D}^{a,b}, R. Arcidiacono \mathbb{D}^{a,c}, S. Argiro \mathbb{D}^{a,b}, M. Arneodo \mathbb{D}^{a,c}, N. Bartosik \mathbb{D}^a,
R. Bellan a, A. Bellora a, C. Biino a, C. Borca a, N. Cartiglia a, M. Costa a,
R. Covarelli a, N. Demaria a, L. Finco a, M. Grippo a, B. Kiani a, F. Legger a,
F. Luongo o<sup>a,b</sup>, C. Mariotti o<sup>a</sup>, L. Markovic o<sup>a,b</sup>, S. Maselli o<sup>a</sup>, A. Mecca o<sup>a,b</sup>, L. Menzio o<sup>a,b</sup>,
E. Migliore • a,b, M. Monteno • R. Mulargia • M.M. Obertino • G. Ortona • L. Pacher • a,b,
N. Pastrone \mathbb{D}^a, M. Pelliccioni \mathbb{D}^a, M. Ruspa \mathbb{D}^{a,c}, F. Siviero \mathbb{D}^{a,b}, V. Sola \mathbb{D}^{a,b}, A. Solano \mathbb{D}^{a,b},
A. Staiano a, C. Tarricone a, D. Trocino a, G. Umoret a, E. Vlasov a, R. White a, b
INFN Sezione di Trieste<sup>a</sup>, Università di Trieste<sup>b</sup>, Trieste, Italy
S. Belforte a, V. Candelise a, M. Casarsa a, F. Cossutti a, K. De Leo a, G. Della Ricca a, b
Kyungpook National University, Daegu, Korea
S. Dogra D, J. Hong D, C. Huh D, B. Kim D, D.H. Kim D, J. Kim, D. Lee, H. Lee, S.W. Lee D,
C.S. Moon, Y.D. Oh, M.S. Ryu, S. Sekmen, B. Tae, Y.C. Yang
Department of Mathematics and Physics — GWNU, Gangneung, Korea
M.S. Kim
Chonnam National University, Institute for Universe and Elementary Particles,
Kwangju, Korea
G. Bak, P. Gwak, H. Kim, D.H. Moon
Hanyang University, Seoul, Korea
E. Asilar, J. Choi, D. Kim, T.J. Kim, J.A. Merlin
Korea University, Seoul, Korea
S. Choi, S. Han, B. Hong, K. Lee, K.S. Lee, S. Lee, J. Park, S.K. Park, J. Yoo
Kyung Hee University, Department of Physics, Seoul, Korea
J. Goh, S. Yang
Sejong University, Seoul, Korea
```

H. S. Kim, Y. Kim, S. Lee

### Seoul National University, Seoul, Korea

J. Almond, J.H. Bhyun, J. Choi $^{\odot}$ , W. Jun $^{\odot}$ , J. Kim $^{\odot}$ , S. Ko $^{\odot}$ , H. Kwon $^{\odot}$ , H. Lee $^{\odot}$ , J. Lee $^{\odot}$ ,

J. Lee, B.H. Oh, S.B. Oh, H. Seo, U.K. Yang, I. Yoon

### University of Seoul, Seoul, Korea

W. Jang, D.Y. Kang, Y. Kang, S. Kim, B. Ko, J.S.H. Lee, Y. Lee, I.C. Park, Y. Roh, I.J. Watson

### Yonsei University, Department of Physics, Seoul, Korea

S. Ha, H.D. Yoo

### Sungkyunkwan University, Suwon, Korea

M. Choi, M.R. Kim, H. Lee, Y. Lee, I. Yu

## College of Engineering and Technology, American University of the Middle East (AUM), Dasman, Kuwait

T. Beyrouthy

### Riga Technical University, Riga, Latvia

K. Dreimanis, A. Gaile, G. Pikurs, A. Potrebko, M. Seidel

### University of Latvia (LU), Riga, Latvia

N.R. Strautnieks

### Vilnius University, Vilnius, Lithuania

M. Ambrozas<sup>10</sup>, A. Juodagalvis<sup>10</sup>, A. Rinkevicius<sup>10</sup>, G. Tamulaitis<sup>10</sup>

### National Centre for Particle Physics, Universiti Malaya, Kuala Lumpur, Malaysia

N. Bin Norjoharuddeen, I. Yusuff<sup>58</sup>, Z. Zolkapli

#### Universidad de Sonora (UNISON), Hermosillo, Mexico

J.F. Benitez, A. Castaneda Hernandez, H.A. Encinas Acosta, L.G. Gallegos Maríñez, M. León Coello, J.A. Murillo Quijada, A. Sehrawat, L. Valencia Palomo

#### Centro de Investigacion y de Estudios Avanzados del IPN, Mexico City, Mexico

G. Ayala<sup>®</sup>, H. Castilla-Valdez<sup>®</sup>, H. Crotte Ledesma, E. De La Cruz-Burelo<sup>®</sup>,

I. Heredia-De La Cruz <sup>59</sup>, R. Lopez-Fernandez , C.A. Mondragon Herrera, A. Sánchez Hernández

#### Universidad Iberoamericana, Mexico City, Mexico

C. Oropeza Barrera, M. Ramírez García

#### Benemerita Universidad Autonoma de Puebla, Puebla, Mexico

I. Bautista, I. Pedraza, H.A. Salazar Ibarguen, C. Uribe Estrada

### University of Montenegro, Podgorica, Montenegro

I. Bubanja, N. Raicevic 🗅

### University of Canterbury, Christchurch, New Zealand P.H. Butler<sup>©</sup>

### National Centre for Physics, Quaid-I-Azam University, Islamabad, Pakistan

A. Ahmad, M.I. Asghar, A. Awais, M.I.M. Awan, H.R. Hoorani, W.A. Khan

### AGH University of Krakow, Faculty of Computer Science, Electronics and Telecommunications, Krakow, Poland

V. Avati, L. Grzanka, M. Malawski

### National Centre for Nuclear Research, Swierk, Poland

H. Bialkowska 👨 , M. Bluj 👨 , B. Boimska 👨 , M. Górski 👨 , M. Kazana 👨 , M. Szleper 👨 , P. Zalewski 👨

### Institute of Experimental Physics, Faculty of Physics, University of Warsaw, Warsaw, Poland

K. Bunkowski, K. Doroba, A. Kalinowski, M. Konecki, J. Krolikowski, A. Muhammad

### Warsaw University of Technology, Warsaw, Poland

K. Pozniak, W. Zabolotny

### Laboratório de Instrumentação e Física Experimental de Partículas, Lisboa, Portugal

- M. Araujo, D. Bastos, C. Beirão Da Cruz E Silva, A. Boletti, M. Bozzo, T. Camporesi, T. Camporesi,
- G. Da Molin<sup>®</sup>, P. Faccioli<sup>®</sup>, M. Gallinaro<sup>®</sup>, J. Hollar<sup>®</sup>, N. Leonardo<sup>®</sup>, G.B. Marozzo,
- T. Niknejad, A. Petrilli, M. Pisano, J. Seixas, J. Varela, J.W. Wulff

### Faculty of Physics, University of Belgrade, Belgrade, Serbia

P. Adzic, P. Milenovic

### VINCA Institute of Nuclear Sciences, University of Belgrade, Belgrade, Serbia

M. Dordevic, J. Milosevic, V. Rekovic

## Centro de Investigaciones Energéticas Medioambientales y Tecnológicas (CIEMAT), Madrid, Spain

- M. Aguilar-Benitez, J. Alcaraz Maestre, Cristina F. Bedoya, Oliver M. Carretero,
- M. Cepeda, M. Cerrada, N. Colino, B. De La Cruz, A. Delgado Peris,
- A. Escalante Del Valle, D. Fernández Del Vallo, J.P. Fernández Ramos, J. Flix, M.C. Fouz
- O. Gonzalez Lopez, S. Goy Lopez, J.M. Hernandez, M.I. Josa, D. Moran,
- C. M. Morcillo Perez , Á. Navarro Tobar , C. Perez Dengra , A. Pérez-Calero Yzquierdo ,
- J. Puerta Pelayo, I. Redondo, D.D. Redondo Ferrero, L. Romero, S. Sánchez Navas,
- L. Urda Gómez, J. Vazquez Escobar, C. Willmott

### Universidad Autónoma de Madrid, Madrid, Spain

J.F. de Trocóniz •

### Universidad de Oviedo, Instituto Universitario de Ciencias y Tecnologías Espaciales de Asturias (ICTEA), Oviedo, Spain

- B. Alvarez Gonzalez, J. Cuevas, J. Fernandez Menendez, S. Folgueras,
- I. Gonzalez Caballero, J.R. González Fernández, P. Leguina, E. Palencia Cortezon,
- C. Ramón Álvarez  $^{\textcircled{\tiny{0}}}$ , V. Rodríguez Bouza  $^{\textcircled{\tiny{0}}}$ , A. Soto Rodríguez  $^{\textcircled{\tiny{0}}}$ , A. Trapote  $^{\textcircled{\tiny{0}}}$ , C. Vico Villalba  $^{\textcircled{\tiny{0}}}$ ,
- P. Vischia

## Instituto de Física de Cantabria (IFCA), CSIC-Universidad de Cantabria, Santander, Spain

- S. Bhowmik, S. Blanco Fernández, J.A. Brochero Cifuentes, I.J. Cabrillo, A. Calderon,
- J. Duarte Campderros, M. Fernandez, G. Gomez, C. Lasaosa García, R. Lopez Ruiz,
- C. Martinez Rivero, P. Martinez Ruiz del Arbol, F. Matorras, P. Matorras Cuevas,
- E. Navarrete Ramos 📵, J. Piedra Gomez 🗓, L. Scodellaro 🗓, I. Vila 🗓, J.M. Vizan Garcia 🗓

### University of Colombo, Colombo, Sri Lanka

M.K. Jayananda, B. Kailasapathy, D.U.J. Sonnadara, D.D.C. Wickramarathna

### University of Ruhuna, Department of Physics, Matara, Sri Lanka

W.G.D. Dharmaratna 61, K. Liyanage 1, N. Perera 1, N. Wickramage 1

### CERN, European Organization for Nuclear Research, Geneva, Switzerland

- D. Abbaneo, C. Amendola, E. Auffray, G. Auzinger, J. Baechler, D. Barney,
- A. Bermúdez Martínez, M. Bianco, B. Bilin, A.A. Bin Anuar, A. Bocci, C. Botta,
- E. Brondolin, C. Caillol, G. Cerminara, N. Chernyavskaya, D. d'Enterria, A. Dabrowski, A. Dabrowski,
- A. David, A. De Roeck, M.M. Defranchis, M. Deile, M. Dobson, L. Forthomme,
- G. Franzoni, W. Funk, S. Giani, D. Gigi, K. Gill, F. Glege, L. Gouskos, M. Haranko,
- J. Hegeman, B. Huber, V. Innocente, T. James, P. Janot, O. Kaluzinska, S. Laurila,
- P. Lecoq, E. Leutgeb, C. Lourenço, L. Malgeri, M. Mannelli, A.C. Marini,
- M. Matthewman, A. Mehta, F. Meijers, S. Mersi, E. Meschi, V. Milosevic, F. Monti,
- F. Moortgat, M. Mulders, I. Neutelings, S. Orfanelli, F. Pantaleo, G. Petrucciani,
- A. Pfeiffer , M. Pierini , D. Piparo , H. Qu , D. Rabady , M. Rovere , H. Sakulin ,
- S. Scarfi, C. Schwick, M. Selvaggi, A. Sharma, K. Shchelina, P. Silva, P. Sphicas, P. Sphicas
- A.G. Stahl Leiton, A. Steen, S. Summers, D. Treille, P. Tropea, A. Tsirou, D. Walter,
- J. Wanczyk 663, J. Wang, S. Wuchterl P. Zehetner, P. Zejdl, W.D. Zeuner

### Paul Scherrer Institut, Villigen, Switzerland

T. Bevilacqua • 64, L. Caminada • 64, A. Ebrahimi •, W. Erdmann •, R. Horisberger •, Q. Ingram •, H.C. Kaestli •, D. Kotlinski •, C. Lange •, M. Missiroli • 64, L. Noehte • 64, T. Rohe •

### ETH Zurich — Institute for Particle Physics and Astrophysics (IPA), Zurich, Switzerland

T.K. Aarrestad, K. Androsov, M. Backhaus, G. Bonomelli, A. Calandri, C. Cazzaniga, K. Datta, P. De Bryas Dexmiers D'archiac, A. De Cosa, G. Dissertori, M. Dittmar, M. Donegà, F. Eble, M. Galli, K. Gedia, F. Glessgen, C. Grab, N. Härringer, T.G. Harte, D. Hits, W. Lustermann, A.-M. Lyon, R.A. Manzoni, M. Marchegiani,

- L. Marchese, C. Martin Perez, A. Mascellani, F. Nessi-Tedaldi, F. Pauss, V. Perovic, V. Perovic,
- S. Pigazzini, C. Reissel, T. Reitenspiess, B. Ristic, F. Riti, R. Seidita,
- J. Steggemann 6<sup>63</sup>, D. Valsecchi , R. Wallny 6

### Universität Zürich, Zurich, Switzerland

- C. Amsler 65, P. Bärtschi , M.F. Canelli, K. Cormier, J.K. Heikkilä, M. Huwiler,
- W. Jin, A. Jofrehei, B. Kilminster, S. Leontsinis, S.P. Liechti, A. Macchiolo,
- P. Meiring, F. Meng, U. Molinatti, A. Reimers, P. Robmann, S. Sanchez Cruz,
- M. Senger, E. Shokr, F. Stäger, Y. Takahashi, R. Tramontano

### National Central University, Chung-Li, Taiwan

C. Adloff<sup>66</sup>, D. Bhowmik, C.M. Kuo, W. Lin, P.K. Rout, P.C. Tiwari, S.S. Yu

### National Taiwan University (NTU), Taipei, Taiwan

- L. Ceard, Y. Chao, K.F. Chen, P.s. Chen, Z.g. Chen, A. De Iorio, W.-S. Hou, T.h. Hsu,
- Y.w. Kao, S. Karmakar, R. Khurana, G. Kole, Y.y. Li, R.-S. Lu, E. Paganis, X.f. Su, X.f. Su,
- J. Thomas-Wilsker, L.s. Tsai, H.y. Wu, E. Yazgan

# High Energy Physics Research Unit, Department of Physics, Faculty of Science, Chulalongkorn University, Bangkok, Thailand

C. Asawatangtrakuldee, N. Srimanobhas, V. Wachirapusitanand

## Çukurova University, Physics Department, Science and Art Faculty, Adana, Turkey

- D. Agyel<sup>®</sup>, F. Boran<sup>®</sup>, Z.S. Demiroglu<sup>®</sup>, F. Dolek<sup>®</sup>, I. Dumanoglu<sup>®</sup>, E. Eskut<sup>®</sup>, Y. Guler<sup>®</sup>,
- E. Gurpinar Guler <sup>68</sup>, C. Isik , O. Kara, A. Kayis Topaksu, U. Kiminsu, G. Onengut,
- K. Ozdemir <sup>69</sup>, A. Polatoz , B. Tali <sup>70</sup>, U.G. Tok , S. Turkcapar , E. Uslan , I.S. Zorbakir

#### Middle East Technical University, Physics Department, Ankara, Turkey

G. Sokmen, M. Yalvac<sup>1</sup>

### Bogazici University, Istanbul, Turkey

B. Akgun, I.O. Atakisi, E. Gülmez, M. Kaya, O. Kaya, S. Tekten, S. Tekten, E. Gülmez, M. Kaya, O. Kaya, S. Tekten, S. Tek

### Istanbul Technical University, Istanbul, Turkey

A. Cakir, K. Cankocak, G.G. Dincer, Y. Komurcu, S. Sen, Sen

### Istanbul University, Istanbul, Turkey

- O. Aydilek <sup>6</sup> <sup>24</sup>, S. Cerci <sup>6</sup> <sup>70</sup>, V. Epshteyn <sup>6</sup>, B. Hacisahinoglu <sup>6</sup>, I. Hos <sup>6</sup> <sup>77</sup>, B. Kaynak <sup>6</sup>,
- S. Ozkorucuklu, O. Potok, H. Sert, C. Simsek, C. Zorbilmez

### Yildiz Technical University, Istanbul, Turkey

B. Isildak <sup>0</sup><sup>78</sup>, D. Sunar Cerci <sup>0</sup><sup>70</sup>

### Institute for Scintillation Materials of National Academy of Science of Ukraine, Kharkiv, Ukraine

A. Boyaryntsev, B. Grynyov

### National Science Centre, Kharkiv Institute of Physics and Technology, Kharkiv, Ukraine

L. Levchuk

### University of Bristol, Bristol, United Kingdom

D. Anthony, J.J. Brooke, A. Bundock, F. Bury, E. Clement, D. Cussans, H. Flacher, M. Glowacki, J. Goldstein, H.F. Heath, M.-L. Holmberg, L. Kreczko, S. Paramesvaran, L. Robertshaw, S. Seif El Nasr-Storey, V.J. Smith, N. Stylianou, K. Walkingshaw Pass

### Rutherford Appleton Laboratory, Didcot, United Kingdom

A.H. Ball, K.W. Bell, A. Belyaev, C. Brew, R.M. Brown, D.J.A. Cockerill, C. Cooke, K.V. Ellis, K. Harder, S. Harper, J. Linacre, K. Manolopoulos, D.M. Newbold, E. Olaiya, D. Petyt, T. Reis, A.R. Sahasransu, G. Salvi, T. Schuh, C.H. Shepherd-Themistocleous, I.R. Tomalin, T. Williams

### Imperial College, London, United Kingdom

R. Bainbridge, P. Bloch, C.E. Brown, O. Buchmuller, V. Cacchio, C.A. Carrillo Montoya, G.S. Chahal, D. Colling, J.S. Dancu, I. Das, P. Dauncey, G. Davies, J. Davies, M. Della Negra, S. Fayer, G. Fedi, G. Hall, M.H. Hassanshahi, A. Howard, G. Iles, M. Knight, J. Langford, J. León Holgado, L. Lyons, A.-M. Magnan, S. Malik, M. Mieskolainen, J. Nash, M. Pesaresi, P.B. Pradeep, B.C. Radburn-Smith, A. Richards, A. Rose, K. Savva, C. Seez, R. Shukla, A. Tapper, K. Uchida, G.P. Uttley, L.H. Vage, T. Virdee, M. Vojinovic, N. Wardle, D. Winterbottom

### Brunel University, Uxbridge, United Kingdom

K. Coldham, J.E. Cole, A. Khan, P. Kyberd, I.D. Reid

#### Baylor University, Waco, Texas, U.S.A.

S. Abdullin, A. Brinkerhoff, B. Caraway, E. Collins, J. Dittmann, K. Hatakeyama, J. Hiltbrand, B. McMaster, J. Samudio, S. Sawant, C. Sutantawibul, J. Wilson

#### Catholic University of America, Washington, DC, U.S.A.

R. Bartek, A. Dominguez, C. Huerta Escamilla, A.E. Simsek, R. Uniyal, A.M. Vargas Hernandez

#### The University of Alabama, Tuscaloosa, Alabama, U.S.A.

B. Bam, R. Chudasama, S.I. Cooper, C. Crovella, S.V. Gleyzer, E. Pearson, C.U. Perez, P. Rumerio, S., E. Usai, R. Yi

#### Boston University, Boston, Massachusetts, U.S.A.

A. Akpinar, D. Arcaro, C. Cosby, G. De Castro, Z. Demiragli, C. Erice, C. Fangmeier, C. Fernandez Madrazo, E. Fontanesi, D. Gastler, F. Golf, S. Jeon, I. Reed, J. Rohlf, K. Salyer, D. Sperka, D. Spitzbart, I. Suarez, A. Tsatsos, S. Yuan, A.G. Zecchinelli

### Brown University, Providence, Rhode Island, U.S.A.

- G. Benelli, X. Coubez, D. Cutts, M. Hadley, U. Heintz, J.M. Hogan, T. Kwon,
- G. Landsberg, K.T. Lau, D. Li, J. Luo, S. Mondal, M. Narain, N. Pervan, N. Pe
- S. Sagir 685, F. Simpson 6, M. Stamenkovic 6, N. Venkatasubramanian, X. Yan 6, W. Zhang

### University of California, Davis, Davis, California, U.S.A.

- S. Abbott, J. Bonilla, C. Brainerd, R. Breedon, H. Cai,
- M. Calderon De La Barca Sanchez, M. Chertok, M. Citron, J. Conway, P.T. Cox,
- R. Erbacher, F. Jensen, O. Kukral, G. Mocellin, M. Mulhearn, D. Pellett, W. Wei,
- Y. Yao, F. Zhang

### University of California, Los Angeles, California, U.S.A.

- M. Bachtis, R. Cousins, A. Datta, G. Flores Avila, J. Hauser, M. Ignatenko, M.A. Iqbal,
- T. Lam, E. Manca, A. Nunez Del Prado, D. Saltzberg, V. Valuev

### University of California, Riverside, Riverside, California, U.S.A.

R. Clare, J.W. Gary, M. Gordon, G. Hanson, W. Si, S. Wimpenny

### University of California, San Diego, La Jolla, California, U.S.A.

- A. Aportela, A. Arora, J.G. Branson, S. Cittolin, S. Cooperstein, D. Diaz, J. Duarte,
- L. Giannini, Y. Gu, J. Guiang, R. Kansal, V. Krutelyov, R. Lee, J. Letts,
- M. Masciovecchio, F. Mokhtar, S. Mukherjee, M. Pieri, M. Quinnan,
- B.V. Sathia Narayanan @ , V. Sharma @ , M. Tadel @ , E. Vourliotis @ , F. Würthwein @ , Y. Xiang @ ,
- A. Yagil

# University of California, Santa Barbara — Department of Physics, Santa Barbara, California, U.S.A.

- A. Barzdukas, L. Brennan, C. Campagnari, J. Incandela, J. Kim, A.J. Li,
- P. Masterson, H. Mei, J. Richman, U. Sarica, R. Schmitz, F. Setti, J. Sheplock, J. Sheplock,
- D. Stuart, T.Á. Vámi, S. Wang

#### California Institute of Technology, Pasadena, California, U.S.A.

- A. Bornheim, O. Cerri, A. Latorre, J. Mao, H.B. Newman, G. Reales Gutiérrez,
- M. Spiropulu, J.R. Vlimant, C. Wang, S. Xie, R.Y. Zhu

### Carnegie Mellon University, Pittsburgh, Pennsylvania, U.S.A.

- J. Alison, S. An, M.B. Andrews, P. Bryant, M. Cremonesi, V. Dutta, T. Ferguson,
- A. Harilal, A. Kallil Tharayil, C. Liu, T. Mudholkar, S. Murthy, P. Palit, K. Park,
- M. Paulini, A. Roberts, A. Sanchez, W. Terrill

### University of Colorado Boulder, Boulder, Colorado, U.S.A.

- J.P. Cumalat , W.T. Ford, A. Hart, A. Hassani, G. Karathanasi, N. Manganelli, A. Hassani, G. Karathanasi, N. Manganelli,
- A. Perloff, C. Savard, N. Schonbeck, K. Stenson, K.A. Ulmer, S.R. Wagner,
- N. Zipper<sup>®</sup>, D. Zuolo<sup>®</sup>

### Cornell University, Ithaca, New York, U.S.A.

- J. Alexander, S. Bright-Thonney, X. Chen, D.J. Cranshaw, J. Fan, X. Fan, S. Hogan,
- P. Kotamnives, J. Monroy, M. Oshiro, J.R. Patterson, M. Reid, A. Ryd, J. Thom,
- P. Wittich, R. Zou

### Fermi National Accelerator Laboratory, Batavia, Illinois, U.S.A.

- M. Albrow, M. Alyari, O. Amram, G. Apollinari, A. Apresyan, L.A.T. Bauerdick,
- D. Berry, J. Berryhill, P.C. Bhat, K. Burkett, J.N. Butler, A. Canepa, G.B. Cerati,
- H.W.K. Cheung, F. Chlebana, G. Cummings, J. Dickinson, I. Dutta, V.D. Elvira,
- Y. Feng , J. Freeman , A. Gandrakota , Z. Gecse , L. Gray , D. Green, A. Grummer ,
- S. Grünendahl, D. Guerrero, O. Gutsche, R.M. Harris, R. Heller, T.C. Herwig,
- J. Hirschauer, L. Horyn, B. Jayatilaka, S. Jindariani, M. Johnson, U. Joshi,
- T. Klijnsma<sup>®</sup>, B. Klima<sup>®</sup>, K.H.M. Kwok<sup>®</sup>, S. Lammel<sup>®</sup>, D. Lincoln<sup>®</sup>, R. Lipton<sup>®</sup>, T. Liu<sup>®</sup>,
- C. Madrid, K. Maeshima, C. Mantilla, D. Mason, P. McBride, P. Merkel, S. Mrenna,
- S. Nahn, J. Ngadiuba, D. Noonan, V. Papadimitriou, N. Pastika, K. Pedro,
- C. Pena 686, F. Ravera , A. Reinsvold Hall 87, L. Ristori , E. Sexton-Kennedy, N. Smith,
- A. Soha, L. Spiegel, S. Stoynev, J. Strait, L. Taylor, S. Tkaczyk, N.V. Tran,
- L. Uplegger, E.W. Vaandering, A. Whitbeck, I. Zoi

### University of Florida, Gainesville, Florida, U.S.A.

- C. Aruta, P. Avery, D. Bourilkov, L. Cadamuro, P. Chang, V. Cherepanov, R.D. Field,
- E. Koenig, M. Kolosova, J. Konigsberg, A. Korytov, K. Matchev, N. Menendez, N. Menendez,
- G. Mitselmakher, K. Mohrman, A. Muthirakalayil Madhu, N. Rawal, D. Rosenzweig,
- S. Rosenzweig, J. Wang

### Florida State University, Tallahassee, Florida, U.S.A.

- T. Adams , A. Al Kadhim, A. Askew, S. Bower, R. Habibullah, V. Hagopian,
- R. Hashmi<sup>®</sup>, R.S. Kim<sup>®</sup>, S. Kim<sup>®</sup>, T. Kolberg<sup>®</sup>, G. Martinez, H. Prosper<sup>®</sup>, P.R. Prova,
- M. Wulansatiti, R. Yohay, J. Zhang

#### Florida Institute of Technology, Melbourne, Florida, U.S.A.

- B. Alsufyani, M.M. Baarmand, S. Butalla, S. Das, T. Elkafrawy, M. Hohlmann,
- R. Kumar Verma<sup>®</sup>, M. Rahmani, E. Yanes

#### University of Illinois Chicago, Chicago, U.S.A., Chicago, U.S.A.

- M.R. Adams, A. Baty, C. Bennett, R. Cavanaugh, R. Escobar Franco, O. Evdokimov,
- C.E. Gerber, M. Hawksworth, A. Hingrajiya, D.J. Hofman, J.h. Lee, D. S. Lemos,
- A.H. Merrit, C. Mills, S. Nanda, G. Oh, B. Ozek, D. Pilipovic, R. Pradhan, E. Prifti,
- T. Roy D, S. Rudrabhatla D, M.B. Tonjes D, N. Varelas D, M.A. Wadud D, Z. Ye D, J. Yoo D

### The University of Iowa, Iowa City, Iowa, U.S.A.

- J.-P. Merlo, A. Mestvirishvili <sup>689</sup>, J. Nachtman <sup>6</sup>, O. Neogi, H. Ogul <sup>690</sup>, Y. Onel <sup>6</sup>, A. Penzo <sup>6</sup>, C. Snyder, E. Tiras <sup>691</sup>

### Johns Hopkins University, Baltimore, Maryland, U.S.A.

B. Blumenfeld, L. Corcodilos, J. Davis, A.V. Gritsan, L. Kang, S. Kyriacou,

P. Maksimovic, M. Roguljic, J. Roskes, S. Sekhar, M. Swartz

### The University of Kansas, Lawrence, Kansas, U.S.A.

A. Abreu, L.F. Alcerro Alcerro, J. Anguiano, S. Arteaga Escatel, P. Baringer, A. Bean,

Z. Flowers, D. Grove, J. King, G. Krintiras, M. Lazarovits, C. Le Mahieu,

J. Marquez, N. Minafra, M. Murray, M. Nickel, M. Pitt, S. Popescu, C. Rogan, C.

C. Royon, R. Salvatico, S. Sanders, C. Smith, Q. Wang, G. Wilson

### Kansas State University, Manhattan, Kansas, U.S.A.

B. Allmond, R. Gujju Gurunadha, A. Ivanov, K. Kaadze, A. Kalogeropoulos,

Y. Maravin, J. Natoli, D. Roy, G. Sorrentino

### Lawrence Livermore National Laboratory, Livermore, California, U.S.A.

F. Rebassoo, D. Wright

### University of Maryland, College Park, Maryland, U.S.A.

A. Baden, A. Belloni, J. Bistany-riebman, Y.M. Chen, S.C. Eno, N.J. Hadley,

S. Jabeen, R.G. Kellogg, T. Koeth, B. Kronheim, Y. Lai, S. Lascio, A.C. Mignerey,

S. Nabili, C. Palmer, C. Papageorgakis, M.M. Paranjpe, L. Wang

### Massachusetts Institute of Technology, Cambridge, Massachusetts, U.S.A.

J. Bendavid, I.A. Cali, P.c. Chou, M. D'Alfonso, J. Eysermans, C. Freer,

G. Gomez-Ceballos, M. Goncharov, G. Grosso, P. Harris, D. Hoang, D. Kovalskyi, J. Krupa, J. Krupa,

L. Lavezzo, Y.-J. Lee, K. Long, A. Novak, C. Paus, D. Rankin, C. Roland,

G. Roland, S. Rothman, G.S.F. Stephans, Z. Wang, B. Wyslouch, T. J. Yang

### University of Minnesota, Minnesota, Minnesota, U.S.A.

B. Crossman, B.M. Joshi, C. Kapsiak, M. Krohn, D. Mahon, J. Mans, B. Marzocchi, B. Marzocchi

S. Pandey 📵, M. Revering 📵, R. Rusack 📵, R. Saradhy 📵, N. Schroeder 📵, N. Strobbe 📵

#### University of Mississippi, Oxford, Mississippi, U.S.A.

L.M. Cremaldi

### University of Nebraska-Lincoln, Lincoln, Nebraska, U.S.A.

K. Bloom, D.R. Claes, G. Haza, J. Hossain, C. Joo, I. Kravchenko, J.E. Siado,

W. Tabb, A. Vagnerini, A. Wightman, F. Yan, D. Yu

#### State University of New York at Buffalo, Buffalo, New York, U.S.A.

H. Bandyopadhyay, L. Hay, H.w. Hsia, I. Iashvili, A. Kharchilava, M. Morris, A. Kharchilava, M. Morris,

D. Nguyen, S. Rappoccio, H. Rejeb Sfar, A. Williams, P. Young

### Northeastern University, Boston, Massachusetts, U.S.A.

G. Alverson, E. Barberis, J. Dervan, Y. Haddad, Y. Han, A. Krishna, J. Li, M. Lu, M. Lu

G. Madigan, R. Mccarthy, D.M. Morse, V. Nguyen, T. Orimoto, A. Parker,

L. Skinnari, D. Wood

### Northwestern University, Evanston, Illinois, U.S.A.

J. Bueghly, Z. Chen, S. Dittmer, K.A. Hahn, Y. Liu, Y. Miao, D.G. Monk, M.H. Schmitt, A. Taliercio, M. Velasco

### University of Notre Dame, Notre Dame, Indiana, U.S.A.

G. Agarwal, R. Band, R. Bucci, S. Castells, A. Das, R. Goldouzian, M. Hildreth, K.W. Ho, K. Hurtado Anampa, T. Ivanov, C. Jessop, K. Lannon, J. Lawrence,

N. Loukas, L. Lutton, J. Mariano, N. Marinelli, I. Mcalister, T. McCauley, C. Mcgrady,

C. Moore, Y. Musienko, H. Nelson, M. Osherson, A. Piccinelli, R. Ruchti, R. Ruchti,

A. Townsend, Y. Wan, M. Wayne, H. Yockey, M. Zarucki, L. Zygala

### The Ohio State University, Columbus, Ohio, U.S.A.

A. Basnet, B. Bylsma, M. Carrigan, L.S. Durkin, C. Hill, M. Joyce, M. Nunez Ornelas, K. Wei, B.L. Winer, B. R. Yates

### Princeton University, Princeton, New Jersey, U.S.A.

F.M. Addesa, H. Bouchamaoui, P. Das, G. Dezoort, P. Elmer, A. Frankenthal, B. Greenberg, N. Haubrich, G. Kopp, S. Kwan, D. Lange, A. Loeliger, D. Marlow, I. Ojalvo, J. Olsen, A. Shevelev, D. Stickland, C. Tully

### University of Puerto Rico, Mayaguez, Puerto Rico, U.S.A.

S. Malik

### Purdue University, West Lafayette, Indiana, U.S.A.

A.S. Bakshi, V.E. Barnes, S. Chandra, R. Chawla, A. Gu, L. Gutay, M. Jones, A.W. Jung, D. Kondratyev, A.M. Koshy, M. Liu, G. Negro, N. Neumeister, G. Paspalaki, S. Piperov, V. Scheurer, J.F. Schulte, M. Stojanovic, J. Thieman, A. K. Virdi, F. Wang, W. Xie,

### Purdue University Northwest, Hammond, Indiana, U.S.A.

J. Dolen, N. Parashar, A. Pathak

#### Rice University, Houston, Texas, U.S.A.

D. Acosta, T. Carnahan, K.M. Ecklund, P.J. Fernández Manteca, S. Freed, P. Gardner, F.J.M. Geurts, W. Li, J. Lin, O. Miguel Colin, B.P. Padley, R. Redjimi, J. Rotter, E. Yigitbasi, Y. Zhang

### University of Rochester, Rochester, New York, U.S.A.

A. Bodek, P. de Barbaro, R. Demina, J.L. Dulemba, A. Garcia-Bellido, O. Hindrichs, A. Khukhunaishvili, N. Parmar, P. Parygin, E. Popova, R. Taus, R. Taus, R. Taus, R. Taus, P. Parygin, P. Parygin, R. Taus, R. T

#### The Rockefeller University, New York, New York, U.S.A.

K. Goulianos •

### Rutgers, The State University of New Jersey, Piscataway, New Jersey, U.S.A.

B. Chiarito, J.P. Chou, S.V. Clark, D. Gadkari, Y. Gershtein, E. Halkiadakis, M. Heindl, C. Houghton, D. Jaroslawski, O. Karacheban, S. Konstantinou, I. Laflotte,

```
A. Lath, R. Montalvo, K. Nash, J. Reichert, H. Routray, P. Saha, S. Salur, S. Schnetzer, S. Somalwar, R. Stone, S.A. Thayil, S. Thomas, J. Vora, H. Wang, University of Tennessee, Knoxville, Tennessee, U.S.A.
```

H. Acharya, D. Ally, A.G. Delannoy, S. Fiorendi, S. Higginbotham, T. Holmes, A.R. Kanuganti, N. Karunarathna, L. Lee, E. Nibigira, S. Spanier

### Texas A&M University, College Station, Texas, U.S.A.

D. Aebi, M. Ahmad, O. Bouhali, R. Eusebi, J. Gilmore, T. Huang, T. Kamon, T. Kamon, T. Kamon, R. Kim, S. Luo, R. Mueller, D. Overton, D. Rathjens, A. Safonov,

### Texas Tech University, Lubbock, Texas, U.S.A.

N. Akchurin, J. Damgov, N. Gogate, V. Hegde, A. Hussain, Y. Kazhykarim, K. Lamichhan, S.W. Lee, A. Mankel, T. Peltola, I. Volobouev

### Vanderbilt University, Nashville, Tennessee, U.S.A.

E. Appelt, Y. Chen, S. Greene, A. Gurrola, W. Johns, R. Kunnawalkam Elayavalli, A. Melo, F. Romeo, P. Sheldon, S. Tuo, J. Velkovska, J. Viinikainen

### University of Virginia, Charlottesville, Virginia, U.S.A.

B. Cardwell, B. Cox, J. Hakala, R. Hirosky, A. Ledovskoy, C. Neu, C.E. Perez Lara

### Wayne State University, Detroit, Michigan, U.S.A.

S. Bhattacharya, P.E. Karchin

### University of Wisconsin — Madison, Madison, Wisconsin, U.S.A.

A. Aravind, S. Banerjee, K. Black, T. Bose, S. Dasu, I. De Bruyn, P. Everaerts,

C. Galloni, H. He<sup>10</sup>, M. Herndon<sup>10</sup>, A. Herve<sup>10</sup>, C.K. Koraka<sup>10</sup>, A. Lanaro, R. Loveless<sup>10</sup>,

J. Madhusudanan Sreekala<sup>®</sup>, A. Mallampalli<sup>®</sup>, A. Mohammadi<sup>®</sup>, S. Mondal, G. Parida<sup>®</sup>,

L. Pétré®, D. Pinna, A. Savin, V. Shang®, V. Sharma®, W.H. Smith®, D. Teague, H.F. Tsoi®, W. Vetens®, A. Warden®

# Authors affiliated with an institute or an international laboratory covered by a cooperation agreement with CERN

S. Afanasiev<sup>®</sup>, V. Andreev<sup>®</sup>, Yu. Andreev<sup>®</sup>, T. Aushev<sup>®</sup>, M. Azarkin<sup>®</sup>, I. Azhgirey<sup>®</sup>,

A. Babaev, A. Belyaev, V. Blinov, E. Boos, V. Borshch, D. Budkouski, V. Bunichev,

V. Chekhovsky, R. Chistov <sup>696</sup>, M. Danilov <sup>696</sup>, A. Dermenev <sup>6</sup>, T. Dimova <sup>696</sup>, D. Druzhkin <sup>697</sup>,

M. Dubinin 686, L. Dudko, A. Ershov, G. Gavrilov, V. Gavrilov, S. Gninenko,

V. Golovtcov, N. Golubev, I. Golutvin, I. Gorbunov, Y. Ivanov, V. Kachanov,

V. Karjavine, A. Karneyeu, V. Kim, M. Kirakosyan, D. Kirpichnikov, M. Kirsanov, M.

V. Klyukhin, O. Kodolova, D. Konstantinov, V. Korenkov, A. Kozyrev, A. Kozyrev,

N. Krasnikov, A. Lanev, P. Levchenko, N. Lychkovskaya, V. Makarenko,

A. Malakhov, V. Matveev, V. Murzin, A. Nikitenko, S. Obraztsov, V. Oreshkin, V. Oreshkin,

V. Palichik, V. Perelygin, M. Perfilov, S. Polikarpov, V. Popov, O. Radchenko, A. Polikarpov, V. Popov, O. Radchenko, V. Popov, O. Radchenko, V. Popov, V. Popov, O. Radchenko, V. Popov, O. Radchenko

R. Ryutin, M. Savina, V. Savrin, V. Shalaev, S. Shmatov, S. Shulha, Y. Skovpen, 496,

S. Slabospitskii, V. Smirnov, A. Snigirev, D. Sosnov, V. Sulimov, E. Tcherniaev,

- A. Terkulov, O. Teryaev, I. Tlisova, A. Toropin, L. Uvarov, A. Uzunian, A. Vorobyev, G. Vorotnikov, N. Voytishin, B.S. Yuldashev, A. Zarubin, I. Zhizhin, A. Zhokin,
  - $^{\dagger}$  Deceased
  - <sup>1</sup> Also at Yerevan State University, Yerevan, Armenia
  - <sup>2</sup> Also at TU Wien, Vienna, Austria
  - <sup>3</sup> Also at Institute of Basic and Applied Sciences, Faculty of Engineering, Arab Academy for Science, Technology and Maritime Transport, Alexandria, Egypt
  - <sup>4</sup> Also at Ghent University, Ghent, Belgium
  - <sup>5</sup> Also at Universidade do Estado do Rio de Janeiro, Rio de Janeiro, Brazil
  - <sup>6</sup> Also at Universidade Estadual de Campinas, Campinas, Brazil
  - $^7$  Also at Federal University of Rio Grande do Sul, Porto Alegre, Brazil
  - <sup>8</sup> Also at UFMS, Nova Andradina, Brazil
  - <sup>9</sup> Also at Nanjing Normal University, Nanjing, China
  - <sup>10</sup> Now at The University of Iowa, Iowa City, Iowa, U.S.A.
  - <sup>11</sup> Also at University of Chinese Academy of Sciences, Beijing, China
  - <sup>12</sup> Also at China Center of Advanced Science and Technology, Beijing, China
  - <sup>13</sup> Also at University of Chinese Academy of Sciences, Beijing, China
  - Also at China Spallation Neutron Source, Guangdong, China
  - $^{15}$  Now at Henan Normal University, Xinxiang, China
  - <sup>16</sup> Also at Université Libre de Bruxelles, Bruxelles, Belgium
  - $^{17}$  Also at an institute or an international laboratory covered by a cooperation agreement with CERN
  - <sup>18</sup> Also at Suez University, Suez, Egypt
  - <sup>19</sup> Now at British University in Egypt, Cairo, Egypt
  - <sup>20</sup> Also at Purdue University, West Lafayette, Indiana, U.S.A.
  - <sup>21</sup> Also at Université de Haute Alsace, Mulhouse, France
  - <sup>22</sup> Also at Department of Physics, Tsinghua University, Beijing, China
  - <sup>23</sup> Also at The University of the State of Amazonas, Manaus, Brazil
  - <sup>24</sup> Also at Erzincan Binali Yildirim University, Erzincan, Turkey
  - <sup>25</sup> Also at University of Hamburg, Hamburg, Germany
- <sup>26</sup> Also at RWTH Aachen University, III. Physikalisches Institut A, Aachen, Germany
- $^{27}$  Also at Bergische University Wuppertal (BUW), Wuppertal, Germany
- <sup>28</sup> Also at Brandenburg University of Technology, Cottbus, Germany
- <sup>29</sup> Also at Forschungszentrum Jülich, Juelich, Germany
- <sup>30</sup> Also at CERN, European Organization for Nuclear Research, Geneva, Switzerland
- <sup>31</sup> Also at Institute of Physics, University of Debrecen, Debrecen, Hungary
- <sup>32</sup> Also at Institute of Nuclear Research ATOMKI, Debrecen, Hungary
- <sup>33</sup> Now at Universitatea Babes-Bolyai Facultatea de Fizica, Cluj-Napoca, Romania
- <sup>34</sup> Also at MTA-ELTE Lendület CMS Particle and Nuclear Physics Group, Eötvös Loránd University, Budapest, Hungary
- 35 Also at HUN-REN Wigner Research Centre for Physics, Budapest, Hungary
- <sup>36</sup> Also at Physics Department, Faculty of Science, Assiut University, Assiut, Egypt
- <sup>37</sup> Also at Punjab Agricultural University, Ludhiana, India
- <sup>38</sup> Also at University of Visva-Bharati, Santiniketan, India
- <sup>39</sup> Also at Indian Institute of Science (IISc), Bangalore, India
- <sup>40</sup> Also at Birla Institute of Technology, Mesra, Mesra, India
- $^{41}$  Also at IIT Bhubaneswar, Bhubaneswar, India
- <sup>42</sup> Also at Institute of Physics, Bhubaneswar, India
- <sup>43</sup> Also at University of Hyderabad, Hyderabad, India
- <sup>44</sup> Also at Deutsches Elektronen-Synchrotron, Hamburg, Germany
- <sup>45</sup> Also at Isfahan University of Technology, Isfahan, Iran
- <sup>46</sup> Also at Sharif University of Technology, Tehran, Iran
- <sup>47</sup> Also at Department of Physics, University of Science and Technology of Mazandaran, Behshahr, Iran

- <sup>48</sup> Also at Department of Physics, Isfahan University of Technology, Isfahan, Iran
- <sup>49</sup> Also at Helwan University, Cairo, Egypt
- <sup>50</sup> Also at Italian National Agency for New Technologies, Energy and Sustainable Economic Development, Bologna, Italy
- <sup>51</sup> Also at Centro Siciliano di Fisica Nucleare e di Struttura Della Materia, Catania, Italy
- <sup>52</sup> Also at Università degli Studi Guglielmo Marconi, Roma, Italy
- <sup>53</sup> Also at Scuola Superiore Meridionale, Università di Napoli 'Federico II', Napoli, Italy
- <sup>54</sup> Also at Fermi National Accelerator Laboratory, Batavia, Illinois, U.S.A.
- <sup>55</sup> Also at Laboratori Nazionali di Legnaro dell'INFN, Legnaro, Italy
- <sup>56</sup> Also at Ain Shams University, Cairo, Egypt
- <sup>57</sup> Also at Consiglio Nazionale delle Ricerche Istituto Officina dei Materiali, Perugia, Italy
- <sup>58</sup> Also at Department of Applied Physics, Faculty of Science and Technology, Universiti Kebangsaan Malaysia, Bangi, Malaysia
- <sup>59</sup> Also at Consejo Nacional de Ciencia y Tecnología, Mexico City, Mexico
- <sup>60</sup> Also at Trincomalee Campus, Eastern University, Sri Lanka, Nilaveli, Sri Lanka
- <sup>61</sup> Also at Saegis Campus, Nugegoda, Sri Lanka
- <sup>62</sup> Also at National and Kapodistrian University of Athens, Athens, Greece
- $^{63}$  Also at Ecole Polytechnique Fédérale Lausanne, Lausanne, Switzerland
- <sup>64</sup> Also at Universität Zürich, Zurich, Switzerland
- <sup>65</sup> Also at Stefan Meyer Institute for Subatomic Physics, Vienna, Austria
- <sup>66</sup> Also at Laboratoire d'Annecy-le-Vieux de Physique des Particules, IN2P3-CNRS, Annecy-le-Vieux, France
- <sup>67</sup> Also at Near East University, Research Center of Experimental Health Science, Mersin, Turkey
- <sup>68</sup> Also at Konya Technical University, Konya, Turkey
- <sup>69</sup> Also at Izmir Bakircay University, Izmir, Turkey
- <sup>70</sup> Also at Adiyaman University, Adiyaman, Turkey
- <sup>71</sup> Also at Bozok Universitetesi Rektörlügü, Yozgat, Turkey
- <sup>72</sup> Also at Marmara University, Istanbul, Turkey
- <sup>73</sup> Also at Milli Savunma University, Istanbul, Turkey
- $^{74}$  Also at Kafkas University, Kars, Turkey
- <sup>75</sup> Now at stanbul Okan University, Istanbul, Turkey
- <sup>76</sup> Also at Hacettepe University, Ankara, Turkey
- <sup>77</sup> Also at Istanbul University Cerrahpasa, Faculty of Engineering, Istanbul, Turkey
- <sup>78</sup> Also at Yildiz Technical University, Istanbul, Turkey
- <sup>79</sup> Also at Vrije Universiteit Brussel, Brussel, Belgium
- <sup>80</sup> Also at School of Physics and Astronomy, University of Southampton, Southampton, United Kingdom
- <sup>81</sup> Also at IPPP Durham University, Durham, United Kingdom
- <sup>82</sup> Also at Monash University, Faculty of Science, Clayton, Australia
- <sup>83</sup> Also at Università di Torino, Torino, Italy
- <sup>84</sup> Also at Bethel University, St. Paul, Minnesota, U.S.A.
- <sup>85</sup> Also at Karamanoğlu Mehmetbey University, Karaman, Turkey
- <sup>86</sup> Also at California Institute of Technology, Pasadena, California, U.S.A.
- <sup>87</sup> Also at United States Naval Academy, Annapolis, Maryland, U.S.A.
- <sup>88</sup> Also at Bingol University, Bingol, Turkey
- <sup>89</sup> Also at Georgian Technical University, Tbilisi, Georgia
- 90 Also at Sinop University, Sinop, Turkey
- <sup>91</sup> Also at Erciyes University, Kayseri, Turkey
- <sup>92</sup> Also at Horia Hulubei National Institute of Physics and Nuclear Engineering (IFIN-HH), Bucharest, Romania
- <sup>93</sup> Now at an institute or an international laboratory covered by a cooperation agreement with CERN
- <sup>94</sup> Also at Texas A&M University at Qatar, Doha, Qatar
- <sup>95</sup> Also at Kyungpook National University, Daegu, Korea
- <sup>96</sup> Also at another institute or international laboratory covered by a cooperation agreement with CERN
- <sup>97</sup> Also at Universiteit Antwerpen, Antwerpen, Belgium

<sup>98</sup> Also at Yerevan Physics Institute, Yerevan, Armenia
99 Also at Northeastern University, Boston, Massachusetts, U.S.A.
100 Also at Imperial College, London, United Kingdom

<sup>&</sup>lt;sup>101</sup> Also at Institute of Nuclear Physics of the Uzbekistan Academy of Sciences, Tashkent, Uzbekistan